NOT TO BE CITED WITHOUT PRIOR
REFERENCE TO THE AUTHOR(S)

Northwest Atlantic Fisheries Organization

Serial No. N7066 **NAFO SCR Doc. 20/020REV**

SCIENTIFIC COUNCIL MEETING – JUNE 2020

Environmental and Physical Oceanographic Conditions on the Eastern Canadian shelves (NAFO Sub-areas 2, 3 and 4) during 2019.

by

F. Cyr[1], P. S. Galbraith[2], C. Layton[3] D. Hebert[3]

[1]Northwest Atlantic Fisheries Centre, Fisheries and Oceans Canada, St. John's (NL)
[2]Maurice-Lamontagne Institute, Fisheries and Oceans Canada, Mont-Joli (QC)
[3]Bedford Institute of Oceanography, Fisheries and Oceans Canada, Dartmouth (NS)

Abstract

Oceanographic and meteorological observations in NAFO Sub-areas 2, 3 and 4 during 2019 are presented and referenced to their long-term (1981-2010) averages. The winter North Atlantic Oscillation (NAO) index, a key indicator of the direction and intensity of the winter wind field patterns over the Northwest Atlantic was positive for a 6th consecutive year (since 2012, only 2013 was negative). The air temperatures across the NW Atlantic were warm in the Arctic, between normal and colder than normal on the Newfoundland and Labrador and Scotian Shelf, and warmer than normal in Boston on the coast of the Gulf of Maine. The sea ice volume across the Newfoundland and Labrador shelf was slightly below normal, characterized by a large negative anomaly in March-April, which also led to an early retreat on Newfoundland shelf. Annual sea surface temperature across the NAFO subareas 2, 3 and 4 were below normal overall for the zone for the first time since 1992, yet they would have been near normal if not for tropical storm Dorian that mixed heat deep into the water column. Observations from the summer AZMP oceanographic survey indicate that after a predominance of colder than average conditions since 2012, the volume of the cold intermediate layer (CIL, <0°C) reduced along Bonavista and Flemish Cap section in 2019 (CIL along Seal Island section was normal this year but was reduced in 2018). The spatially averaged bottom temperature in 3LNOPs during the spring was close to normal, except along the slopes of the Grand Banks where it was above normal. For the fall, bottom temperature in 2HJ3KLNO was also above normal, especially in 2J (+1.1 SD) and 3K (+1.0 SD). Deep water temperatures on the Scotian shelf were very warm: record high in Cabot Strait (nearly 5SD above the climatology) and Emerald Basin, and second warmest year in George Basin. The Labrador Current transport index along the Labrador and northern Newfoundland slope in 2019 was back to normal after the 2018 record high since the beginning of the time series that started in 1993.

Introduction

This manuscript presents an overview of the 2019 environmental and physical oceanographic conditions in NAFO sub-areas 2, 3 and 4 on eastern Canadian shelves (see Figure 1). This report complements similar reviews of environmental conditions on the Northeast US Shelf, the Labrador Sea and West Greenland Waters as part of the Scientific Council's annual review of environmental conditions in the NAFO Convention Area.

The information presented for 2019 is derived from various sources:

1. Observations made throughout the year at historical monitoring stations 27 (near St. John's, NL), Prince-5 (Bay of Fundy) and Halifax-2 (Scotian Shelf);
2. Measurements made during the summer along standard NAFO and Atlantic Zone Monitoring Program (AZMP) (Therriault et al. 1998) cross-shelf sections (see Figure 1);
3. Oceanographic observations made during multi-species and ground fish resource assessment surveys (NAFO sub-areas 2 to 4);
4. SST data based on infrared satellite imagery (Advance Very High Resolution Radiometer, or AVHRR) of the Northwest Atlantic
5. Other multi-source historical data (ships of opportunity, international campaign, other DFO regions surveys, Argo program, etc.);
6. Ice data are from the Canadian Ice Service and meteorological data are from Environment Canada and other sources cited in the text.

Unless otherwise specified, these data are available from MEDS archives and maintained in a regional data archive at the Northwest Atlantic Fisheries Centre (NAFC) in St. John's, NL and at the Bedford Institute of Oceanography (BIO) in Dartmouth, NS.

Time series of temperature and salinity anomalies and other derived climate indices were constructed by removing the annual cycle computed over a standard climatological period from 1981 to 2010. "*Normal"* is thus defined here as the average over this period. Annual or seasonal anomalies were sometimes normalized by dividing the values by the standard deviation (SD) of the data time series over the climatological period. A value of 2, for example, indicates that the index was 2 SD higher than its long-term average. As a general guide, anomalies within ±0.5 SD are considered to be normal.

The normalized values of water properties and derived climate indices presented in this document are color-coded in "scorecards" with gradations of 0.5 SD (Figure 2). Shades of blue represent cold-fresh environmental conditions and reds warm-salty conditions. In some instances (NAO, ice and cold water areas or volumes, for example) negative anomalies may indicate warm conditions and hence are colored red. Most of the colormaps used in this report are taken from the *cmocean* colormaps package for oceanography (Thyng et al., 2016).

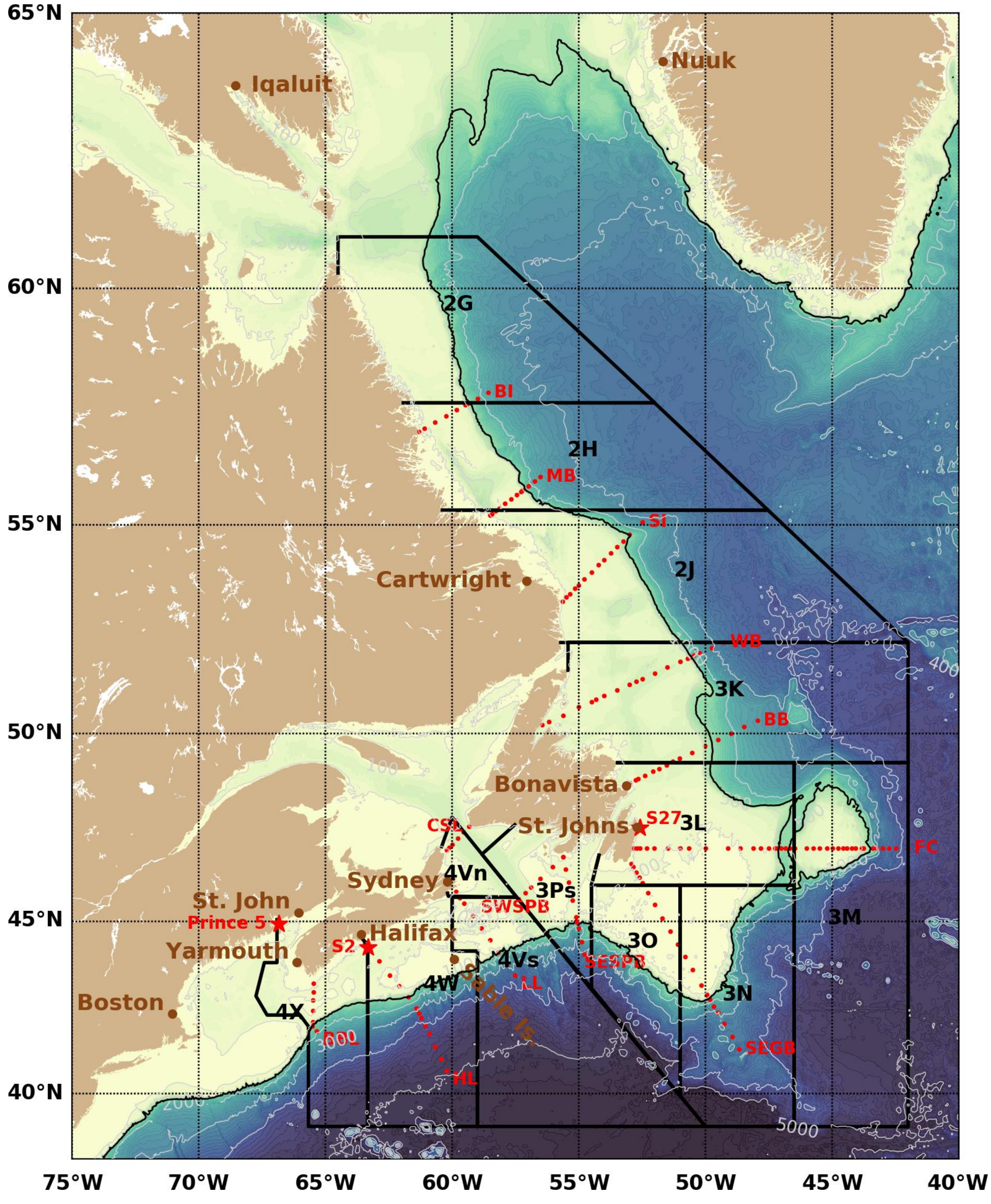

Figure 1. Map showing NAFO Divisions and main bathymetric features of the Northwest Atlantic. The hydrographic sections reported here are shown with red dots and the fixed stations by red stars. The stations used for air temperature time series and in brown. The black contour is the isobath 1000m that is used here to delimit the continental shelf.

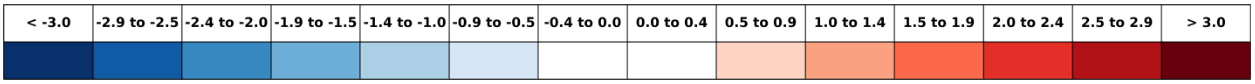

Figure 2. Colorscale used for the presentation of normalized anomalies. Color levels are incremented by 0.5 standard deviations (SD), where blue is below normal and red above normal. Values between 0 and ±0.5 SD remain white indicating normal conditions.

Meteorological Conditions

The winter North Atlantic Oscillation (NAO) is defined as anomaly in the sea-level pressure (SLP) difference between the sub-tropical high (average location near the Azores) and the sub-polar low (average location near Iceland). Several definitions of the NAO exists and the definition used here is the one from the National Center for Environmental Information of the National Oceanic and Atmospheric Administration (NOAA) and available online. The winter NAO (defined here as the average of monthly values from December to March) is considered a measure of the strength of the winter westerly and north westerly winds over the Northwest Atlantic. A high NAO index (positive phase) occurs during an intensification of the Icelandic Low and Azores High. Except for some years for which the SLP patterns are spatially shifted (e.g. 1999, 2000 and 2018, where the location of high and low SLP were reversed in March), positive winter NAO years favor strong northwestly winds, cold air and sea surface temperatures, and heavy ice conditions on the NL shelves (Colbourne et al., 1994; Drinkwater 1996; Petrie et al., 2007). In 2019, the winter NAO was positive (+0.68; first row in Figure 3) for a 6th consecutive year. A predominance of strongly positive winter NAO phase is ongoing since 2012 (all years except 2013 were positive), including the record high of +1.6 in 2015, whereas the record low of -1.5 was in 2010.

The Arctic Oscillation (AO) is a larger scale index intimately linked with the NAO. During a positive phase, the arctic air outflow to the Northwest Atlantic increases, resulting in colder winter air temperatures over much of the NL and adjacent shelf regions. In 2019, the AO was above normal at +0.5 (Figure 3), indicative of cold air temperature. AO in 2015 was the highest value since 1990 at +1.6, and the record low was reached in 2010 when it was below normal at -1.5 (warm air temperatures).

The Atlantic Multidecadal Oscillation (AMO) is also provided in Figure 3. This index, based on the Sea Surface Temperature of the Atlantic Ocean, evolves as part of a 65-80 year cycle that influences the regional climate and has consequences on the ocean circulation in the North Atlantic (e.g., Kerr, 2000). In 2019, the AMO was normal for a second year in a row.

Air temperature anomalies (winter and annual values) from five coastal communities around the Northwest Atlantic (Nuuk Greenland, Iqaluit Baffin Island, Cartwright Labrador, Bonavista and St. John's Newfoundland) are shown in Figure 3 as normalized anomalies between 1980 and 2019, and in Figure 4 and Figure 5 as cumulative annual and monthly anomalies, respectively. Except for Nuuk for which data are obtained from the Danish Meteorological Institute, the air temperature data from Canadian sites are from the second generation of Adjusted and Homogenized Canadian Climate Data (AHCCD) that accounts for shifts in station location and changes in observation methods (Vincent et al., 2012).

On average, winter values in 2019 were normal for the three southern sites, but above normal for Iqaluit and Nuuk (+0.8 and +1.0 SD, respectively). The annual values show similar trends with normal values at the three southern sites, but above normal for Iqaluit and Nuuk (+1.3 and +1.2 SD, respectively). The predominance of warmer-than-normal air temperatures at all sites from the mid-1990s to 2013 is evident, where values in

2010 at Cartwright and Iqaluit reached 2.5 and 2.7 SD above normal setting 77 and 65 year records, respectively. Figure 4 shows that the cumulative annual air temperature index was above normal for the two northern sites, with monthly average temperatures in Iqaluit being 3.6°C to 4.6°C above normal for 5 months out of 12 in 2019 (Figure 5). In contrast, temperature in Newfoundland (Bonavista and St. John's) were colder than average in February, and between May to July.

Annual air temperature anomalies for six sites in the Scotian Shelf-Gulf of Maine region (location in Figure 1) are shown in Figure 6 and Table 1. In 2019, the mean annual air temperature anomalies were negative or normal at all sites with anomalies ranging from -0.6 to 0.0 SD. Boston was 1.7 SD above the climatology. The time series of annual anomalies indicates that all sites have increasing temperatures over the long term with decadal scale variability superimposed. Over shorter periods, there are times when there is no trend or a decreasing trend in the temperature. Linear trends from 1900 to present for Sydney, Sable Island, Halifax, Yarmouth, Saint John and Boston correspond to changes (and 95% confidence limits) per century of +0.6°C (+0.4°C, +0.9°C), +1.3°C (+1.0°C, +1.6°C), +1.1°C (+0.8°C, +1.3°C), +1.0°C (+0.8°C, +1.2°C), +1.0°C (+0.8°C, +1.3°C) and +2.5°C (+2.2°C, +2.7°C), respectively.

The anomalies for all 6 sites are displayed in Figure 7 as a composite sum and illustrate two points: 1) In the 120 year time series shown, 2019 was the 31st warmest year for the region as a whole (with 2012 being the warmest). For most years the anomalies have the same sign. Since 1900, 96 of the 120 years had five or more stations with the annual anomalies having the same signs; for 67 years, all six stations had anomalies with the same sign. This indicates that the spatial scale of the air temperature patterns is greater than the largest spacing among sites.

	80	81	82	83	84	85	86	87	88	89	90	91	92	93	94	95	96	97	98	99
-- Climate indices --																				
NAO_{winter}	0.0	0.2	0.3	0.9	0.6	-0.5	0.5	-0.2	0.5	1.4	0.7	0.5	0.6	0.8	1.1	1.3	-0.5	0.3	0.0	0.5
AO	-0.6	-0.4	0.3	0.0	-0.2	-0.5	0.1	-0.5	0.0	1.0	1.0	0.2	0.4	0.1	0.5	-0.3	-0.5	0.0	-0.3	0.1
AMO	0.0	-0.1	-0.2	-0.1	-0.2	-0.3	-0.3	0.1	0.0	-0.1	-0.1	-0.1	-0.2	-0.2	-0.2	0.1	-0.1	0.0	0.4	0.1
-- Winter Air Temperature --																				
Nuuk	0.8	0.3	0.2	-2.1	-2.5	0.5	1.8	-0.1	0.4	-0.8	-0.3	-0.7	-0.9	-1.7	-0.4	-0.8	0.5	0.2	0.1	-0.1
Iqaluit	0.6	0.9	1.0	-1.8	-1.6	0.8	1.7	-0.9	-0.1	-1.3	-0.8	-1.3	-0.6	-1.7	-0.5	0.1	0.4	0.3	-0.4	0.1
Cartwright	0.5	1.0	0.3	-1.2	-0.9	-0.1	0.2	-0.1	0.1	-1.2	-1.2	-1.3	-1.5	-1.4	-1.0	-0.7	0.7	0.3	0.8	0.5
Bonavista	0.2	0.9	0.0	0.1	0.0	-0.7	-0.1	-0.5	0.2	-1.1	-2.0	-1.1	-1.5	-1.9	-1.5	-0.6	0.8	0.1	0.5	1.1
StJohns	-0.3	0.9	0.0	0.8	0.6	-0.6	-0.1	-0.9	0.0	-1.4	-2.1	-1.1	-1.6	-1.5	-1.2	-0.8	0.4	0.2	0.3	1.3
-- Annual Air Temperature --																				
Nuuk	0.6	0.1	-1.1	-1.8	-2.0	1.2	0.1	0.0	0.3	-1.2	-0.7	-0.4	-1.4	-1.6	-0.6	-0.3	0.4	0.1	0.2	0.0
Iqaluit	0.6	1.3	-0.8	-1.5	-1.1	1.1	-0.7	-0.7	-0.1	-1.1	-1.2	-0.5	-1.7	-1.7	-0.4	0.5	0.5	0.3	0.2	0.1
Cartwright	-0.1	1.1	-1.3	-0.5	-1.1	-0.6	-0.9	0.5	-0.3	-0.6	-1.3	-1.6	-1.4	-1.3	-0.6	-0.3	0.5	-0.3	0.6	1.1
Bonavista	-1.0	0.7	-1.0	0.1	-0.4	-1.4	-0.9	-0.2	0.2	-0.2	-0.6	-1.8	-1.8	-1.8	-0.7	-0.7	0.6	-0.9	0.6	1.5
StJohns	-1.2	1.0	-1.0	0.5	0.2	-1.7	-1.0	-0.5	0.2	-0.6	-0.5	-1.4	-1.7	-1.5	-0.5	-0.7	0.3	-1.1	0.6	1.9

	00	01	02	03	04	05	06	07	08	09	10	11	12	13	14	15	16	17	18	19	$\bar{x}$	sd
-- Climate indices --																						
NAO_{winter}	1.2	-0.3	0.4	0.0	0.3	0.2	-0.2	0.6	0.5	0.1	-1.5	-0.4	1.3	-0.4	0.8	1.6	1.2	0.7	0.7	0.7		
AO	0.0	-0.2	0.1	0.2	-0.2	-0.4	0.1	0.3	0.2	-0.3	-1.0	0.5	-0.2	0.0	-0.1	0.6	-0.1	0.3	0.2	0.6		
AMO	0.0	0.1	0.0	0.2	0.2	0.3	0.3	0.1	0.1	0.0	0.3	0.1	0.2	0.2	0.1	0.1	0.3	0.3	0.1	0.1		
-- Winter Air Temperature --																						
Nuuk	0.2	0.3	0.3	0.8	1.2	0.4	0.6	0.9	-1.0	0.6	1.9	1.1	0.1	0.6	0.3	-0.6	0.2	0.2	-0.2	1.0	-7.7	3.0
Iqaluit	0.4	0.5	0.1	0.5	0.9	-0.3	0.6	1.3	-0.7	0.2	2.3	2.2	0.8	0.8	0.7	-0.8	0.3	0.5	0.3	0.8	-25.0	3.4
Cartwright	0.3	0.0	0.4	0.3	1.8	0.0	0.7	0.9	-0.8	0.2	2.9	2.2	0.1	0.9	-0.7	-1.2	0.4	-0.1	0.3	-0.2	-12.3	2.5
Bonavista	1.3	0.0	0.6	-0.6	1.2	0.7	1.8	0.3	-0.2	0.7	1.4	2.3	1.0	0.9	-1.0	0.4	1.0	0.3	1.4	-0.4	-3.5	1.3
StJohns	1.5	-0.6	0.3	-0.6	1.0	0.7	1.7	0.3	0.0	1.1	1.3	2.5	1.2	0.7	-0.7	0.7	1.0	0.3	1.5	-0.4	-3.7	1.2
-- Annual Air Temperature --																						
Nuuk	0.4	0.7	0.2	1.2	0.6	1.1	0.8	0.6	0.2	0.5	2.6	-0.2	1.0	0.7	0.4	-1.0	1.1	0.4	-0.5	1.2	-1.4	1.5
Iqaluit	0.4	0.6	-0.1	0.8	0.1	0.9	1.4	0.2	-0.1	0.5	2.7	0.5	0.6	0.2	0.4	-1.2	0.4	0.7	-0.2	1.3	-9.1	1.8
Cartwright	0.5	0.6	-0.3	0.4	1.1	0.9	1.8	0.1	0.1	0.4	2.5	0.7	1.4	0.5	0.0	-1.2	-0.3	0.2	-0.2	0.1	0.1	1.3
Bonavista	0.8	0.6	-0.1	0.5	1.0	1.2	1.7	0.0	0.7	0.5	1.6	0.8	1.7	1.1	0.5	-0.5	0.6	0.1	0.8	-0.3	4.7	0.9
StJohns	1.0	0.3	-0.4	0.4	0.6	0.7	1.6	-0.1	0.8	0.9	1.7	0.6	2.3	0.8	0.4	-0.7	0.7	0.4	0.4	-0.4	5.0	0.8

Figure 3. Scorecard of standardized air temperature anomalies (winter and annual) from 1980 to 2019.

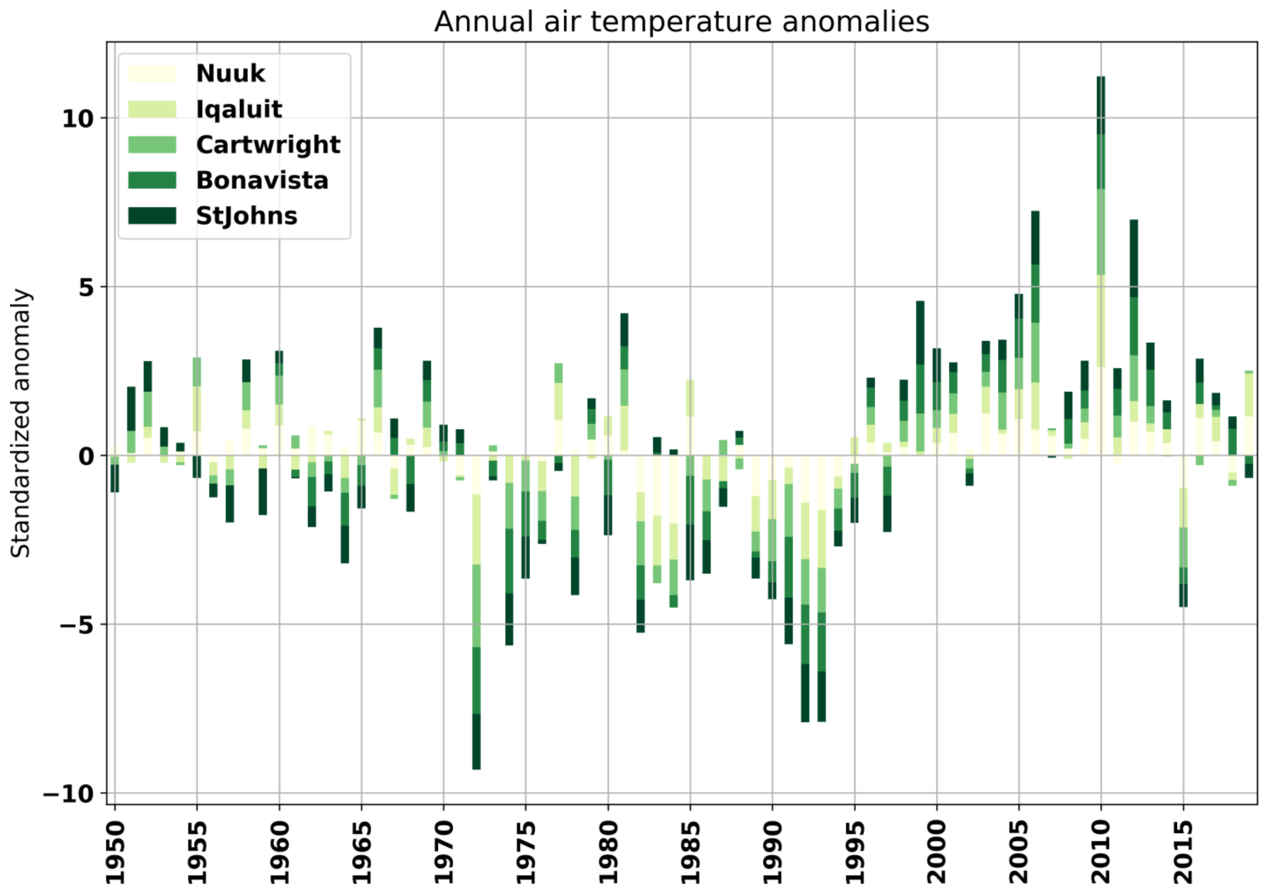

Figure 4. Cumulative standardized annual air temperature anomalies time series at Nuuk, Iqaluit, Cartwright, Bonavista and St. John's.

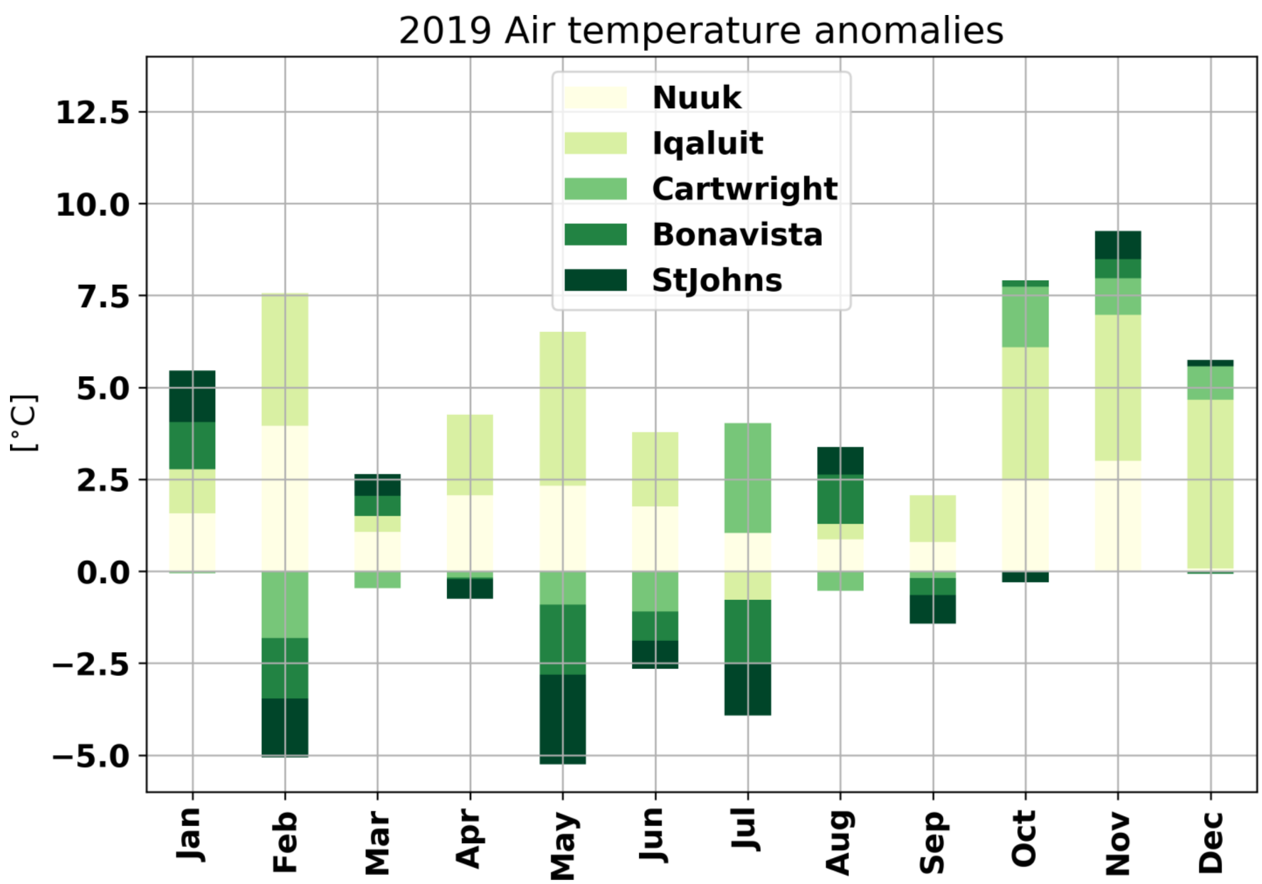

Figure 5. Cumulative monthly air temperature anomalies at Nuuk, Iqaluit, Cartwright, Bonavista and St. John's for 2019.

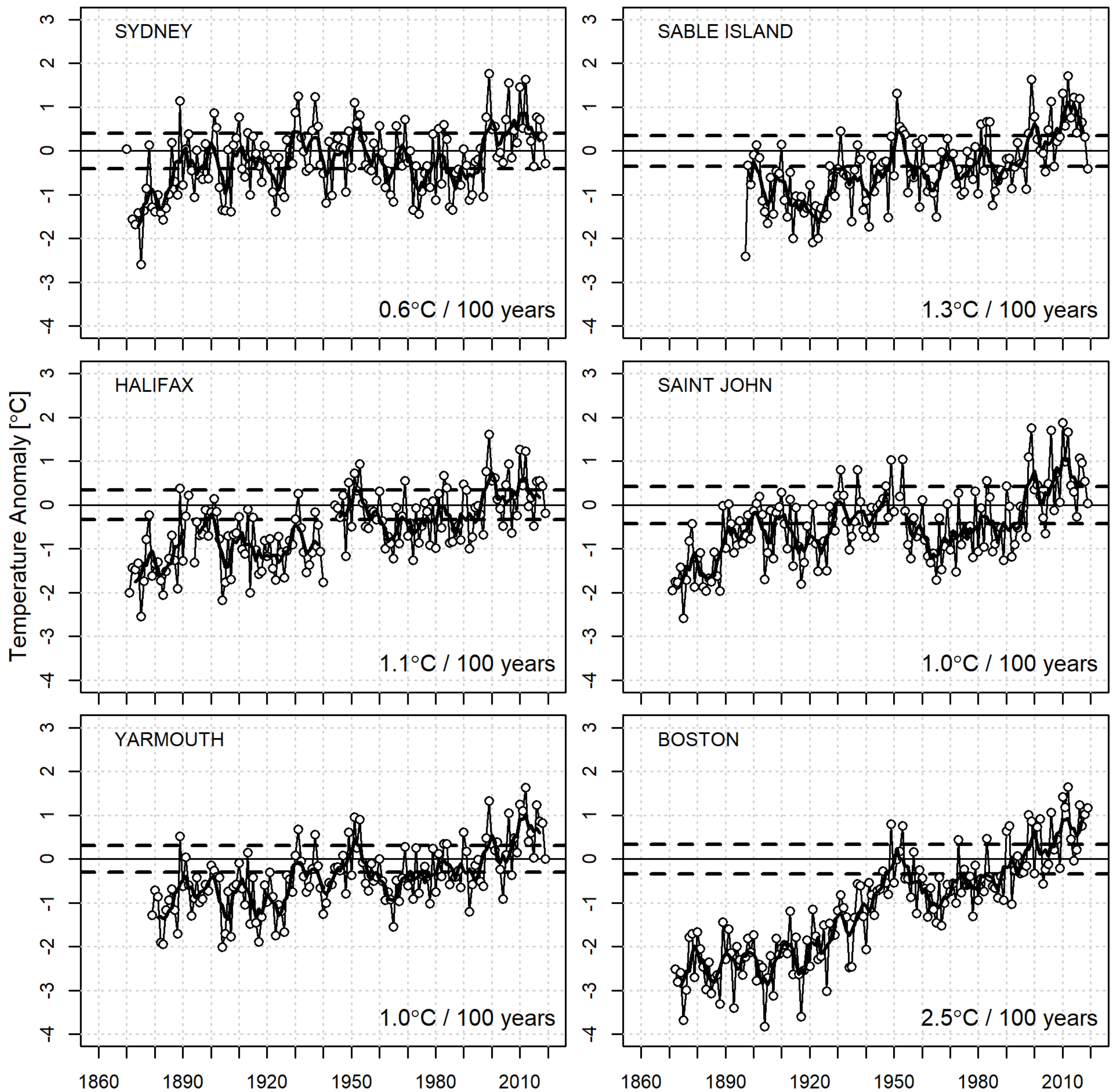

Figure 6. Annual air temperature anomalies in °C (dashed line) and five year running means (solid line) at selected sites (Sydney, Sable Island, Shearwater, Yarmouth, Saint John and Boston) in Scotian Shelf-Gulf of Maine region (years 1860 to 2018). Horizontal dashed lines represent the1981-2010 climatological average ±0.5 SD.

Table 1. The 2019 annual mean air temperature anomaly in degrees and standardize anomaly (relative to the 1981-2010 climatology) for Scotian Shelf and Gulf of Maine.

Site	Annual Anomaly		1981-2010 Climatology	
	Observed (°C)	Normalized	Mean (°C)	SD (°C)
Sydney	-0.3	-0.4	5.87	0.81
Sable Island	-0.4	-0.6	7.88	0.68
Shearwater (Halifax)	-0.2	-0.3	6.99	0.74
Yarmouth	0.0	0.0	7.16	0.62
Saint John	0.0	0.0	5.19	0.74
Boston	+1.2	+1.7	10.91	0.60

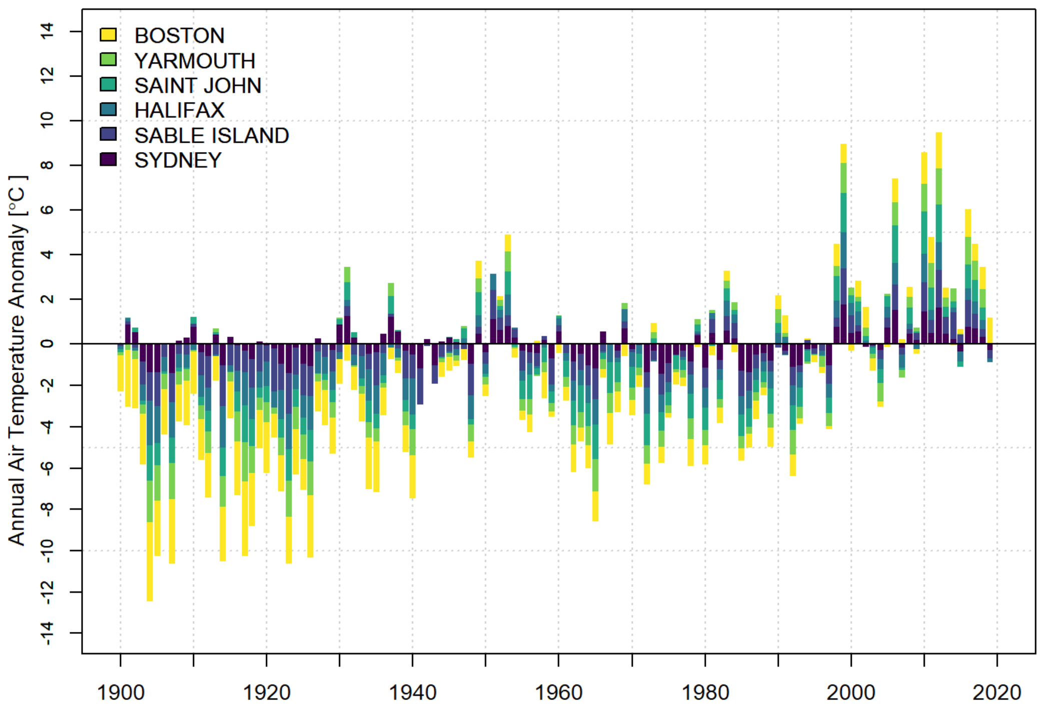

Figure 7. The contributions of each of the annual temperature anomalies for 6 Scotian Shelf-Gulf of Maine sites (Boston, Saint John, Yarmouth, Shearwater, Sable Island and Sydney) are shown as a stacked bar. Anomalies are referenced to the 1981-2010 period.

Sea-Ice Conditions

Ice cover area, volume and seasonal duration are estimated from ice cover products obtained from the Canadian Ice Service (CIS). These parameters consist of weekly Geographic Information System (GIS) charts covering the period 1969-2019 and daily charts covering the period 2009-2019. All charts were further processed into regular 0.01° latitude by 0.015° longitude grids (approximately 1 km resolution), with ice concentrations and growth stages attributed to each grid point. Average thicknesses (and therefore regional volumes) are estimated from standard thicknesses attributed to each stage of ice growth from new ice and nilas (5 cm), grey ice (12.5 cm), grey-white ice (22.5 cm), thin first year ice (50 cm), medium first year ice (95 cm) and thick first year ice (160 cm). Prior to 1983, the CIS reported ice categories with fewer classifications, where a single category of first year ice (≥ 30 cm) was used with a suggested average thickness of 65 cm. We have found this value to lead to underestimates of the seasonal maximum thickness and volume based on high interannual correlations between the estimated volume of the weekly seasonal maximums and its area or sea-ice season duration. The comparisons of these correlations pre- and post-1983 provided estimates of first-year ice thickness of 85 cm in the Gulf of St. Lawrence and 95 cm on the Newfoundland and Labrador Shelf for this single first year ice category, which were used instead of the suggested 65 cm.

Several products were computed to describe the sea-ice cover inter-annual variability. The day of first and last occurrence, ice season duration (Figure 8) and distribution of ice thickness during the week of maximum volume (Figure 9) are presented as maps. Regional scorecards of anomalies in the first and last day of ice, duration of the sea ice season and maximum ice volume are presented in Figure 10 for the Labrador and Newfoundland shelves. Here, the area defined as Labrador shelf spans from 52° 15’ N to 55° 20’ N, matching the latitude limits of NAFO Division 2J, and the area defined as the Newfoundland Shelf is to the south. Daily evolution of the ice volume during the 2019 ice season is presented in Figure 11 for Labrador (left) and Newfoundland (right) shelves in relation to the climatology and historical extremes. Time series of seasonal maximum ice volume, area (excluding thin new ice) and ice season duration in relation to the December-to-April air temperature anomaly at Cartwright are presented for Labrador (top) and Newfoundland (bottom) shelves in Figure 12

Ice typically starts forming in December along the Labrador coast and only by late February at the southern extent of sea-ice presence (Figure 8). Last occurrence is typically in late June to early July on the Labrador coast, leading to sea-ice season durations of 23 weeks or more. There has been a declining trend in ice cover severity since the early 1990s reaching the lowest values in 2011 and 2010, with a rebound in 2014 (Figure 10 and Figure 12). On the Newfoundland Shelf, the sea ice metrics of annual maximum ice area, volume, and ice cover duration are well correlated with each other (R^2 = 0.70 to 0.77; Figure 12). The best correlation with air temperature was found between the December-April air temperature anomaly at Cartwright and the sea-ice metrics of the Newfoundland Shelf (R^2 = 0.65-0.81), indicative of the advective nature of the Newfoundland Shelf sea ice; i.e. strong ice cover is associated with cold air temperatures in the source area. Sensitivity of the Newfoundland Shelf ice cover to air temperature increase (e.g. through climate change) can thus be estimated using 1969-2019 co-variations between winter air temperature and sea-ice parameters, which indicate losses of 15 km^3, 26,000 km^2 and 9 days of sea-ice season for each 1°C increase in winter air temperature.

In 2019, the sea-ice cover first appeared at a date ranging from near-normal to later than normal by a few weeks (Figure 8) leading to regional average that was near normal on the Labrador Shelf and slightly later than normal on the Newfoundland Shelf (Figure 10). Last occurrence varied between earlier than normal on the shelves to later than normal at the edge of the distribution (Figure 8), averaging to near-normal timing (Figure 10). Sea ice volume progressed mostly below normal until late March on the Labrador Shelf, and up to late February on the Newfoundland Shelf (Figure 11). The ice cover declined sharply on the Newfoundland Shelf in March. It also declined sharply on the Labrador Shelf in April but rebounded somewhat by late April. The seasonal maximum combined ice volume was below normal at 72 km^3 (-1.2 SD) during the week of March 11th (Figure 8) which is a bit early. The durations of 168 and 101 days on the Labrador and Newfoundland Shelves respectively were normal and slightly below-normal (-0.5 SD).

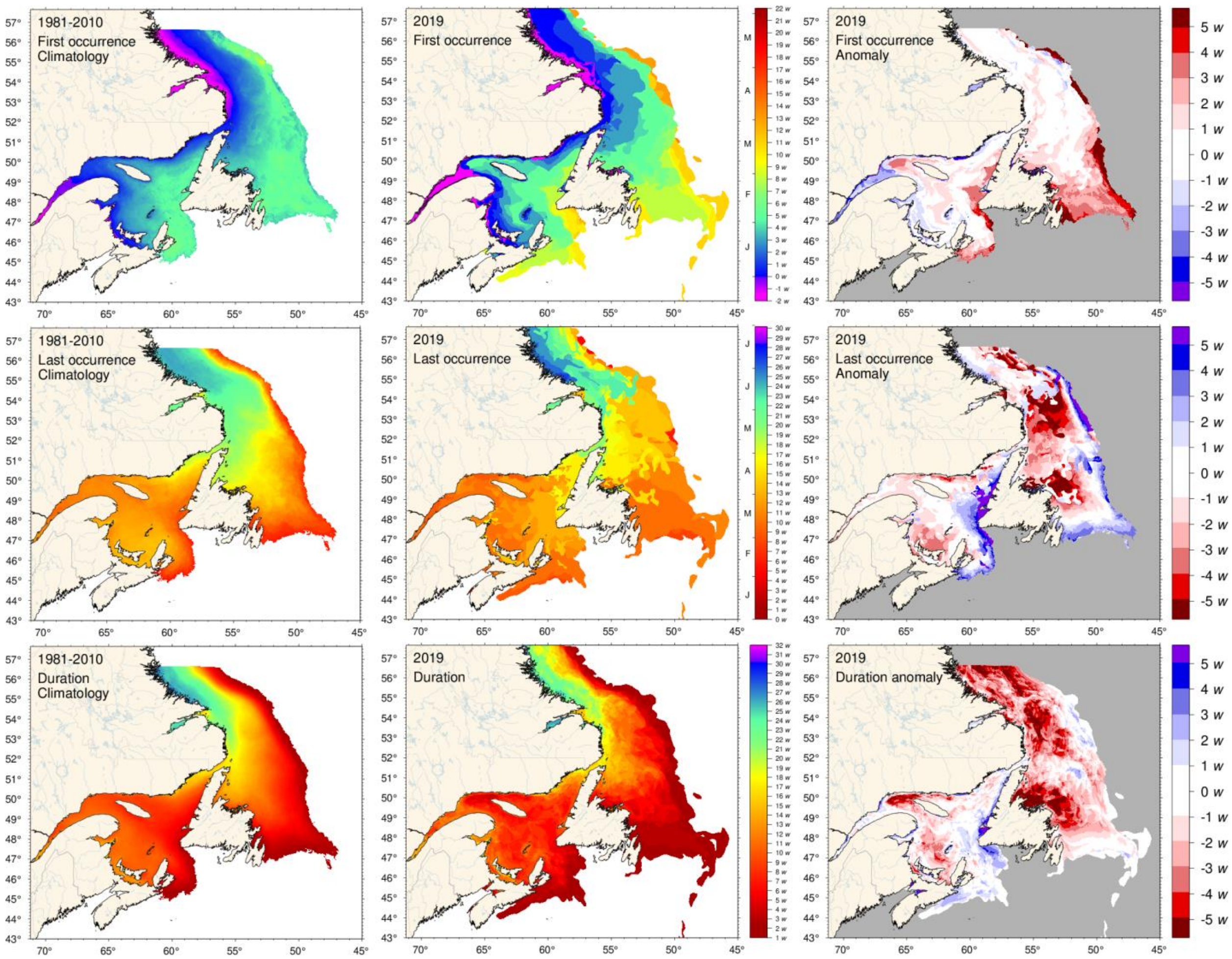

Figure 8. First (top) and last (middle) occurrence of ice and ice season duration (bottom) based on weekly data. The 1981-2010 climatologies are shown (left) as well as the 2019 values (middle) and anomalies (right). First and last occurrences are defined here as the first and last weekly chart in which any amount of ice is recorded for each pixel and are illustrated as day-of-year. Ice duration sums the number of weeks with ice cover for each pixel. Climatologies are shown for pixels that had at least 15 years out of 30 with occurrence of sea-ice, and therefore also show the area with 50% likelihood of having some sea-ice at any time during any given year. The duration

anomaly map includes pixels with no ice cover where some was expected based on the climatology.

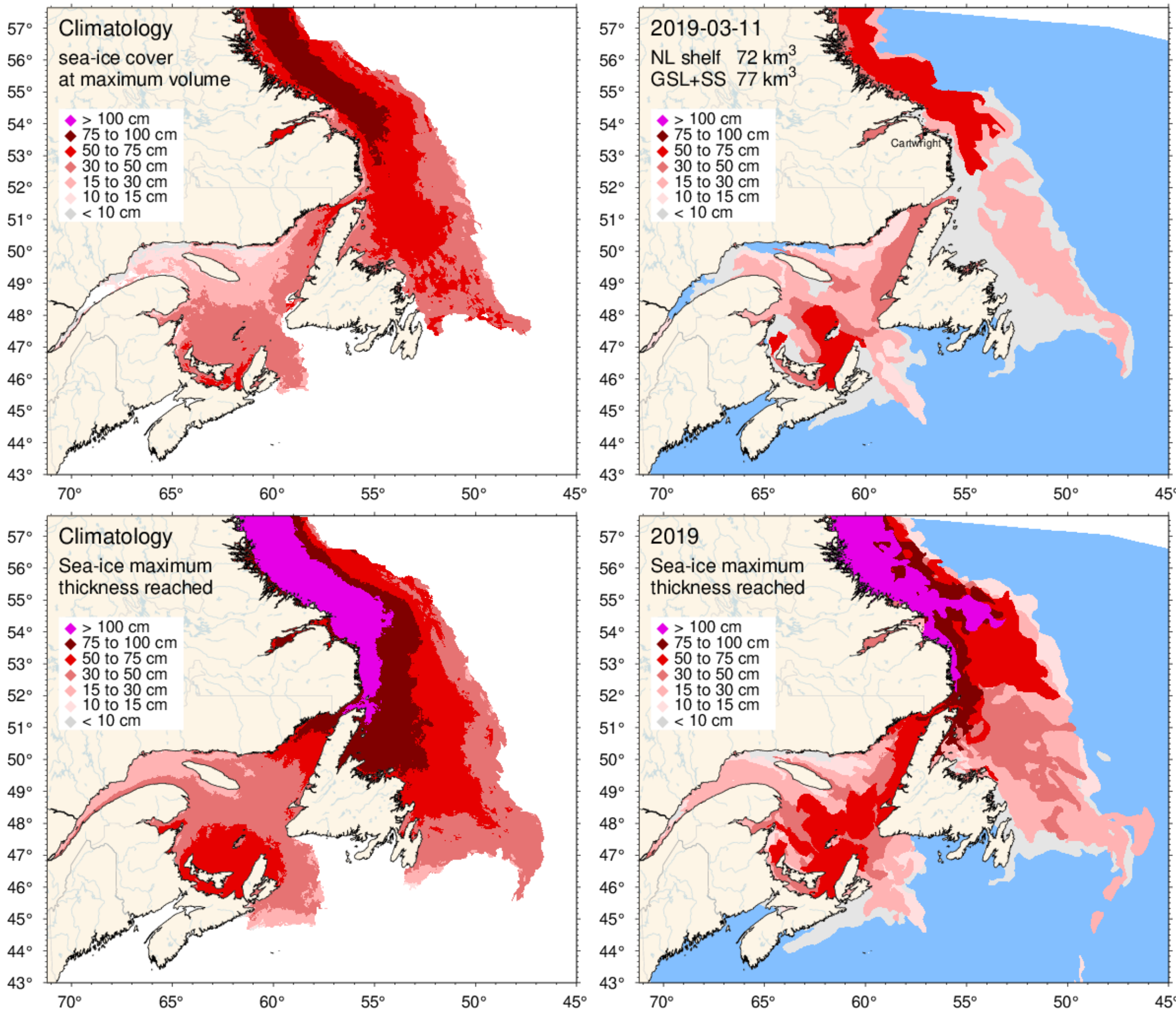

Figure 9. Ice thickness map for 2019 for the week with the maximum annual volume on the Newfoundland and Labrador Shelf (upper right panel) and similarly for the 1981-2010 climatology of the weekly maximum (upper left panel). Note that these maps reflect the ice thickness distribution on that week. The maximum ice thickness observed at any given location during the year is presented in the lower panels, showing the 1981-2010 climatology and 2019 distribution of the thickest ice recorded during the season at any location.

.

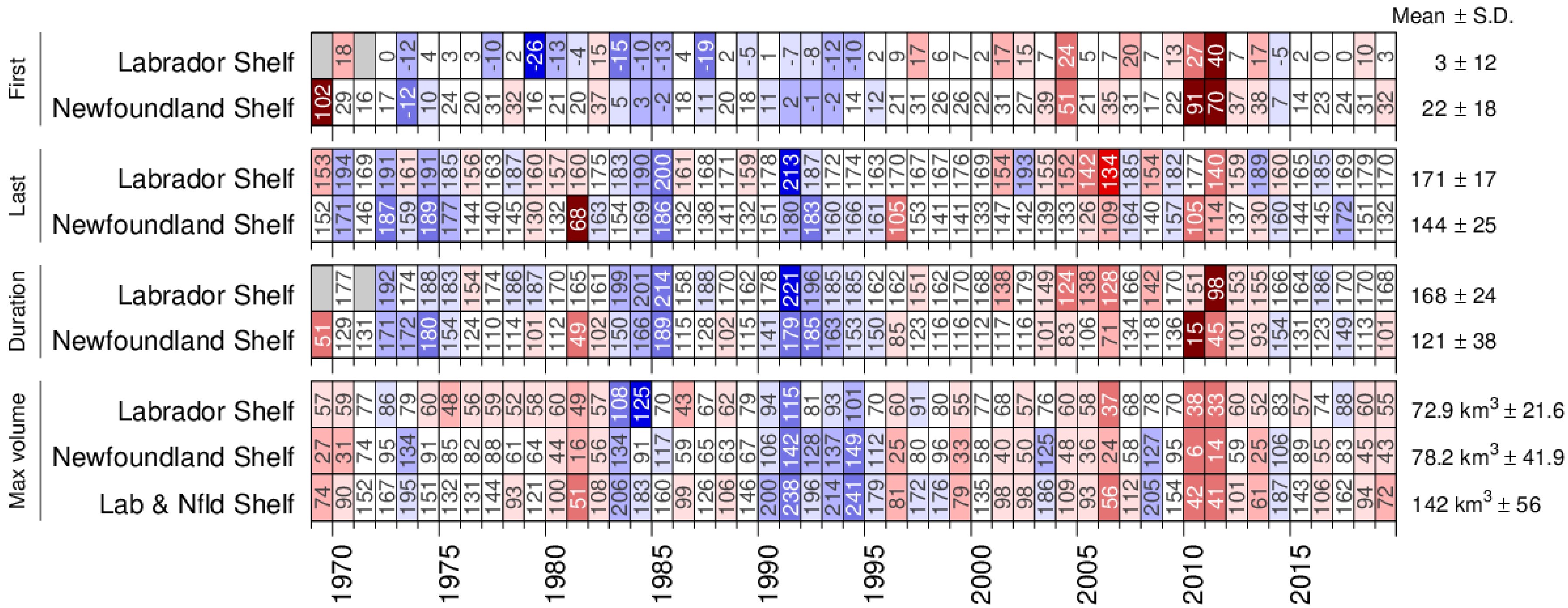

Figure 10. First and last day of ice occurrence, ice duration, and maximum seasonal ice volume by region. The moment when ice was first and last observed in days from the beginning of each year is indicated for each region, and the color code expresses the anomaly based on the 1981–2010 climatology, with blue (cold) representing earlier first occurrence and later last occurrence. The threshold is 5% of the climatological average of the seasonal maximum ice volume. Numbers in the table are the actual day of the year or volume, but the color coding is according to normalized anomalies based on the climatology of each region. Duration is the numbers of days that the threshold was exceeded.

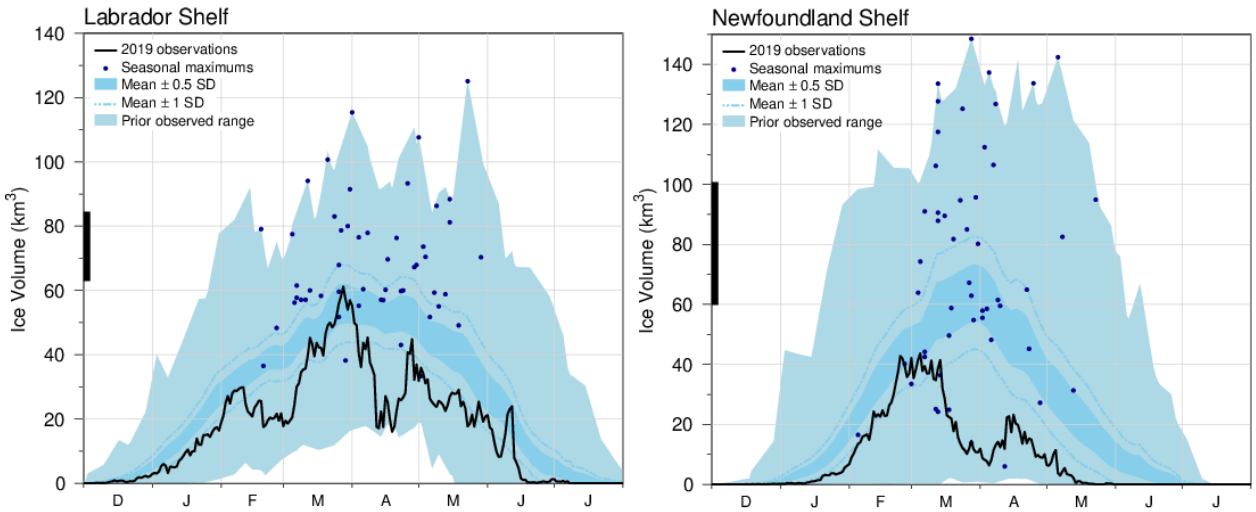

Figure 11. Time series of the 2018-2019 daily mean ice volume (black lines) for the Labrador Shelf (left) and Newfoundland Shelf (right), the 1981-2010 climatological mean volume ±0.5 and ±1 SD (dark blue area and dashed line respectively), the minimum and maximum span of 1969-2019 observations (light blue), and the date and volumes of 1969-2019 seasonal maximums (blue dots). The black thick line on the left indicates the mean volume ±0.5 SD of the annual maximum ice volume, which is higher than the peak of the mean daily ice volume distribution.

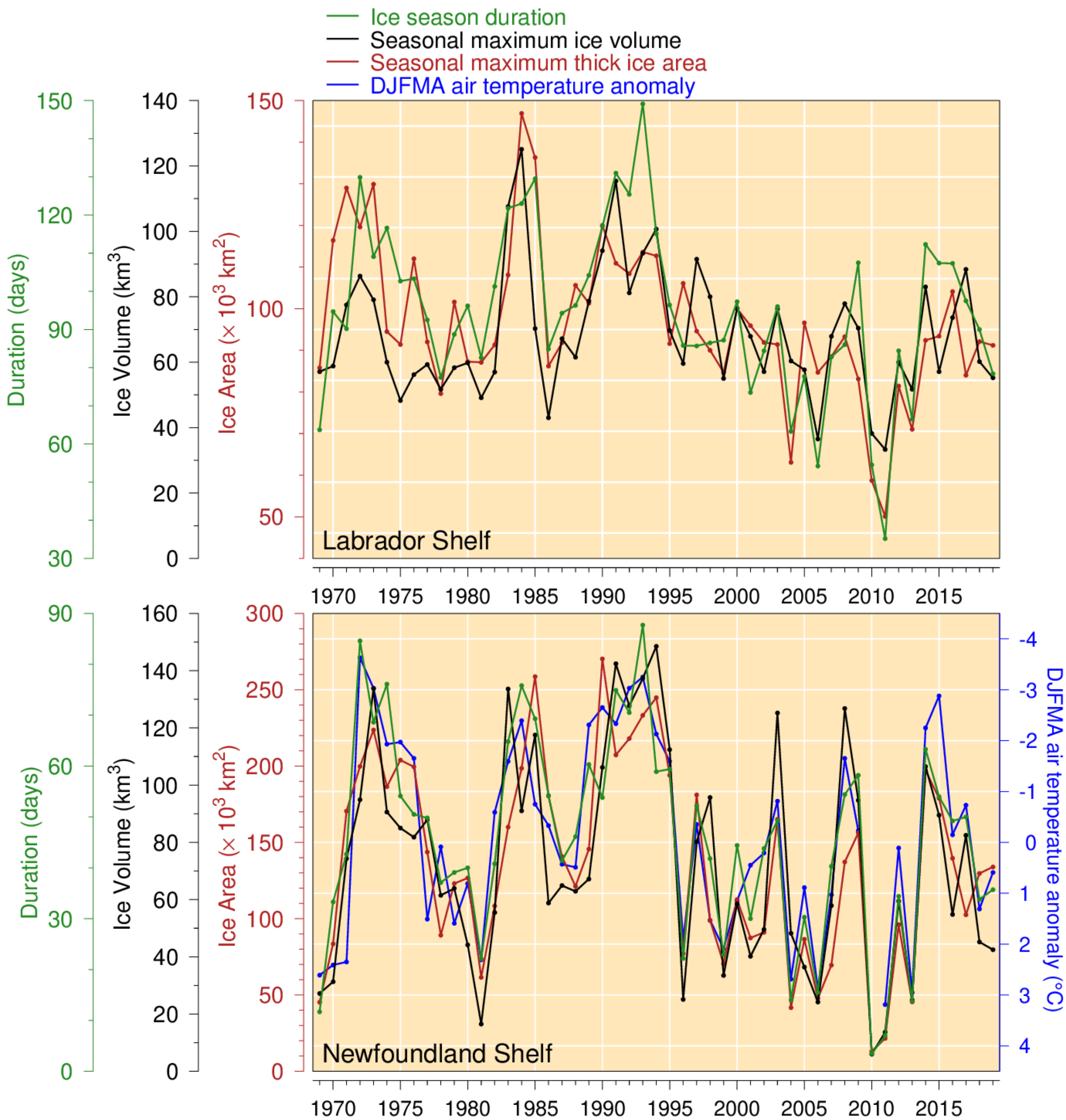

Figure 12. Seasonal maximum ice volume and area (excluding ice less than 15 cm thick), and ice season duration for the Labrador Shelf (top) and Newfoundland Shelf (bottom), and December-to-April air temperature anomaly at Cartwright.

Satellite Sea-Surface Temperature Conditions

Sea Surface Temperatures (SSTs) used here is a blend of data from Pathfinder version 5.3 (1982-2014), Maurice Lamontagne Institute (1985-2013) and Bedford Institute of Oceanography (1997-2019) and monthly temperature composites are based on averaged daily anomalies to which monthly climatological average temperatures are added (see Galbraith et al. 2020 for details). This eliminates the bias that would occur when averaging temperature data that are not evenly distributed. A difference from Galbraith et al. (2020) is that the coverage was extended northward and eastward to include NAFO Divisions 2G, 2H and 3M. In addition, because of the general differences of SST patterns, Division 4V was split into north and south portions (4Vn and 4Vs) and 4X was split into the Scotian Shelf (4X SS) and Gulf of Maine and Bay of Fundy (4X eGoM+BoF).

Averaged over ice-free periods of the year as short as June to November on the Labrador Shelf, May to November in the Gulf, to the entire year on the Scotian Shelf, air temperature has been found to be a good proxy of sea surface temperature, and the warming trend observed in air temperature since the 1870s of about 1°C per century is also expected to have occurred in surface water temperatures across Atlantic Canada (Galbraith et al. 2020). The Zone experienced its warmest surface temperatures in 2012 when all regions had positive anomalies over ice-free months, with records reached in the Bay of Fundy-Gulf of Maine (4X eGoM+BoF), Scotian Shelf (4X SS, 4W, 4Vn, 4Vs), St. Pierre Bank (3P) and Flemish pass (3M).

In 2019, monthly average SSTs were generally below normal to normal in ice-free months until July, including record lows (since 1982) in May in NAFO Divisions 3P and 4V (Figure 13 to Figure 15). They were normal to above normal for the seasonal maximum reached in August, but decreased remarkably with the passage of tropical storm Dorian in early September. The 100+ km/h winds mixed the water column to depths as high as 45 m-decreasing surface temperatures by as much as 8°C and increasing it equally at depth (Galbraith et al. 2020). September average surface temperatures were at record lows in the Gulf of St. Lawrence and well as on St. Pierre Bank and the Scotian Shelf (NAFO Divisions 3P, 4V and 4W), but not because of heat lost to the atmosphere but rather because of redistribution within the water column. Surface temperatures remained stable in the thick mixed layer until air temperatures cooled to below water temperatures. Surface temperatures were above normal in November on the Scotian Shelf and Gulf of Maine-Bay of Fundy.

Sea-surface temperatures were normal to above normal on the Labrador Shelf and the northern Newfoundland Shelf, but varied from below normal to normal elsewhere (Figure 15). On average across the zone, seasonal sea-surface temperatures were below normal for the first time since 1992 (Figure 16, scorecard at the bottom). However, the zonal average would have been near-normal had it not been for tropical storm Dorian.

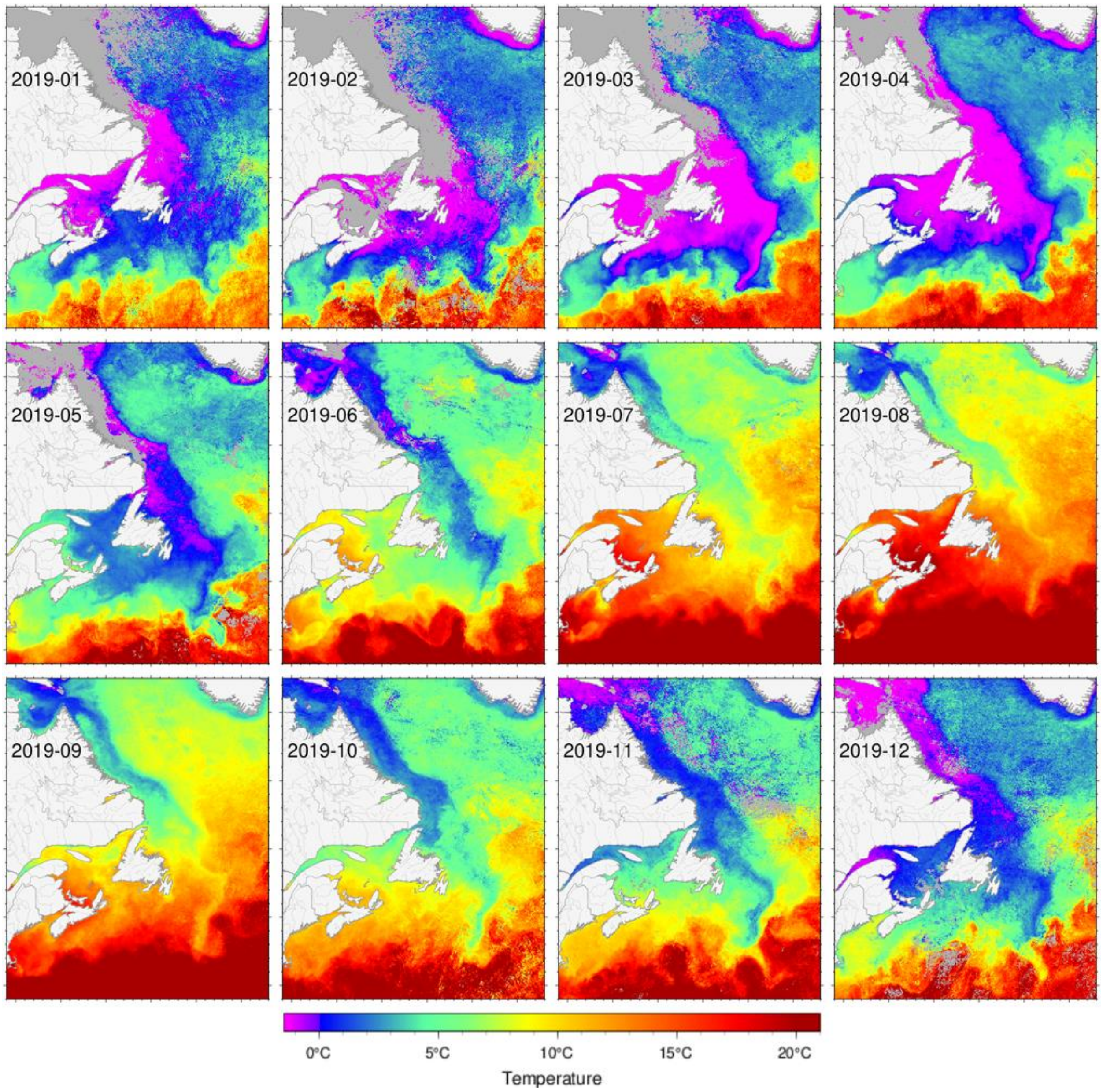

Figure 13. Sea-surface temperature monthly averages for 2019 in the Atlantic zone.

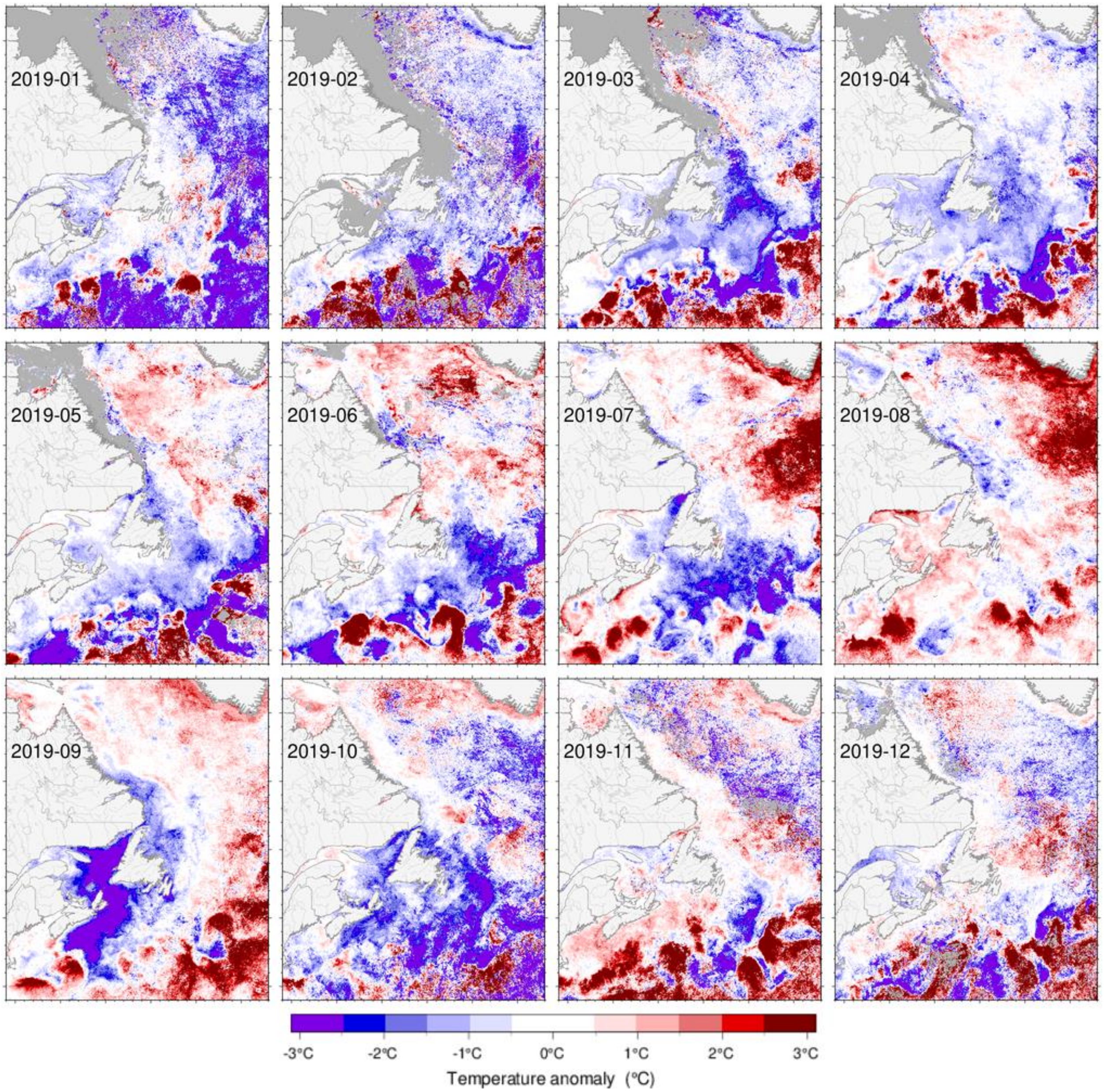

Figure 14. Sea-surface temperature monthly anomalies for 2019 in the Atlantic zone. Temperature anomalies are based on a 1982-2010 climatology.

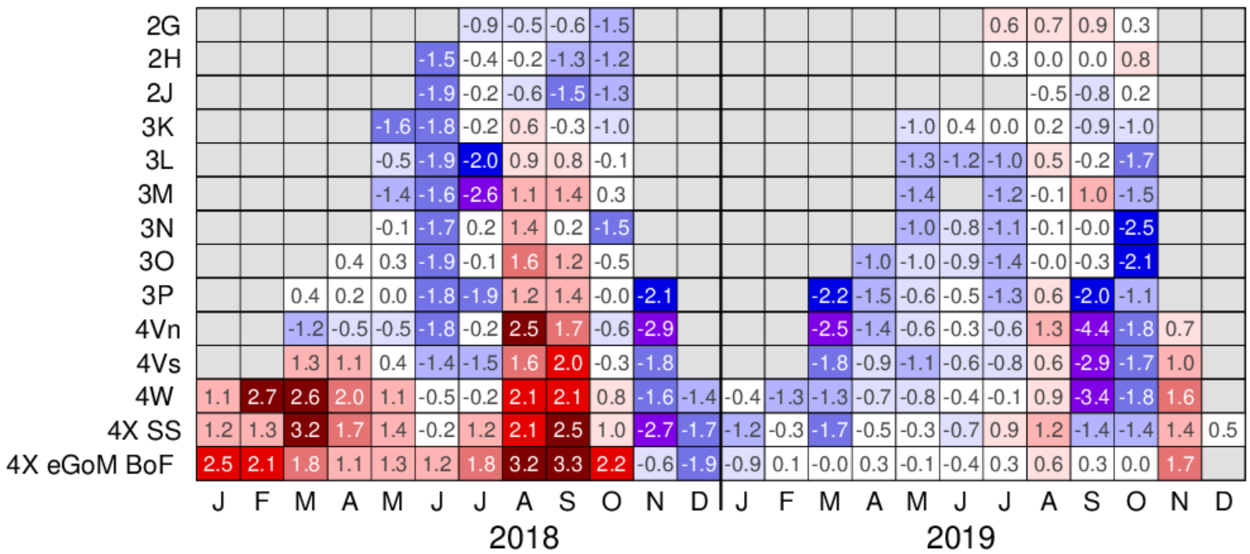

Figure 15. Monthly standardized anomalies of SST for NAFO subareas 2, 3 and 4 during 2018 and 2019. The area used for each division is limited to the continental shelf (see black contour in Figure 1). Grayed boxes represent months ignored because more than 15% of the pixel were invalid during this month (e.g., ice or fog).

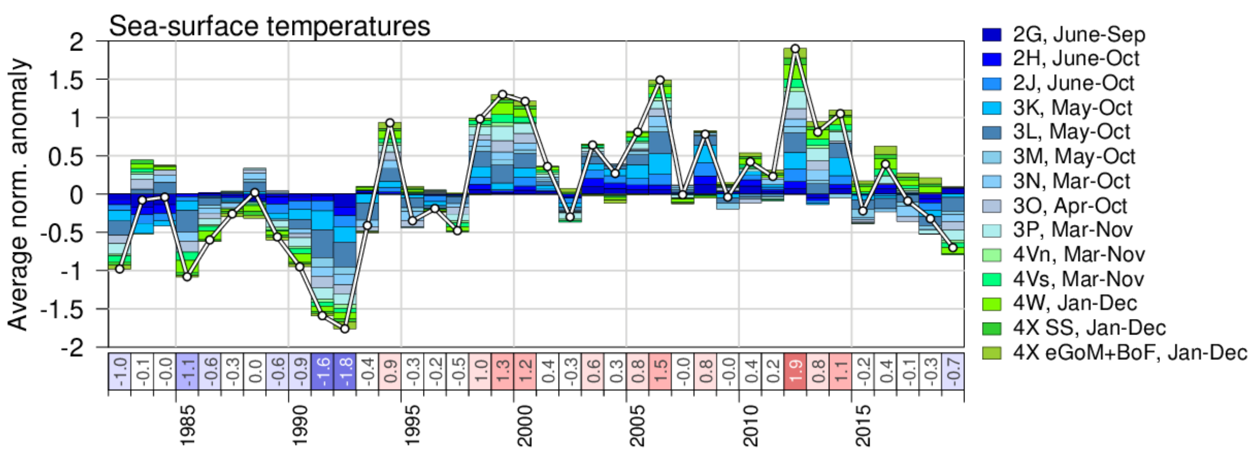

Figure 16. Sea Surface Temperature (SST) composite index in NAFO sub-areas 2 (dark blue), 3 (light blue) and 4 (green) since 1982. This index is built by performing a weighted average of the seasonal SST mean for each NAFO division (divisions and months used are provide on the right-and side of the figure).The scorecard at the bottom of the figure represent the normalized anomaly of the seasonal average.

Ocean Conditions on the Newfoundland and Labrador Shelf (NAFO Sub-areas 2 and 3)

Long-term observations at Station 27

Station 27 (47° 32.8’ N, 52° 35.2’ W), is located in the Avalon Channel off Cape Spear, NL (Figure 1). It is one of longest hydrographic time series in Canada with frequent occupations (near-monthly basis) since 1948. In 2019, the station was occupied 44 times (41 CTD casts, including 22 biogeochemical sampling and 3 XBT). No observations were made in January or February and the first occupation of the year was made on March 30th. Such late first occupation is a recurrent problem since 2016, and 2019 represent the latest first occupation of the station since 1949.

In addition to the traditional hydrographic sampling described above, a total of 262 CTD profiles were collected from an automatic profiling system installed on a surface buoy (type Viking) between June 27th and November 26th 2019. The addition of the Viking buoy to our sampling effort in 2017 really improved our ability to detect short-term variations of ocean properties at Station 27. In 2019, for example, the buoy well captured the rapid cooling and deepening of the isopycnals that occurred during the first half of September as a result of wind-driven mixing cause by tropical storm Dorian.

Station occupation and Viking buoy automatic casts were combined to obtain the annual evolution of temperature and salinity at Station 27, as well as the anomaly compared to the 1981-2010 climatology, shown in Figure 17 and Figure 18. These figures demonstrate the seasonal warming of the top layer (~20m), with temperature peaking in August before being mixed during the fall. The cold intermediate layer (CIL; Petrie et al., 1988), a remnant of the previous winter cold layer and defined as temperature below 0^{o}C (thick black line in Figure 17) is also evident below 100m throughout the summer. The surface layer is generally freshest between early-September and mid-October, with salinities <31 (Figure 18). These low near-surface salinities, generally from early summer to late fall, are a prominent feature of the salinity cycle on the Newfoundland Shelf and is largely due to the melting of coastal sea-ice.

In 2019, the surface layer was colder than normal for most of the spring and early summer, and warmer in October-December (Figure 17). Until the storm Dorian hit the region, waters were saltier than normal in near-surface waters and fresher at depth (Figure 18, bottom). Overall over the year, the vertically averaged temperature and salinity were normal (Figure 19). This contrasts with 2018 that exhibited the second largest fresh anomaly of the time series after 1970, a period commonly referred to as the Great Salinity Anomaly in the North Atlantic (Dickson et al., 1988).

The CIL summer (May-July) statistics at Station 27 since 1950 are presented in Figure 20. The striking feature in this figure is the anomalously warm and thin CIL anomaly present from the early 1960s to the mid-1970s. This anomaly is accentuated by the fact that the climatological reference period (1981-2010) encompasses a rather cold period that spanned the mid-1980s to the mid-1990s. The CIL core depth (last panel) seems uncorrelated to the three other panels that are well correlated between them. After the prevalence of a warm CIL in the early 2010s (with some of the warmest years since the mid-1970s), there has been a cooling trend since about 2014. In 2018 and 2019, however, the CIL was warmer than normal (mean temperature 1.7 SD and 1.2 SD above normal, respectively).

The monthly mean mixed layer depth (MLD) at Station 27 was also estimated from the density profiles as the depth of maximum buoyancy frequency (*N) calculated from the monthly averaged density profiles (ρ(z)) :*

$$N^2 = -\frac{g}{\rho_0}\frac{\Delta\rho(z)}{\Delta z};$$

with g = 9.8 ms^{-2} as the gravitational acceleration, z the depth and ρ_0 as a reference density.

Climatological monthly MLD values, as well as for 2019, are presented in Figure 21. The climatological annual cycle shows a gradual decrease of the MLD between late fall and summer (mixed layer thickest in November-December and shallowest in July-August). In 2019, the MLD was much thicker than normal in May (note that no values are available between January and March) with a mean value of more than 80 m compared to the climatological value of less than 30 m. The MLD was shallower than normal in September and deeper than normal in October. Figure 22 shows a time series of the annual mean values of the MLD (solid gray line) and its 5-year moving average (dashed-black line). In general, there is a strong interannual and decadal oscillation in MLD, with a recent increase since the mid-2000's.

Stratification is an important characteristic of the water column since it influences, for example, the transfer of solar heat to lower layers and the vertical exchange of biogeochemical tracers between the deeper layers and the surface. The seasonal development of stratification is also an important process influencing the formation and evolution of the CIL on the shelf regions of Atlantic Canada. It essentially insulates the lower water column from the upper layers, thus slowing vertical heat flux from the seasonally heated surface layer.

The stratification index at Station 27 is computed from the density (ρ) difference between 5 and 50 m for each monthly average density profiles (i.e. $\Delta\rho/\Delta z$). The annual anomalies are then calculated as the average of monthly anomalies. The 2019 and climatological evolution of the stratification throughout the year are shown in Figure 23 The stratification is generally weakest between December and April, before rapidly increasing at the onset of spring until it peaks in August. In 2019, the stratification was weaker than normal for most of the year. Note however that no data are available for January and February, and that March has been excluded because the only occupation was realized at the end of the month. The interannual evolution of the stratification anomaly since 1950 is shown in Figure 24. While strong decadal variations are observed, a positive trend is distinguishable since the mid-1970s, with the highest annual anomaly since 1950 observed in 2017 (+0.9 SD). In 2019, the annual stratification was weaker than normal at -1.0 SD, a further decrease after -0.7 SD in 2018. A scorecard of annual standardized anomalies since 1980 of all parameters discussed in this section is presented in Figure 25.

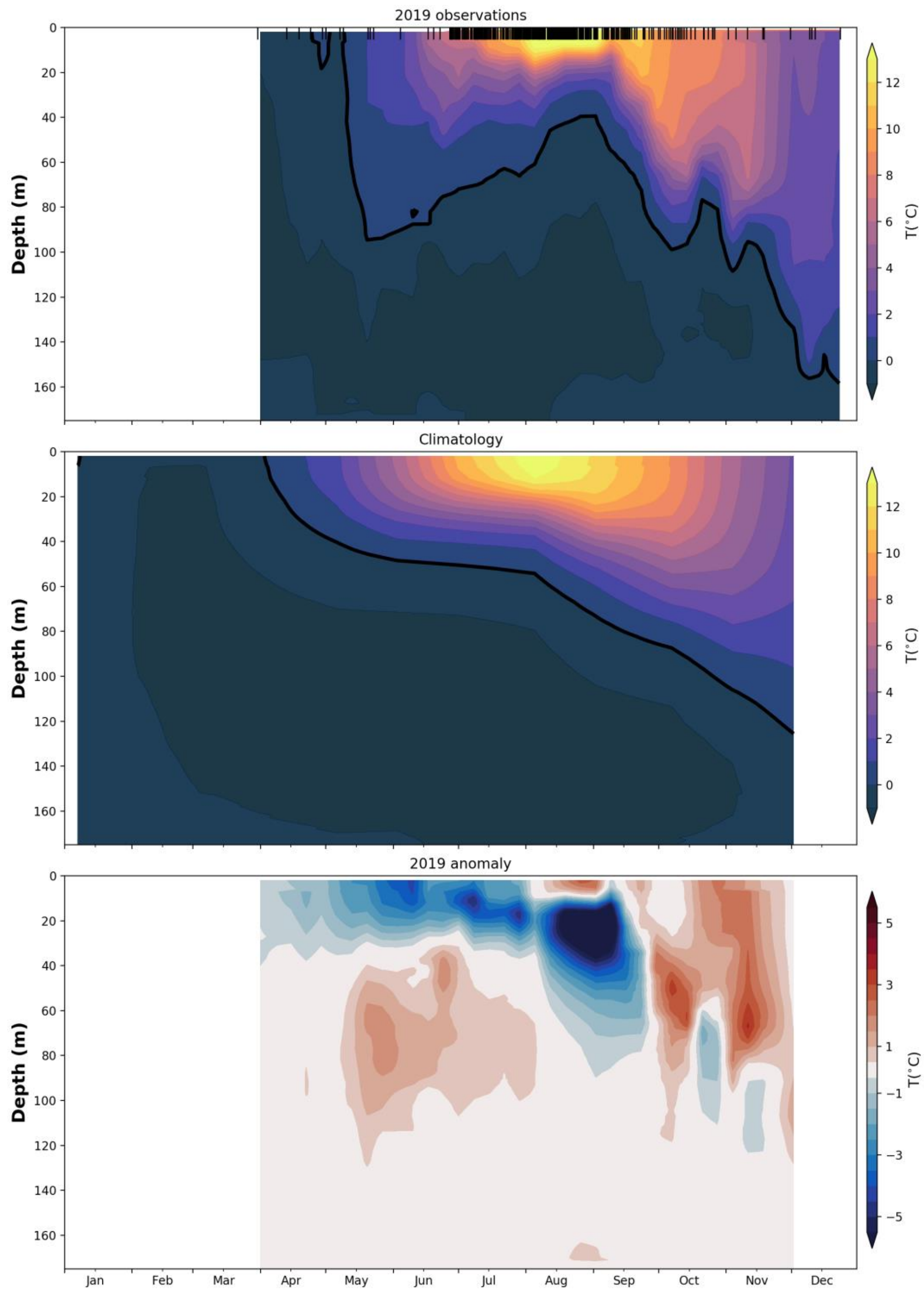

Figure 17. Annual evolution of temperature at Station 27. The 2019 contour plot (top panel) is generated from weekly averaged profiles from all available data, including station occupation and Viking buoy casts (indicated by black tick marks on top of panel). The solid black contour delineates the cold intermediate layer defined as water below 0°C. The 1981-2010 climatology (middle panel)

is plotted from monthly-averaged temperature profiles. The anomaly (bottom panel) is the difference between the 2019 field and the climatology.

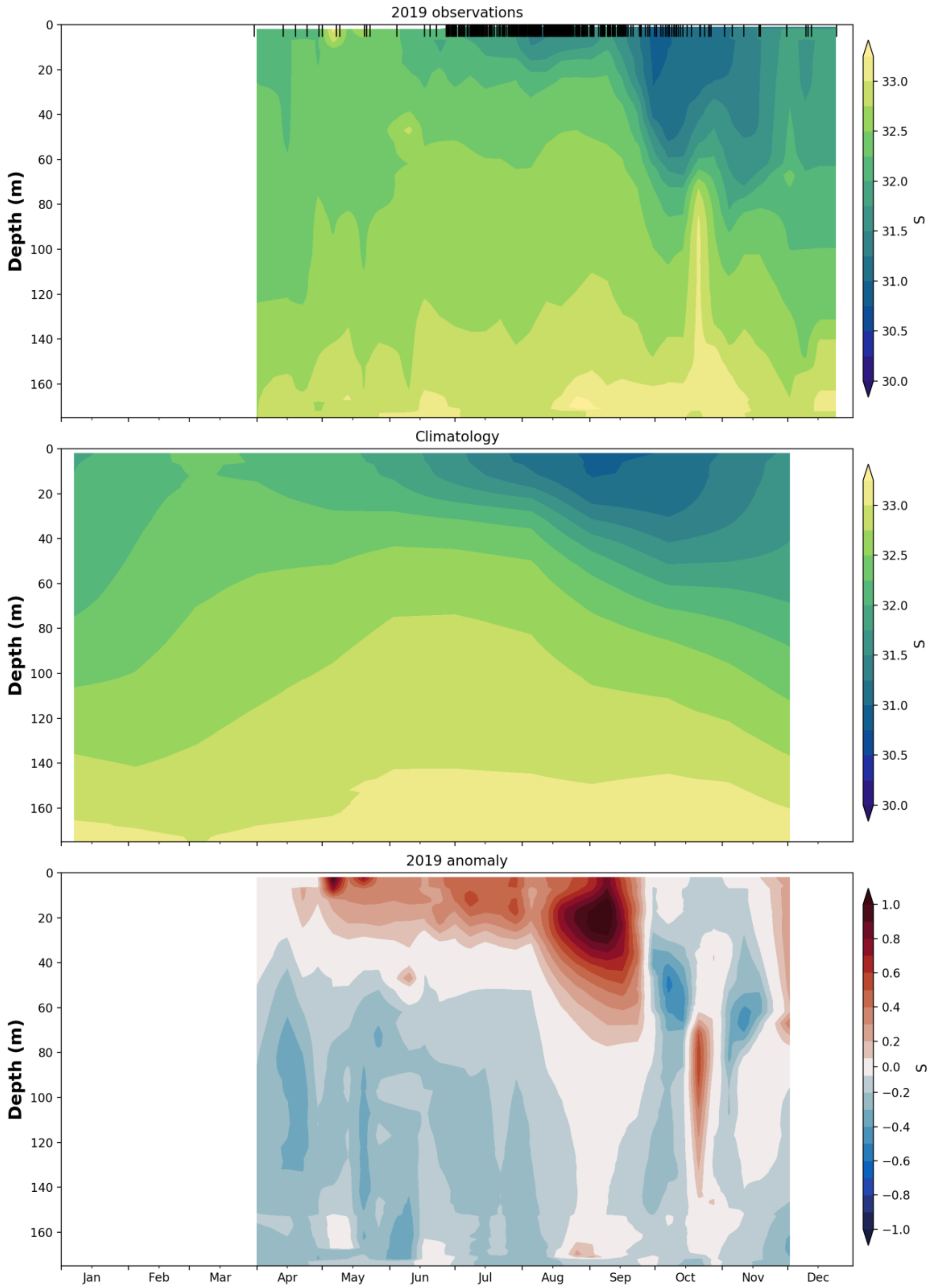

Figure 18. Same as in Figure 17, but for salinity.

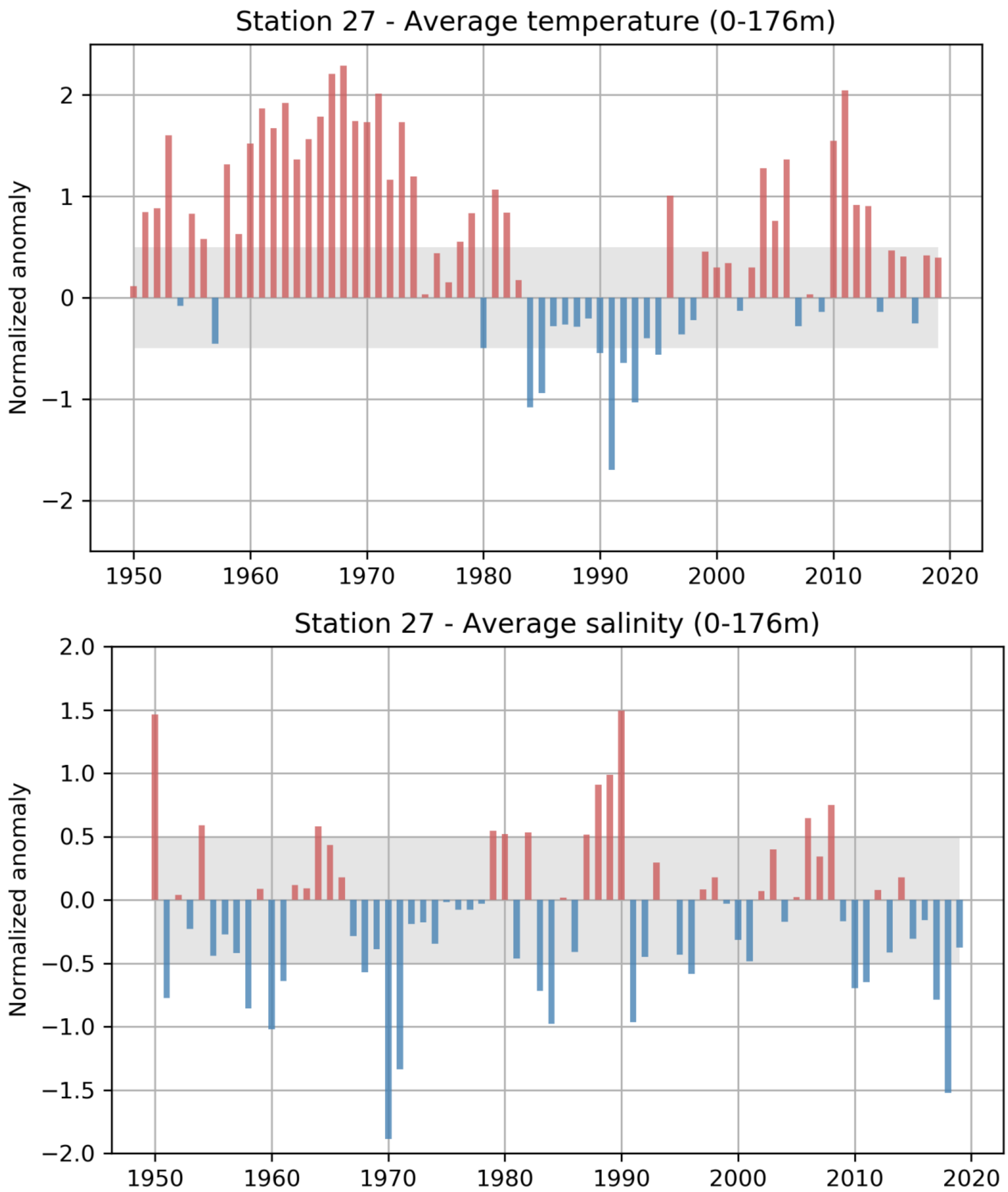

Figure 19. Annual normalized anomaly of vertically averaged (0-176m) temperature (top) and salinity (bottom) at Station 27 calculated from all occupations since 1950. Shaded gray areas represent the ±0.5 SD range considered "normal".

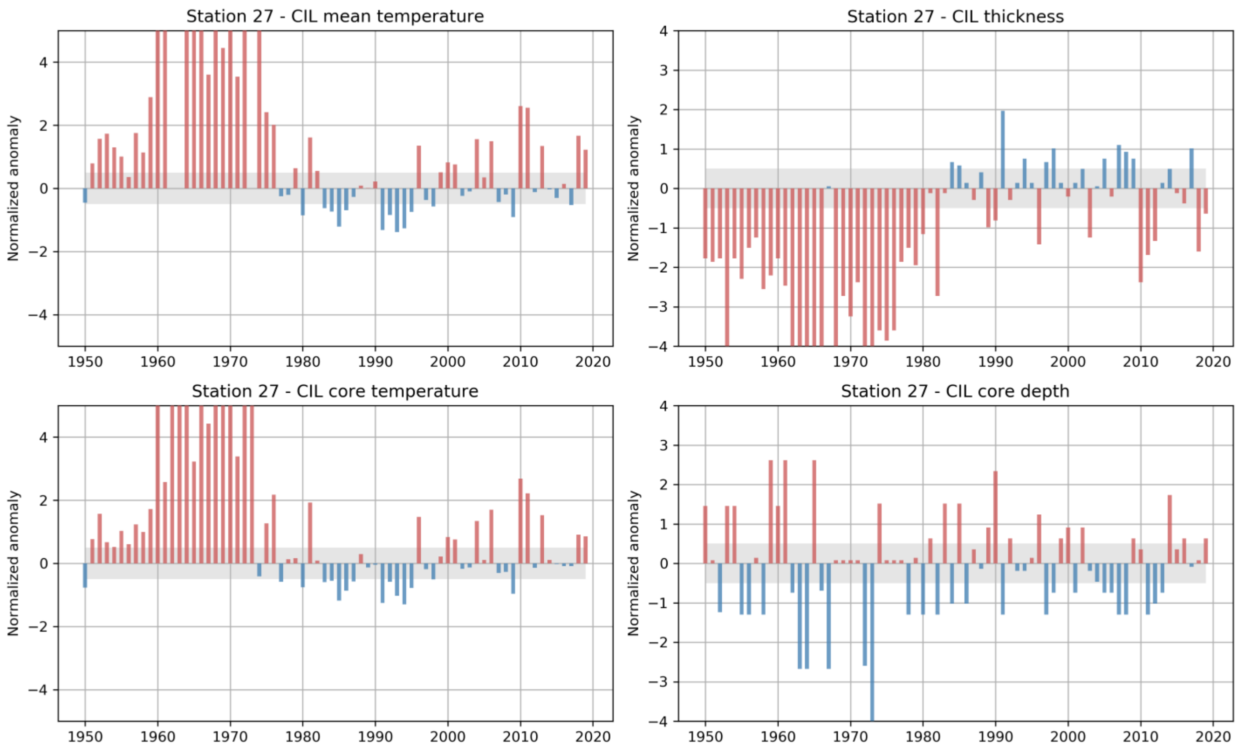

Figure 20. Normalized anomalies of summer (May-July) cold intermediate layer (CIL) statistics at Station 27 since 1950. The top row shows the CIL mean temperature and thickness, while the bottom row

shows its core temperature (minimum temperature of the CIL) and its depth. Shaded gray areas represent the ±0.5 SD range considered "normal".

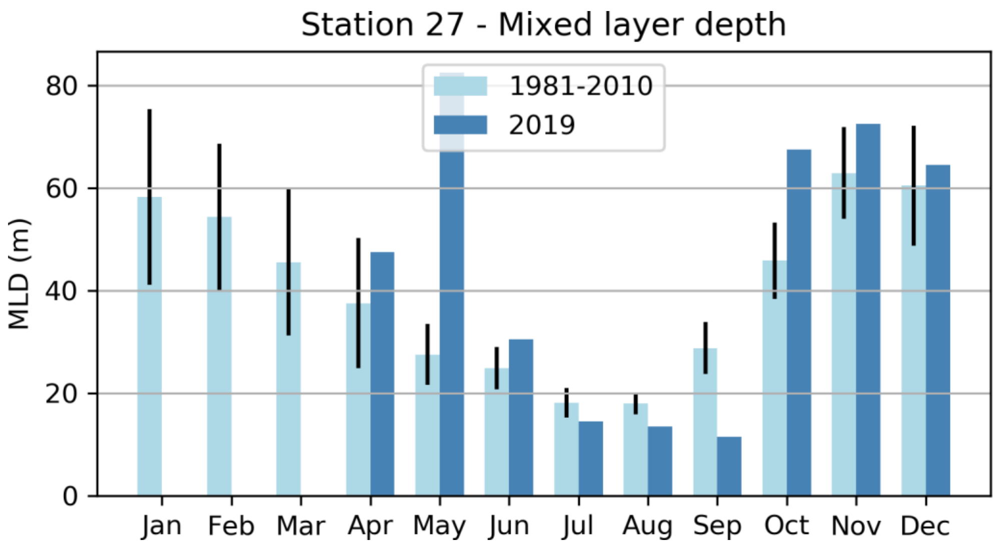

Figure 21. Bar plot of the monthly averaged mixed layer depth (MLD) at Station 27. The 1981-2010 climatology is shown in light blue while the update for 2019 is shown in dark blue. The black lines represent 0.5 SD above and below the climatology.

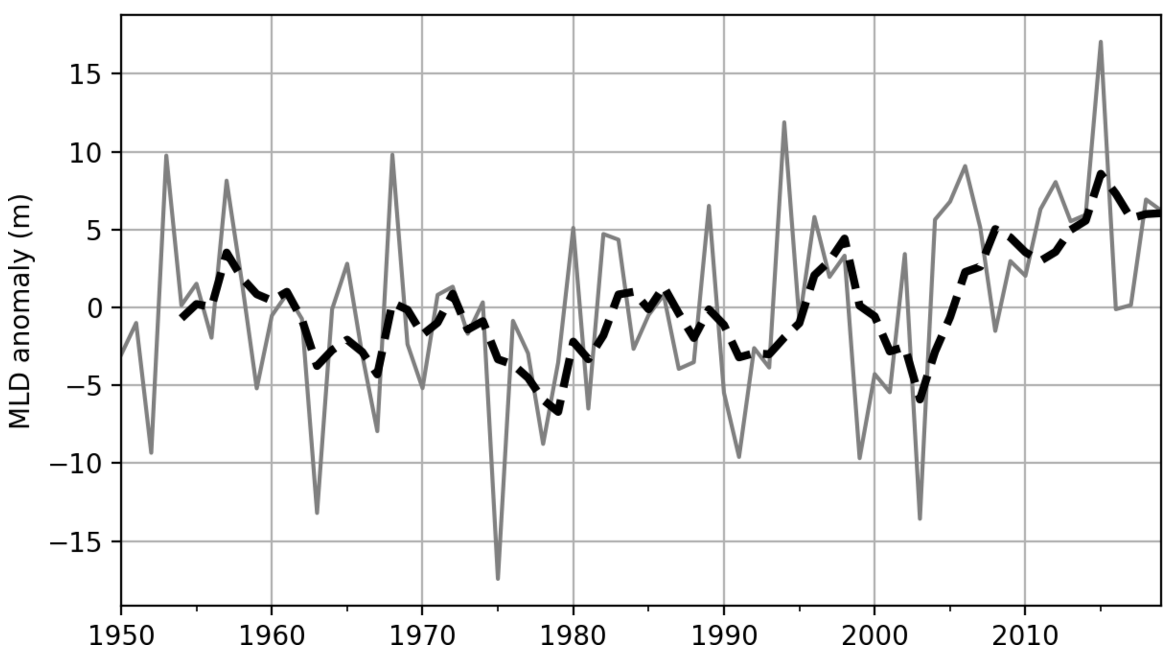

Figure 22. Time series of the annual mixed layer depth (MLD) average at Station 27 since 1950 (gray solid line) and its 5-year running mean (dashed-black line).

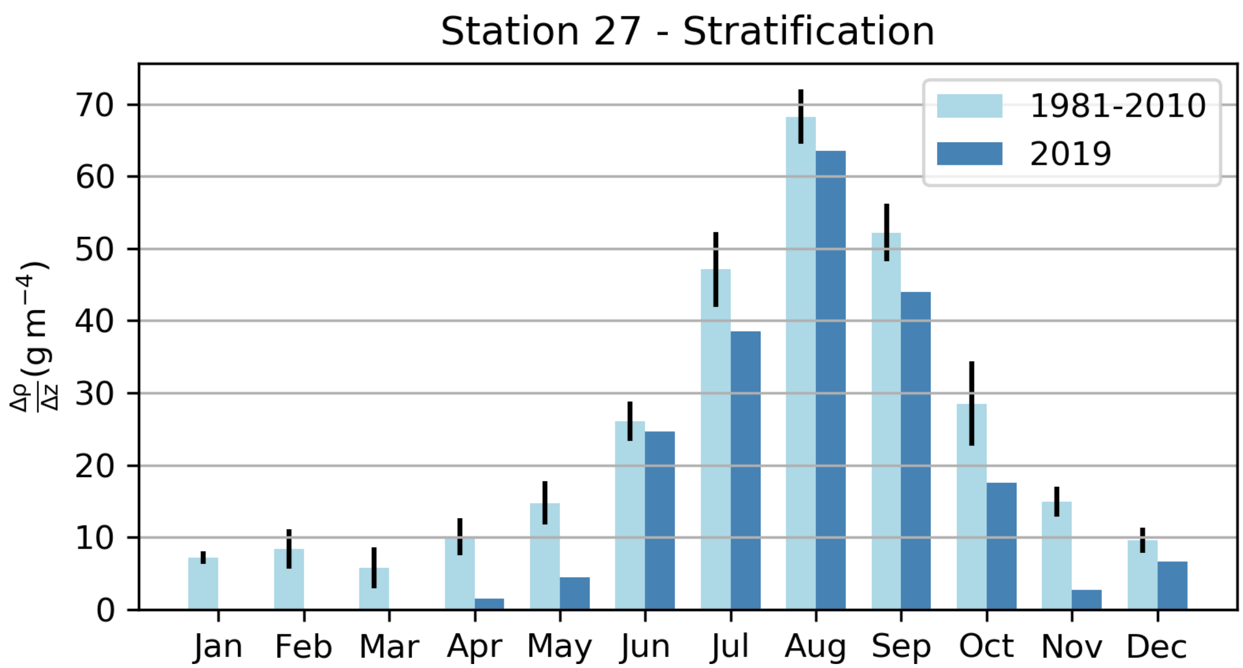

Figure 23. Bar plot of the monthly average stratification (defined as the density difference between 0 and 50m) at Station 27. The 1981-2010 climatology is shown in light blue while the update for 2019 is shown in dark blue. The black lines represent 0.5 SD above and below the climatology.

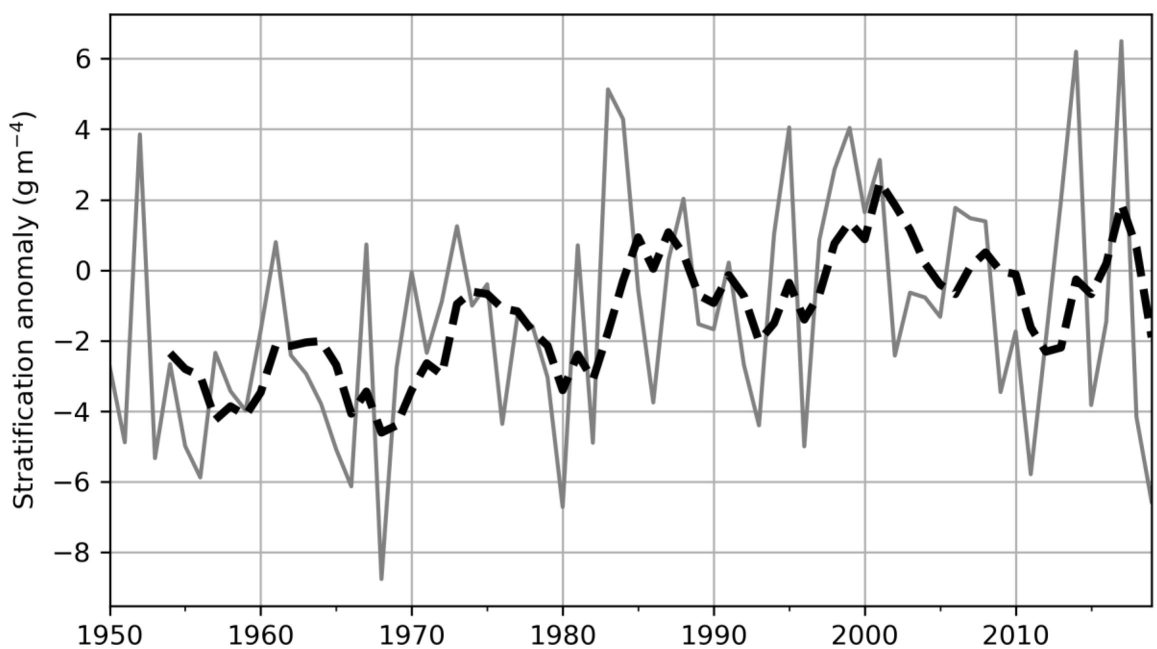

Figure 24. Time series of the annual average stratification at Station 27 since 1950 (gray solid line) and its 5-year running mean (dashed-black line).

	80	81	82	83	84	85	86	87	88	89	90	91	92	93	94	95	96	97	98	99	00	01	02	03	04	05	06	07	08	09	10	11	12	13	14	15	16	17	18	19	x̄	sd
-- Vertically averaged temperature --																																										
Temp 0-176m	-0.5	1.1	0.8	0.2	-1.1	-0.9	-0.3	-0.3	-0.3	-0.2	-0.5	-1.7	-0.6	-1.0	-0.4	-0.6	1.0	-0.4	-0.2	0.5	0.3	0.3	-0.1	0.3	1.3	0.8	1.4	-0.3	0.0	-0.1	1.5	2.0	0.9	0.9	-0.1	0.5	0.4	-0.3	0.4	0.4	0.4	0.4
Temp 0-50m	-0.8	0.7	0.1	0.2	-1.1	-0.8	-0.2	-0.2	-0.4	-0.3	-0.5	-1.5	-0.5	-0.8	0.0	-0.4	0.7	-0.4	0.1	0.5	0.4	0.5	-0.3	0.3	0.9	0.8	1.5	-0.4	0.6	-0.3	1.1	1.4	1.0	0.8	0.1	0.4	0.7	-0.2	0.0	-0.2	3.2	0.7
Temp 150-176m	-0.1	0.4	-0.1	-0.4	-0.8	-1.3	-0.3	-0.2	-0.2	-0.5	-0.8	-1.2	-0.9	-1.3	-1.1	-0.6	0.5	0.2	0.5	0.7	0.5	0.7	0.1	0.0	1.9	1.3	1.5	0.4	0.1	-0.3	1.6	3.2	0.8	1.1	-0.5	-0.5	-0.4	-0.5	0.9	0.5	-1.0	0.3
-- Vertically averaged salinity --																																										
Sal 0-176m	0.5	-0.5	0.5	-0.7	-1.0	0.0	-0.4	0.5	0.9	1.0	1.5	-1.0	-0.5	0.3	0.0	-0.4	-0.6	0.1	0.2	0.0	-0.3	-0.5	0.1	0.4	-0.2	0.0	0.6	0.3	0.7	-0.2	-0.7	-0.6	0.1	-0.4	0.2	-0.3	-0.2	-0.8	-1.5	-0.4	32.5	0.1
Sal 0-50m	0.5	-0.2	1.0	-0.7	-1.2	0.2	0.4	0.8	0.9	1.1	1.4	-1.3	-0.4	-0.1	-0.1	-0.9	-0.4	-0.2	-0.2	-0.2	-0.6	-0.7	0.6	0.8	0.1	0.1	0.3	0.1	0.4	0.1	-0.8	-0.5	0.1	-0.2	-0.1	-0.2	0.0	-1.0	-0.8	0.4	31.9	0.2
Sal 150-176m	-0.1	0.4	-0.1	-0.4	-0.8	-1.3	-0.3	-0.2	-0.2	-0.5	-0.8	-1.2	-0.9	-1.3	-1.1	-0.6	0.5	0.2	0.5	0.7	0.5	0.7	0.1	0.0	1.9	1.3	1.5	0.4	0.1	-0.3	1.6	3.2	0.8	1.1	-0.5	-0.5	-0.4	-0.5	0.9	0.5	33.1	0.1
-- Cold intermediate layer (CIL) properties --																																										
CIL temp	-0.9	1.6	0.6	-0.6	-0.7	-1.2	-0.7	-0.3	0.1	0.0	0.2	-1.3	-0.8	-1.4	-1.3	-0.7	1.3	-0.4	-0.6	0.5	0.8	0.8	-0.2	-0.1	1.6	0.3	1.5	-0.4	-0.2	-0.9	2.6	2.6	-0.1	1.3	0.0	-0.3	0.1	-0.5	1.7	1.2	-1.0	0.2
CIL core T	-0.8	1.9	0.1	-0.6	-0.5	-1.2	-0.9	-0.6	0.3	-0.1	0.0	-1.3	-0.6	-1.0	-1.3	-0.8	1.5	-0.2	-0.5	0.2	0.8	0.8	-0.2	-0.1	1.3	0.1	1.7	-0.3	-0.3	-1.0	2.7	2.2	-0.1	1.5	0.1	0.0	-0.1	-0.1	0.9	0.9	-1.4	0.2
CIL core depth	-1.3	0.6	-1.3	1.5	-1.0	1.5	-1.0	0.4	-0.1	0.9	2.3	-1.3	0.6	-0.2	-0.2	0.1	1.2	-1.3	-0.7	0.6	0.9	-0.7	0.9	-0.2	-0.5	-0.7	-0.7	-1.3	-1.3	0.6	0.4	-1.3	-1.0	-0.7	1.7	0.4	0.6	-0.1	0.1	0.6	125.5	18.1
CIL thickness	-1.2	-0.1	-2.7	-0.1	0.7	0.6	0.1	-0.3	0.4	-1.0	-0.8	2.0	-0.3	0.1	0.8	0.1	-1.4	0.7	1.0	0.1	-0.2	0.1	0.5	-1.2	0.1	0.8	-0.2	1.1	0.9	0.8	-2.4	-1.7	-1.3	0.1	0.5	-0.1	-0.4	1.0	-1.6	-0.6	124.4	11.5
-- Mixed layer depth (MLD) --																																										
MLD winter	0.6	-0.3	1.0	0.8	0.3	-1.0	-0.6	-0.2		0.3	-0.2	-0.5	0.0	-1.1	0.8	-0.1	0.1	1.2	0.7	-0.2	-0.5	-0.1	0.1	-1.3	0.6	0.8	1.3	0.7	0.3	-1.1	-0.8	0.3	0.6	1.6	1.2	0.8	0.0				54.8	23.4
MLD spring	-0.2	-0.3	-0.3	-0.4	-1.3	0.3	-0.2	0.0	-0.3	0.8	0.4	-0.8	0.3	-0.3	1.1	-0.5	0.0	0.7	-0.8	-0.6	0.6	-0.3	0.4	-0.7	0.5	-0.4	0.2	-0.3	-0.2	0.4	1.9	-0.4	1.5	0.6	0.1	1.3	0.2	0.3	1.7	1.9	30.1	10.5
MLD summer	-0.7	-0.5	0.1	0.0	-0.4	0.2	0.6	-0.3	0.0	0.9	0.1	-0.3	0.1	1.0	0.8	1.1	0.3	0.3	-0.8	-0.4	-1.1	0.2	0.0	0.0	-0.8	-0.7	0.2	-0.3	-0.8	0.9	-0.4	1.6	-1.0	-0.1	-1.1	1.4	0.9	-0.6	-0.6	-1.1	21.7	3.9
MLD fall	0.8	-0.2	-0.8	0.6	0.3	1.1	1.1	-0.2	-0.7	-0.2	-1.5	-0.8	-0.4	0.9	-0.2	0.0	0.9	-0.6	0.4	-0.7	0.0	-0.7	0.1	-0.7	0.3	0.7	-0.4	0.1	0.1	1.3	-0.3	0.8	0.7	-0.6	0.4	0.3	-0.3	0.2	0.1	0.7	55.8	13.3
MLD annual	0.1	-0.3	0.1	0.2	-0.3	0.1	0.2	-0.2	-0.3	0.5	-0.2	-0.6	0.0	0.1	0.6	0.1	0.3	0.2	-0.2	-0.5	-0.3	-0.2	0.2	-0.6	0.2	0.0	0.3	0.1	-0.2	0.5	0.3	0.6	0.4	0.2	-0.1	0.9	0.2	0.0	0.4	0.5	39.4	6.3
-- Stratification --																																										
strat winter	1.4		0.1		-0.2	0.3	-0.1	-0.6		-0.2	1.5	-0.6	3.9	-1.9	-0.8	-1.5	-0.4	0.4	0.3	0.2	0.6	0.5	0.9	0.0	-0.2	-0.5	-0.3	0.1	0.1	0.2	0.5	0.2	-0.6	-0.2	-0.4	-0.2	-0.8				0.008	0.005
strat spring	-0.7	0.3	-0.5	2.6	1.5	-0.8	-0.3	1.6	0.0	-0.6	-0.3	0.1	-1.1	-0.7	-0.5	1.2	-0.7	0.0	0.6	0.8	-0.4	-0.1	-0.9	-1.0	-0.4	-0.1	0.4	0.2	-0.4	0.1	-0.9	-0.3	-0.6	-0.3	-0.7	-0.2	-0.7	1.4	-1.1	-1.2	0.017	0.005
strat summer	-0.9	0.3	-0.5	0.8	1.3	0.6	-0.6	-0.7	0.1	-0.6	-0.3	-0.8	-1.4	-0.5	1.2	0.3	-1.3	0.0	0.7	0.9	0.2	0.5	0.1	-0.8	0.2	0.2	0.1	1.0	0.3	-1.2	-0.4	-2.0	0.1	0.9	2.9	-1.1	-0.5	1.8	-0.5	-0.8	0.055	0.007
strat fall	-1.6	-0.7	-1.6	-0.9	-0.1	-0.5	-1.1	-0.4	0.5	0.3		1.3	0.5	-0.4	0.0	1.7	-0.5	0.3	0.0	0.1	0.5	1.0	-0.9	0.1	-0.3	-0.5	0.5	-0.3	1.2	-0.9	0.2	-0.8	-0.9	-0.1	-0.2	-1.1	1.3	-0.2	-0.5	-1.6	0.018	0.005
strat annual	-0.5	0.0	-0.5	0.8	0.7	-0.1	-0.5	0.0	0.2	-0.2	-0.1	0.1	-0.2	-0.7	0.0	0.6	-0.7	0.1	0.4	0.6	0.2	0.5	-0.3	-0.4	-0.2	-0.2	0.2	0.2	0.2	-0.4	-0.3	-0.7	-0.5	0.1	0.6	-0.6	-0.1	0.9	-0.7	-1.2	0.026	0.004

Figure 25. Annual normalized anomalies of hydrographic parameters for Station 27. The different boxes from top to bottom are: vertically averaged temperature and salinity for different depth ranges, cold intermediate layer (CIL) properties, mixed layer depth (MLD), and stratification for the 4 seasons and annual average. The cells are color-coded according to Figure 2. Gray cells indicate absence of data.

Standard Hydrographic Sections

In the early 1950s, several countries under the auspices of the International Commission for the Northwest Atlantic Fisheries (ICNAF) carried out systematic monitoring along hydrographic sections in Newfoundland and Labrador waters. In 1976, ICNAF normalized a suite of oceanographic monitoring stations along sections in the Northwest Atlantic Ocean from Cape Cod (USA) to Egedesminde (West Greenland) (ICNAF 1978). In 1998 under the Atlantic Zone Monitoring Program (AZMP) of Fisheries and Oceans Canada, the Seal Island (SI), Bonavista Bay (BB), Flemish Cap (47°N) (FC) and Southeast Grand Bank (SEGB) historical stations were selected as core monitoring sections. The White Bay section (WB) continued to be sampled during the summer as a long time series ICNAF/NAFO section (see Figure 1).

Two ICNAF sections on the mid-Labrador Shelf, the Beachy Island (BI) and the Makkovik Bank (MB) sections, were selected to be sampled during the summer if survey time permitted. Starting in the spring of 2009, a section crossing south-west over St. Pierre Bank (SWSPB) and one crossing south-east over St. Pierre Bank (SESPB) were added to the AZMP surveys.

In 2019, our three annual surveys suffered from significant reduction of ship times of various origins. During the spring survey (11-18 April), only section FC was realized. Sections MB, SI, BB and FC were sampled during the summer survey (June 26th to July 13th), while BB, FC, SEGB and part of SWSPB were sampled during the fall (November 17th to December 10th). In this manuscript we present the summer cross sections of temperature and salinity and their anomalies along the SI, BB and FC sections to represent the vertical temperature and salinity structure across the NL Shelf during 2019.

Temperature and Salinity Variability

The water mass characteristics observed along the standard sections crossing the NL Shelf are typical of subpolar waters with a subsurface temperature range of -1.5°C to 2°C and salinities from 31.5 to 33.5. Labrador Slope water flows southward along the shelf edge and into the Flemish Pass and Flemish Cap regions. This water mass is generally warmer and saltier than the subpolar shelf waters with a temperature range of 3° to 4°C and salinities in the range of 34 to 34.75. Surface temperatures normally warm to between 10° and 12°C during late summer while bottom temperatures remain < 0°C over much of the Grand Banks but increase to between 1° and 3.5°C near the shelf edge below 200 m and in the deep troughs between the banks. In the deeper (> 1000 m) waters of the Flemish Pass and across the Flemish Cap, bottom temperatures generally range from 3° to 4°C. In general, the near-surface water mass characteristics along the standard sections undergo seasonal modification from annual cycles of air-sea heat flux, wind forced mixing, and the formation and melting of sea ice. These mechanisms cause intense vertical and horizontal temperature and salinity gradients, particularly along the frontal boundaries separating the shelf and slope water masses. The seasonal changes in the temperature and salinity fields along the Bonavista section are presented in Colbourne et al. (2015).

The summer temperature and salinity structures along the Seal Island, Bonavista Bay and Flemish Cap (47ºN), hydrographic sections during 2019 are highlighted in Figure 26 to Figure 28. The dominant thermal feature along these sections is associated with the cold and relatively fresh waters overlying the shelf. This water mass is separated from the warmer and denser water of the continental slope region by strong temperature and salinity fronts. The cross sectional area (or volume) of the CIL is bounded by the 0°C isotherm and highlighted as a thick black contour in the temperature panels. The CIL parameters are generally regarded as robust indices of ocean climate conditions on the eastern Canadian Continental Shelf. While the CIL area undergoes significant seasonal variability, the changes are highly coherent from the

Labrador Shelf to the Grand Banks. The CIL remains present throughout most of the summer until it gradually decays during the fall as increasing winds and storm episodes deepen the surface mixed layer.

During 2019, temperatures were generally above normal for most of the SI and BB sections, except in the near surface (Figure 26 and Figure 27, bottom left). For FC section, temperatures were much colder than normal at the surface (by more than 3°C below normal in some areas; Figure 28, bottom left). At depth, temperatures were slightly warmer than normal temperature, which signifies warmer bottom conditions in a large portion of the Grand Banks (see section on bottom observations).

The corresponding salinity cross sections show a relatively fresh upper water layer over the shelf with sources from arctic outflow and the Labrador Shelf with values < 33, in contrast to the saltier Labrador Slope water further offshore with values > 34 (Figure 26 to Figure 28, right panels). In 2019, salinities corresponding to the CIL were generally lower than normal for all sections, while the slope waters were above normal. This is likely due to an unusual extension of the saltier Labrador Current onto the slope in 2019 compared to the climatology. This is especially evident for sections BB and FC (see difference in salinity field between the top two right panels of all three figures).

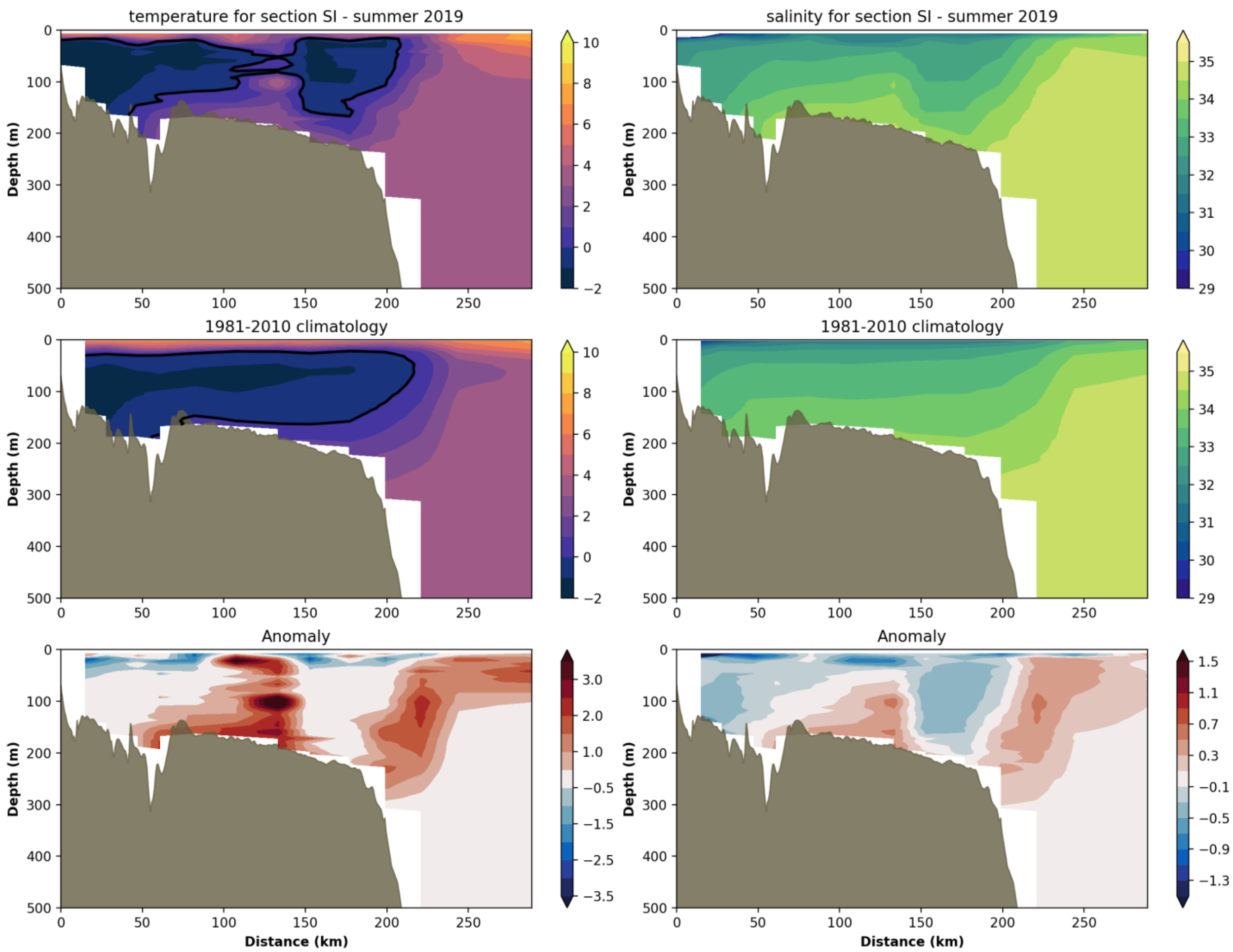

Figure 26. Contours of temperature (°C) and salinity during summer 2019 (top row) and climatological average (middle row) for Seal Island (SI) hydrographic section (see map Figure 1 for location). Their respective anomalies for 2019 are plotted in the bottom panels.

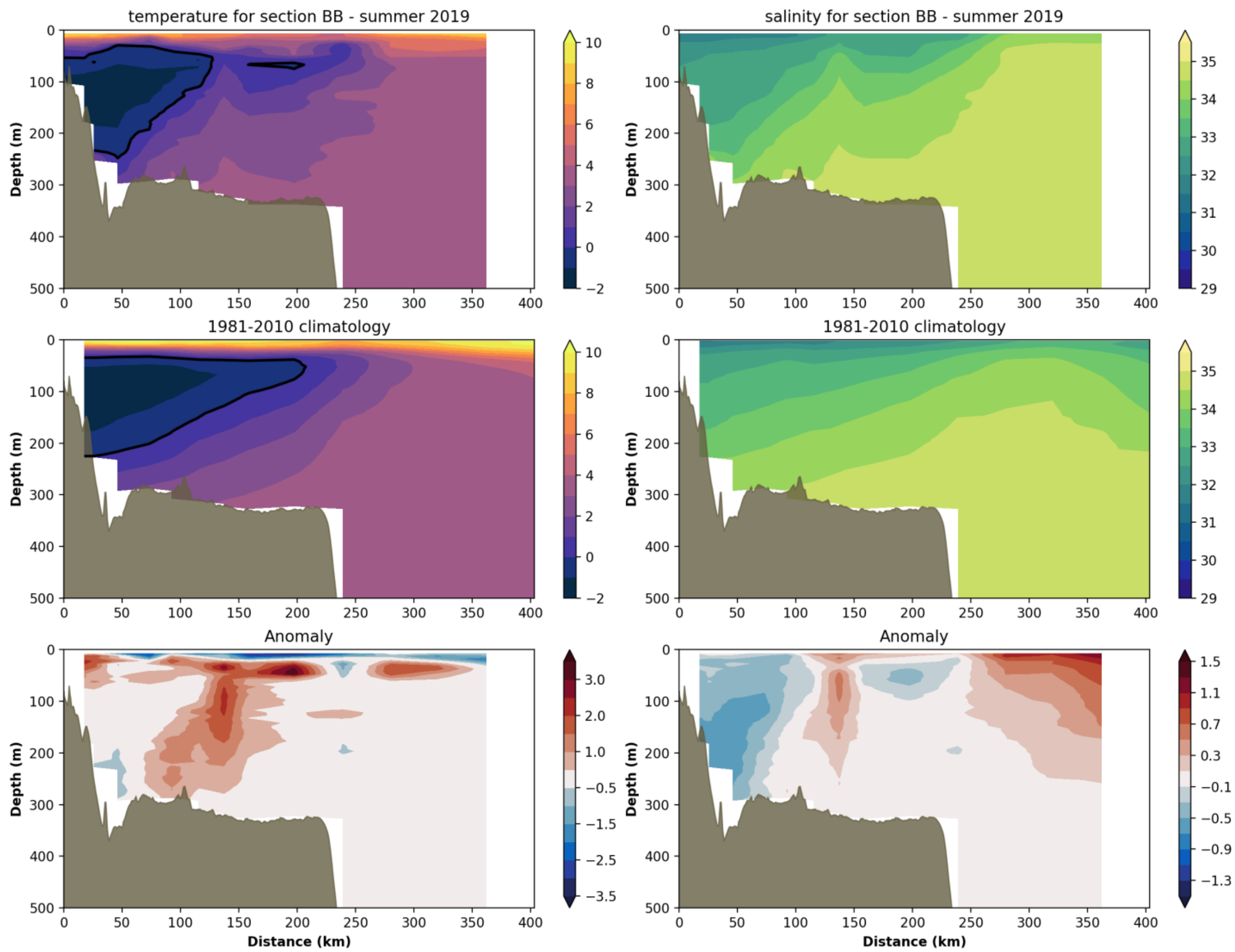

Figure 27. Same as in Figure 26, but for Bonavista (BB) hydrographic section (see map Figure 1 for location).

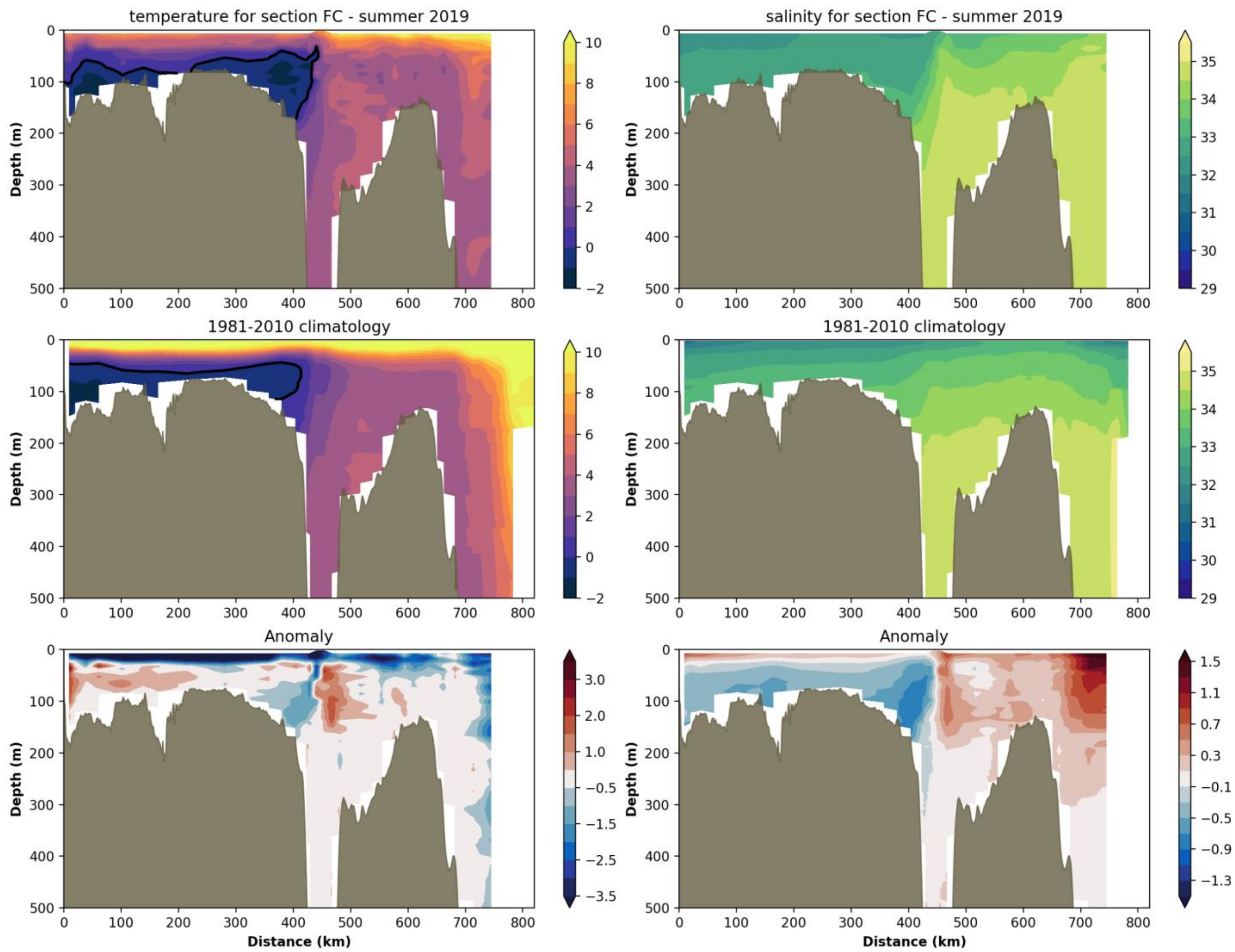

Figure 28. Same as in Figure 26, but for Flemish Cap (FC) hydrographic section (see map Figure 1 for location).

Cold Intermediate Layer Variability

Statistics of summer CIL anomalies for the three sections discussed above (Seal Island, Bonavista and Flemish Cap) are presented in a scorecard in Figure 29. The climatological average cross sectional area of the summer CIL along these sections are 20.3 ± 4.5 km^2, 23.8 ± 8.2 km^2 and 11.7 ± 8.9 km^2, respectively. The averaged anomalies of the CIL core temperature (minimum temperature of this layer) and volume (defined as the cross sectional area) for these three sections are summarized in Figure 30 as a time series going back to 1950. In general, the summer CIL has been predominantly warmer/smaller than average since the mid 1990's, with a cooling trend emerging since about 2012 or 2014 to 2017. However, the most striking aspect of this long time series is the warm conditions that prevailed in the 1960's (that stands as a unique feature for this nearly 70-year time series, although measurements during this period were largely made from reversing thermometers that might have missed the CIL core), followed by a cold period that lasted from the mid-1980's to the mid-1990's.

In 2019, the CIL conditions were generally warmer than normal (except for the CIL core at SI), in agreement with 2018 that saw a return to warmer than normal conditions after 4 years of mostly colder conditions (Figure 29). Interestingly, the very warm CIL core temperature found on SI section in 2018 (+2.5 SD) is back to cold conditions (-0.5 SD) in 2019.

	80	81	82	83	84	85	86	87	88	89	90	91	92	93	94	95	96	97	98	99
-- Seal Island section --																				
CIL area (km^2)	-0.3	-2.0	0.3	-1.3	1.8	0.5	-0.5	-0.2	0.0		1.7	1.8	1.1	1.5	-0.2	-0.6	0.1	-0.9	-0.1	-1.8
CIL core (°C)	0.5	0.7	0.2	-1.3	-1.3	-1.0	0.8	0.2	0.0		-0.8	-1.2	-1.0	-1.3	-0.7	2.0	-0.3	-0.6	-0.4	1.0
core depth (m)	0.3	0.7	-0.7	0.7	-0.7	-0.5	1.7	1.7	0.1		1.7	1.7	-0.3	0.1	1.1	-0.3	-0.9	0.3	0.5	-0.7
-- Bonavista section --																				
CIL area (km^2)	-1.0	-0.4		0.6	3.0	1.3	-0.4	-0.6	0.5	0.1	1.6	2.2	0.0	0.5	0.3	-0.7	-0.2	-0.9	-0.3	-0.5
CIL core (°C)	2.7	1.3		-1.8	-1.2	-0.9	0.3	0.4	1.2	-1.0	-0.9	-1.1	-0.2	-0.6	-1.0	-0.3	0.8	-0.4	-0.6	0.0
core depth (m)	-0.3	-0.5		1.3	-1.1	-0.7	0.1	0.5	-0.3	0.3	1.7	0.5	0.7	0.9	0.3	2.7	-0.1	-0.1	-0.9	0.7
-- Flemish Cap section --																				
CIL area (km^2)	0.2	0.3	-1.3	2.0	1.2	0.9	0.2	-0.4	-0.2	0.8	1.7	1.3	0.3	0.9	-0.4	0.0	-0.3	-0.6	0.9	-0.6
CIL core (°C)	-0.4	0.5	2.9	-0.9	-0.3	-0.9	-0.6	-0.7	0.0	-0.8	-0.5	-0.9	-0.7	-0.7	-0.7	-1.4	0.0	-0.3	-0.6	0.4
core depth (m)	-1.5	-2.1	-0.4	-0.7	-0.1	-0.1	1.6	-0.9	-0.7	-0.9	0.2	-0.9	-0.9	1.3	-0.9	1.0	2.1	0.2	0.7	1.6

	00	01	02	03	04	05	06	07	08	09	10	11	12	13	14	15	16	17	18	19	x̄	sd
-- Seal Island section --																						
CIL area (km^2)	-0.4	0.8	-0.2	0.7	-1.3	-0.1	-0.3	-0.3	-0.5	1.0	-0.3	-1.2	1.8	-1.0	0.0	1.7	-0.8	1.5	-2.1	-0.3	20.8	3.7
CIL core (°C)	-0.6	1.1	-0.6	0.6	2.3	1.0	1.1	-0.1	-0.7	-0.3	1.1	2.7	-0.4	1.1	-1.3	0.1	-0.3	-0.7	3.1	-0.5	-1.5	0.2
core depth (m)	-1.5	-1.3	0.1	0.5	-0.1	-1.3	-0.1	0.9	-0.1	-1.3	-1.7	-0.9	0.1	0.1	2.7	-0.1	0.3	-0.9	0.7	0.9	69.3	25.1
-- Bonavista section --																						
CIL area (km^2)	0.2	-0.6	-0.5	0.1	-1.5	-1.0	-1.1	-0.4	-1.0	0.0	-0.3	-2.4	-0.3	-0.7	1.3	0.7	0.2	0.0	-0.6	-1.5	24.5	7.1
CIL core (°C)	-0.2	0.4	-0.1	-0.3	2.0	0.9	2.6	0.9	-0.3	-0.7	0.8	2.5	-0.8	0.4	-1.0	-0.9	-0.6	-0.9	0.8	0.4	-1.6	0.1
core depth (m)	0.3	-0.9	1.1	0.3	-0.3	-1.3	-0.5	-1.7	0.1	-1.3	-1.3	0.3	1.1	-0.5	0.7	1.9	-0.9	-0.3	-0.1	1.3	89.4	24.9
-- Flemish Cap section --																						
CIL area (km^2)	-1.1	-1.3	-0.8	-0.9	-1.0	-0.4	0.0	2.0	-1.0	-1.2	-0.9	-1.1	-1.3	-0.6		0.0	-0.2	-1.3	-0.3	-1.1	11.7	8.9
CIL core (°C)	0.3	3.1	0.2	0.4	0.3	0.1	0.9	0.1	-0.2	0.0	0.9	1.2	0.3	1.1		0.1	0.0	0.0	0.0	-0.1	-1.3	0.5
core depth (m)	-0.1	1.3	-0.1	-0.7	-0.7	-0.9	-0.1	1.1	0.2	-0.9	1.0	-1.2	1.6	1.0		-0.7	-0.1	1.6	1.6	2.1	83.4	18.0

Figure 29. Scorecards of the cold intermediate layer (CIL) summer statistics along Seal Island, Bonavista and Flemish Cap hydrographic sections. The CIL area is defined as all water below 0°C (see black contours in Figure 26 to Figure 28), and the CIL core temperature and depth are the minimum temperature of the CIL and the depth at which it is encountered respectively. Color codes for the area and depth have been reversed (positive is blue and negative is red) because they represent cold conditions. Grayed cells indicate absence of data.

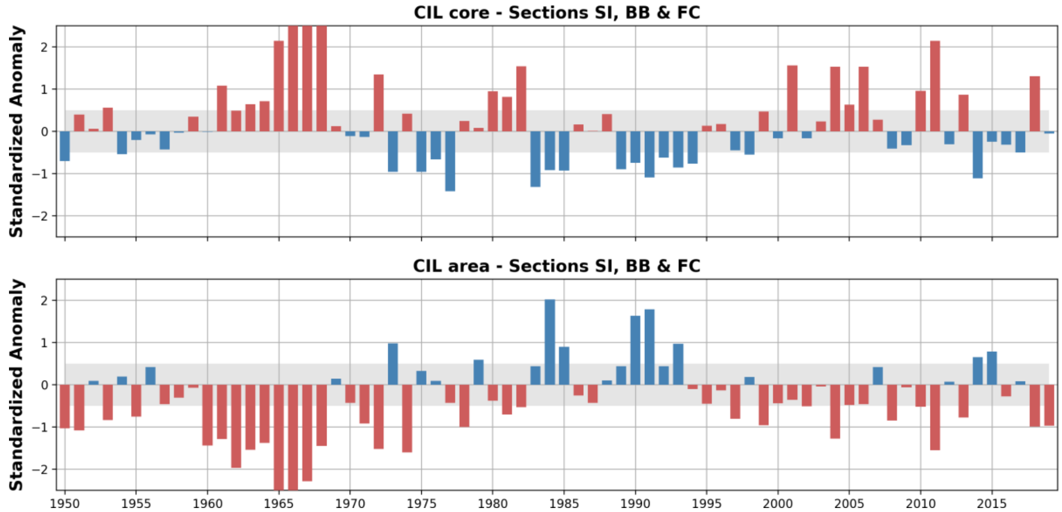

Figure 30. Mean normalized anomalies of the summer CIL core temperature (top) and area (bottom) over Seal Island, Bonavista and Flemish Cap sections since 1950 (values for each separate section since 1980 can be found in Figure 29). Shaded gray areas represent the ±0.5 SD range considered "normal".

Bottom Observations in NAFO sub-areas

Canada has been conducting stratified random bottom trawl surveys in NAFO Sub-areas 2 and 3 on the NL Shelf since 1971. Areas within each division, with a selected depth range, were divided into strata, and the number of fishing stations in an individual stratum was based on an area-weighted proportional allocation (Doubleday, 1981). Temperature profiles (and salinity profiles since 1990) are available for most fishing sets in each stratum. These surveys provide large spatial-scale oceanographic data sets for the Newfoundland and Labrador Shelf. NAFO Subdivision 3Ps on the Newfoundland south coast and Divisions 3LNO on the Grand Banks are surveyed in the spring, and Divisions 2HJ off Labrador in the north, 3KL off eastern Newfoundland, and 3NO on the southern Grand Bank are surveyed in the fall. The hydrographic data collected on these surveys are routinely used to assess the spatial and temporal variability in the thermal habitat of several fish and invertebrate species. A number of products based on the data are used to characterize the oceanographic bottom habitat. Among these are contour maps of the bottom temperatures and their anomalies, the area of the bottom covered by water in various temperature ranges, etc. In addition, species-specific *thermal habitats* indices are often used in marine resource assessments for snow crab and northern shrimp.

The current method to derive the bottom temperature was introduced by Cyr et al. (2019) and is similar to the approach presented in reports of the annual physical oceanographic conditions for the Gulf of St. Lawrence (Galbraith et al. 2020) and Newfoundland and Labrador Shelves (Cyr et al. 2020). First, all available annual profiles of temperature and salinity (from AZMP hydrographic campaigns, multi-species resources assessments, surveys from other DFO regions, international oceanographic campaigns, Argo program, etc.) are vertically averaged in 5 m bins and vertically interpolated to fill missing bins. Then, for each season (April-June for spring and September-December for fall), all data are averaged on a regular 0.1° x 0.1° (latitudinal x longitudinal) grid to obtain one seasonal profile per grid cell. Since this grid has missing data in many cells, each depth level is horizontally linearly interpolated. For each grid point, the bottom observation is considered as the data at the closest depth to the GEBCO_2014 Grid bathymetry (version 20141103), to a maximum 50 m difference. Lastly, bottom observations deeper than 1000 m are clipped. This method is applied for all years between 1980 and 2019 from which the 1981-2010 climatology is derived. Anomalies for 2019 are calculated as the difference between annual observations and the climatology.

Spring Conditions

Spring climatological bottom temperature and salinity maps, together with 2019 observations and anomalies for NAFO divisions 3LNOPs are presented in Figure 31 and Figure 32, respectively (see center panel for station occupation coverage). In 2019, bottom temperatures in 3L are generally below 0°C except in the northern part and near the shelf edge where they range from 2° to 4°C. Over the central and southern areas of the Grand Bank (3NO), bottom temperatures ranged from 0° on the bank to 6°C on the slopes. Bottom temperature anomalies were slightly warmer than normal over 3LNO where anomalies of 0.5 to 3.5°C are observed. On St. Pierre Bank (eastern 3Ps) temperatures were generally below 0° in the shallower shelf and above 5°C in the Laurentian Channel. Bottom temperatures were also warmer than normal by 0.5 to 2.5°C.

Spring bottom in 3LNO generally range from 32 – 33 over the central Grand Bank, and from 33 – 35 closer to the shelf edge. In 3Ps, salinities are between 32 and 33 over shallower areas and above 34.5 in the Laurentian channel. A widespread fresh anomaly is observed over the entire 3LNOPs, reaching -0.4 to -0.6 salinity units lower than normal.

Climate indices based on normalized spring temperature anomalies between 1980 and 2019 are shown in a color-coded scorecard in Figure 33. Overall, the table colors visually highlight two main periods of this time series that are the cold period of the late 80's / early 90's (mostly blue cells) and the warm period of the early 2010's (mostly red cells). During the spring of 2011 in Divisions 3LNO, none of the bottom area was covered by <0°C water, the only such occurrence since the surveys began in the early 1970s, corresponding to 2.1 SD below normal. This warm period lasted between 2010 and 2013 before returning towards to normal values: between 2015 and 2017 the bottom area that was covered by <0°C was only -0.1 to 0.1 SD above normal. In 2019, the average bottom temperature for 3LNO was again above below by 0.5 SD.

In Division 3Ps bottom temperatures exhibit some similarities with 3LNO, with warm years of 1999-2000 and 2005-2006 separated by a colder period between 2001-2004 (2003 is the coldest year on record since 1991 at -1.0 SD). With the exception of 2007 (cold at -0.6 SD) and 2008 (normal), all years between 2005 and 2019 were warmer than normal with the warmest year being 2016 at 1.9 SD above normal. 2019 was +1.4 SD above normal. The spring of 2011 had the lowest area of <0°C bottom water of the time series at 1.7 SD below normal, also corresponding to little or no bottom waters with temperatures of <0°C. The area of <0°C water increased somewhat in recent years, including in 2019 (+1.0 SD).

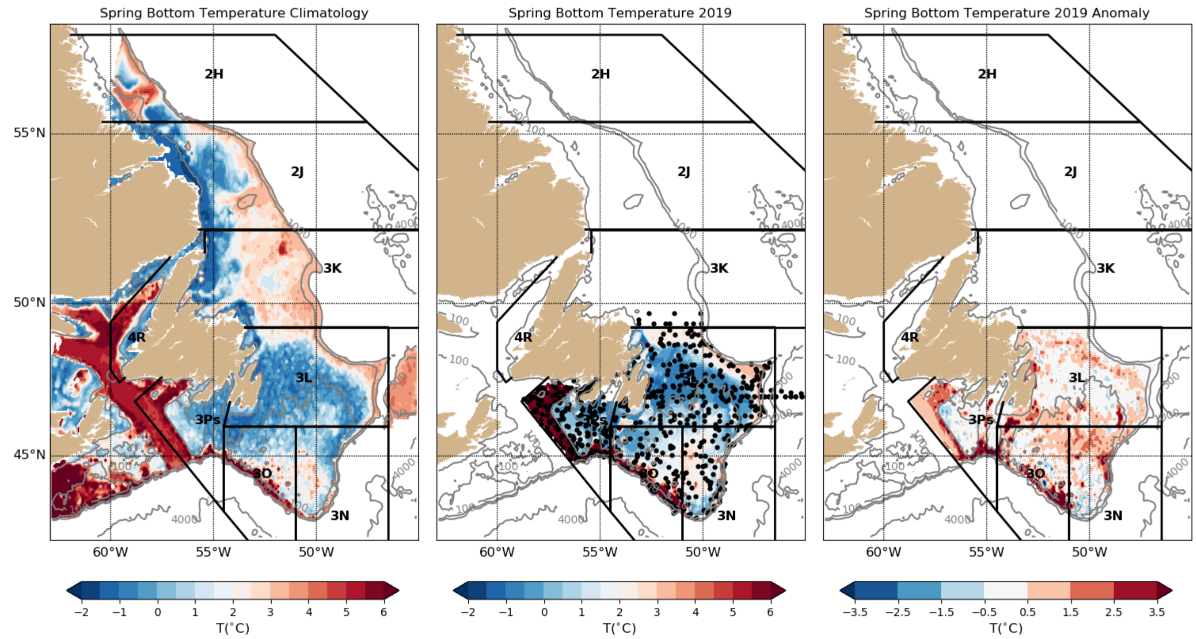

Figure 31. Maps of the mean 1981-2010 spring bottom temperature (left), and spring 2019 bottom temperature (center) and anomalies (right) for NAFO Divisions 3LNOPs only. The location of observations used to derive the temperature field is shown as black dots in the center panel.

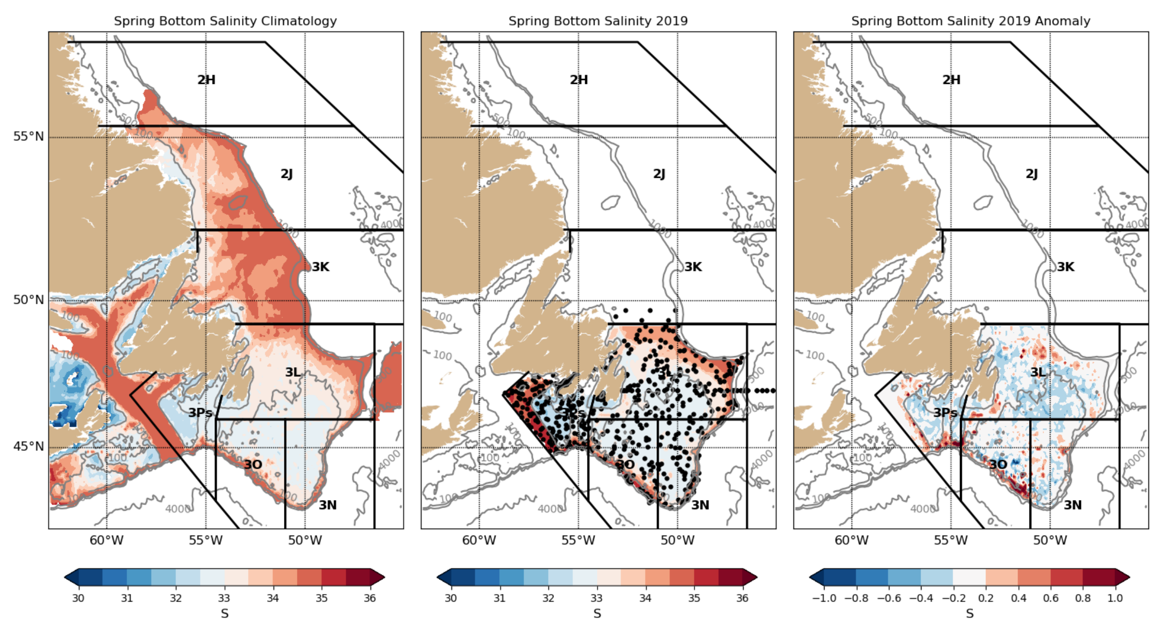

Figure 32. Maps of the mean 1981-2010 spring bottom salinity (left), and spring 2019 bottom salinity (center) and anomalies (right) for NAFO Divisions 2J3KLNO only. The location of observations used to derive the salinity field is shown as black dots in the center panel.

-- NAFO division 3LNO --

	80	81	82	83	84	85	86	87	88	89	90	91	92	93	94	95	96	97	98	99	00	01	02	03	04	05	06	07	08	09	10	11	12	13	14	15	16	17	18	19	$\bar{x}$	sd
T_{bot}	0.2	1.7	-0.4	0.7	-0.6	-1.1	-0.9	-0.2	0.3	-1.0	-1.7	-1.7	-1.4	-0.9	-1.2	-0.5	0.3	-0.5	0.9	1.6	0.9	0.4	0.2	-0.7	1.6	0.9	0.9	0.5	0.5	0.5	1.2	2.4	1.7	1.4	-0.2	0.3	0.0	0.2	0.7	0.5	0.9	0.6
$T_{bot_{<200m}}$	0.1	1.8	-0.3	1.0	-0.5	-1.1	-1.0	-0.1	0.3	-0.8	-1.7	-1.7	-1.4	-0.9	-1.2	-0.5	0.3	-0.7	0.9	1.7	1.0	0.3	0.1	-0.9	1.5	0.8	0.7	0.4	0.3	0.5	1.1	2.4	1.6	1.4	-0.3	0.2	0.0	0.1	0.5	0.6	0.5	0.6
$Area_{>2^{\circ}C}$	0.1	1.5	-1.1	0.8	-0.4	-1.2	-0.9	-0.1	0.2	-1.1	-1.7	-1.4	-1.5	-0.7	-1.1	-0.2	0.1	-0.5	0.6	1.7	0.7	-0.1	0.1	-0.6	2.0	0.9	0.8	0.7	0.9	0.9	0.6	2.8	1.7	0.8	-0.2	0.8	-0.1	0.3	0.3	0.2	63.7	22.4
$Area_{<0^{\circ}C}$	-0.6	-1.4	-0.1	0.0	0.7	1.0	0.9	0.6	0.2	0.8	1.3	1.5	1.1	1.0	1.0	0.5	-0.4	0.6	-0.9	-1.4	-0.4	-0.4	-0.1	0.7	-2.0	-1.1	-1.8	-0.1	-0.1	0.2	-1.9	-2.2	-1.1	-1.3	0.5	0.1	0.0	-0.2	-0.5	-0.5	104.0	43.9

-- NAFO division 3Ps --

	80	81	82	83	84	85	86	87	88	89	90	91	92	93	94	95	96	97	98	99	00	01	02	03	04	05	06	07	08	09	10	11	12	13	14	15	16	17	18	19	$\bar{x}$	sd
T_{bot}			-0.3	0.5	0.6									-1.1	-1.1	-0.6	0.1	-1.0	0.1	1.5	1.8	-0.9	-0.1	-1.8	0.2	1.2		-1.2	0.2	0.9	1.2	2.0	1.7	1.4	1.2	1.3	2.6	0.8	1.9	1.5	2.2	0.4
$T_{bot_{<200m}}$			0.4	0.7	1.1									-1.6	-1.3	-0.7	0.1	-1.1	0.3	1.3	1.5	-0.8	-0.4	-1.8	0.2	1.2		-0.7	0.2	0.8	0.6	1.7	1.1	1.0	0.5	0.6	1.4	-0.1	1.1	0.3	0.8	0.6
$Area_{>2^{\circ}C}$			0.3	1.1	-1.2									-0.5	-0.8	0.2	-0.7	-0.9	0.3	2.5	1.9	-1.2	-0.5	-1.1	-0.4	0.4		-0.9	0.6	0.4	0.3	1.7	-0.1	0.6	0.4	0.5	1.0	-0.4	1.8	0.1	27.4	3.3
$Area_{<0^{\circ}C}$			-0.4	-0.6	-0.9									1.6	1.1	1.1	-0.5	1.3	-0.1	-0.8	-1.2	0.6	0.2	2.0	-1.1	-1.5		0.6	0.0	-0.3	-0.9	-1.7	-1.4	-1.4	-0.4	-0.8	-1.2	0.2	-1.0	0.2	16.3	9.5

Figure 33. Scorecards of normalized spring bottom temperature anomalies for 3LNO and 3Ps.

Fall Conditions

Fall bottom temperature and salinity climatological maps, together with 2019 observations and anomalies for NAFO divisions 2HJ3KLNO, are presented in Figure 34 and Figure 35, respectively (see center panel for station occupation coverage). Except for 2H that was approximately normal, there is a north-south gradient of bottom temperature anomalies in 2HJ3KLNO, with warmer than normal conditions in the north: up to +2.5°C in most of 2J; +0.5°C to +2.5°C in 3K, +0.5°C to +1.5°C in 3L, and a mixture of both colder and warmer than normal in 3NO, except for the southwest slope the Grand Banks which was warmer than normal by 3.5°C.

Bottom salinities in divisions 2HJ and 3K generally display an inshore-offshore gradient between <33 close to the coast and 34 to 35 at the shelf edge. The Grand Banks bottom salinities range from <33 to 35, with the lowest values on the southeast shoal. In 2019 the bottom salinities were close to normal in most 2HJ3KLN, except the eastern part of 3L near the Flemish Pass that was saltier than normal. Division 3O was slightly fresh in its center and salty along the southwest slope of the Grand Banks.

Normalized bottom temperature and other derived indices anomalies are presented in the scorecard in Figure 36. While bottom temperature for 2017 was normal in 2J3K and below normal in 3LNO (first negative occurrence in a decade), they are above normal everywhere in 2HJ3KLNO in 2019, a further increase after 2018.

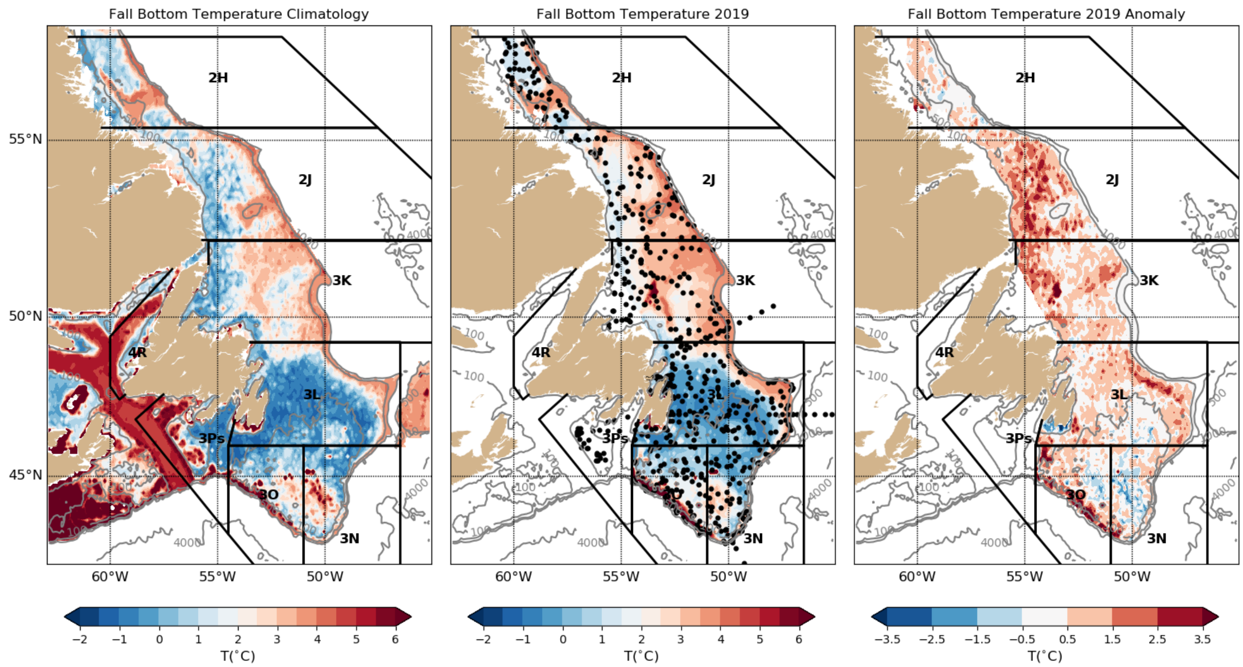

Figure 34. Maps of the mean 1981-2010 fall bottom temperature (left), and fall 2019 bottom temperature (center) and anomalies (right) for NAFO Divisions 2HJ3KLNO only. The location of observations used to derive the temperature field is shown as black dots in the center panel.

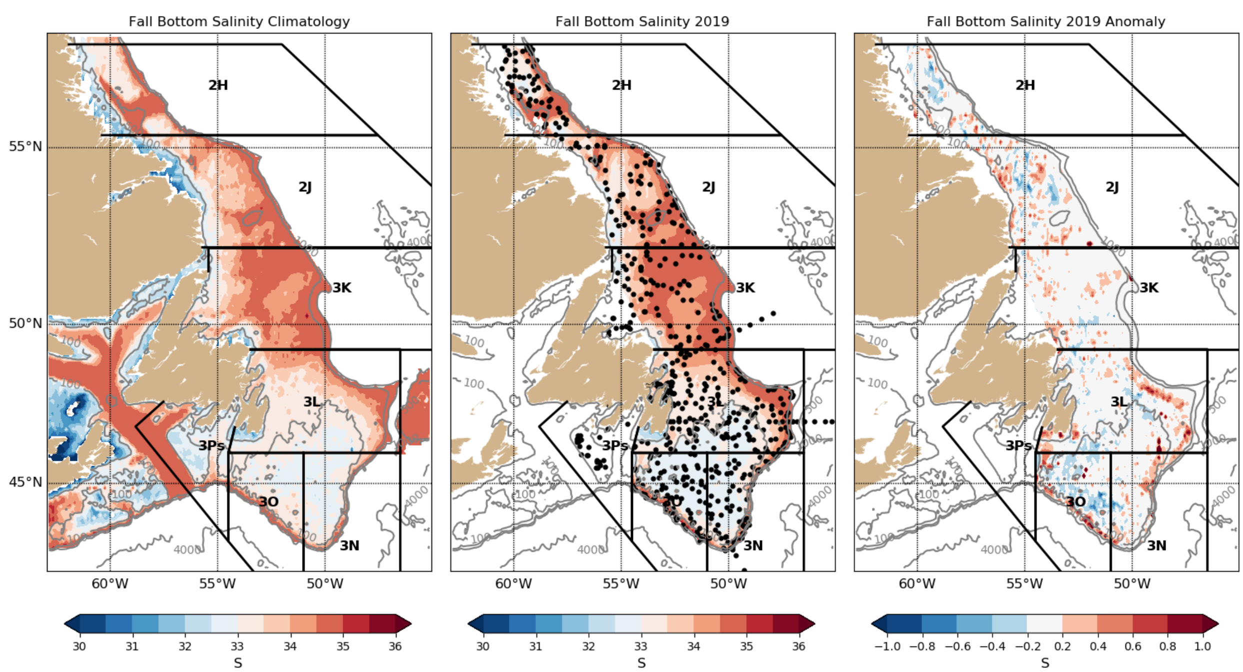

Figure 35. Maps of the mean 1981-2010 fall bottom salinity (left), and fall 2019 bottom salinity (center) and anomalies (right) for NAFO Divisions 2HJ3KLNO only. The location of observations used to derive the salinity field is shown as black dots in the center panel.

	80	81	82	83	84	85	86	87	88	89	90	91	92	93	94	95	96	97	98	99	00	01	02	03	04	05	06	07	08	09	10	11	12	13	14	15	16	17	18	19	$\bar{x}$	sd
-- NAFO division 2H --																																										
T_{bot}		0.0		-2.0								-1.3						0.2	0.2	0.5		-0.6			1.0		0.0		0.5		1.5	1.6	0.4	0.0	0.0	-0.2	0.0	-0.9	0.4	0.5	2.1	0.5
$T_{bot<200m}$		0.5		-1.8								-1.3						0.6	0.3	0.4		-1.1			1.0		0.0		0.1		1.4	1.6	0.5	-0.1	-0.1	0.3	0.2	-0.6	0.4	0.7	1.0	0.7
$Area_{>2°C}$		-0.6		-1.4								-1.1						0.2	0.2	0.0		-1.2			1.5		0.2		0.4		1.7	1.7	-0.4	-0.1	-0.6	-1.2	-0.5	-1.3	-0.2	0.0	22.7	5.4
$Area_{<1°C}$		-0.9		1.7								1.5						-0.9	0.1	-0.7		0.4			-0.8		0.5		0.4		-1.2	-1.2	-0.4	0.5	0.1	-0.3	-0.2	0.6	-0.6	-0.8	13.1	10.6
-- NAFO division 2J --																																										
T_{bot}	-0.2	0.3	-0.9	-0.8	-1.9	-1.5	0.2	-1.2	0.1	-0.3	-1.1	-0.7	-1.4	-1.4	-0.8		0.7	0.4	0.4	0.7	0.1	0.8	0.6	1.0	1.2	1.4	0.1	1.5	0.4	0.5	1.8	1.8	0.4	0.4	-0.1	-0.1	0.6	0.2	1.1	1.1	2.0	0.6
$T_{bot<200m}$	0.0	0.4	-0.8	-1.2	-1.8	-1.2	0.4	-1.2	0.1	-0.4	-0.9	-0.9	-1.5	-1.4	-0.7		0.8	0.3	0.2	0.8	0.0	1.0	0.7	1.0	1.1	1.5	-0.3	1.5	0.2	0.5	1.8	1.9	0.2	0.0	-0.5	-0.3	1.1	0.1	1.0	1.4	0.7	0.8
$Area_{>2°C}$	-0.1	0.1	-1.2	-0.6	-1.5	-1.4	0.3	-1.1	0.0	-0.5	-1.2	-0.7	-1.1	-1.3	-0.8		1.0	0.5	0.2	0.2	0.1	0.9	0.6	1.0	1.2	1.6	0.1	1.9	-0.2	0.1	2.1	2.3	-0.1	0.1	-0.2	-0.1	0.6	0.0	0.9	1.2	46.9	15.1
$Area_{<1°C}$	0.0	-0.5	1.2	1.1	1.5	1.3	-0.5	1.4	-0.5	0.4	1.1	1.0	1.3	1.3	0.8		-0.7	-0.5	-0.2	-1.1	0.1	-1.0	-0.7	-1.1	-0.9	-1.5	0.2	-1.4	0.1	-0.5	-1.6	-1.6	0.1	-0.1	0.3	0.2	-1.4	-0.1	-1.0	-1.5	26.4	16.9
-- NAFO division 3K --																																										
T_{bot}	0.2	0.1	-0.2	-0.5	-1.1	-2.0	-0.1	-0.9	-0.3	-0.2	-1.6	-0.8	-1.6	-1.6	-1.2	-0.6	0.0	0.7	0.6	1.0	0.6	0.3	0.8	1.0	1.6	1.1	0.4	1.2	0.9	0.5	1.7	2.3	0.5	0.7	0.0	0.2	0.0	-0.3	0.9	1.0	2.4	0.5
$T_{bot<200m}$	0.3	0.1	-1.4	-1.2	-1.4	-1.3	0.4	-1.1	-0.5	-0.3	-1.1	-1.0	-1.1	-1.3	-0.9	0.5	0.9	0.2	0.0	0.8	0.0	0.7	0.9	1.1	1.5	1.2	0.2	1.4	0.2	0.3	2.2	2.0	0.4	0.1	-0.3	0.3	1.3	0.1	1.2	1.8	0.2	0.8
$Area_{>2°C}$	0.2	0.3	0.1	-0.6	-0.9	-2.0	0.2	-1.0	-0.3	-0.4	-1.5	-0.5	-1.5	-1.5	-1.3	-0.9	0.0	0.9	0.8	0.9	0.7	0.2	1.1	0.7	1.3	1.2	0.4	1.1	0.9	-0.2	1.8	1.6	0.4	0.8	-0.2	0.3	-0.4	-0.4	1.1	1.1	72.2	14.5
$Area_{<1°C}$	-0.1	-0.2	0.1	0.7	0.9	2.0	-0.8	0.4	-0.2	-0.1	2.1	0.9	1.4	1.9	1.3	-0.2	-0.8	-0.3	-0.2	-0.7	0.0	-0.4	-0.9	-1.0	-1.4	-1.2	0.0	-1.3	-0.2	-0.1	-1.6	-1.7	-0.1	-0.5	0.1	-0.3	-1.0	0.3	-1.2	-1.6	17.1	10.0
-- NAFO division 3LNO --																																										
T_{bot}	0.5	0.0	1.3	0.3	-0.3	-1.0	0.2	-0.6	-1.1	0.3	-1.0	-1.4	-1.3	-2.2	-1.5	-0.2	0.3	0.1	1.0	2.2	-0.2	0.3	0.1	-0.1	1.2	0.5	0.9	0.1	-0.4	0.8	1.8	3.1	0.7	0.9	0.5	0.1	0.6	-1.0	0.4	0.5	1.1	0.4
$T_{bot<200m}$	0.8	0.1	1.6	0.4	-0.3	-0.9	0.4	-0.7	-1.0	0.4	-0.7	-1.4	-1.1	-2.2	-1.4	0.0	0.4	-0.1	1.0	2.3	-0.5	0.2	0.0	-0.3	1.0	0.4	0.8	-0.2	-0.8	0.8	1.8	3.1	0.6	0.9	0.6	-0.2	0.7	-1.1	0.3	0.6	0.7	0.5
$Area_{>2°C}$	0.2	-0.2	0.7	0.7	0.3	-1.4	0.3	-0.5	-1.6	0.9	-1.0	-1.0	-1.3	-1.8	-1.3	-0.4	0.0	0.0	1.3	2.6	0.0	0.1	-0.1	-0.2	1.0	0.4	0.5	0.1	-0.5	0.7	1.6	2.8	0.9	1.0	0.8	0.3	0.8	-0.8	0.0	0.4	70.4	19.9
$Area_{<0°C}$	-1.1	0.7	-0.1	0.8	1.1	0.2	-0.3	0.3	0.2	0.0	0.5	1.5	1.1	2.2	1.5	-0.5	-0.2	0.1	-0.6	-1.8	0.7	-0.2	-0.7	-0.2	-2.3	-0.9	-1.3	-0.1	0.3	-0.3	-1.7	-3.4	0.0	-0.3	-0.2	-0.1	0.1	1.3	-0.8	-0.4	99.0	26.6

Figure 36. Scorecards of normalized fall bottom temperature anomalies for 2H, 2J, 3K and 3LNO.

Ocean Conditions on the Scotian Shelf and Gulf of Maine (NAFO Sub-area 4)

Coastal Temperatures and Salinities

Coastal sea surface temperatures have been collected at Halifax (Nova Scotia) and St. Andrews (New Brunswick) since the 1920s (Figure 37). In 2019, the SST anomalies were +0.1°C (+0.2 SD) for Halifax, a decrease of 0.3°C from 2018 and +0.4°C (+0.6 SD) for St. Andrews, a decrease of 0.7°C from 2018.

Temperature and salinity measurements through the water column, for the most part sampled monthly, have been taken since 1924 at Prince 5, at the entrance to the Bay of Fundy (Figure 1). It is the longest continuously operating hydrographic monitoring site in eastern Canada. Its waters are generally well-mixed from the surface to the bottom (90 m). The depth-averaged (0-90 m) temperature, salinity and density anomaly time series are shown in Figure 37 (C-E). In 2019, the annual temperature anomaly was +0.4°C (+0.8 SD) and the salinity anomaly was -0.1 (-0.7 SD). These represent changes of -0.7°C and -0.3 from the 2018 values. The below-normal density anomaly is accounted for by both positive temperature anomaly and negative salinity anomaly.

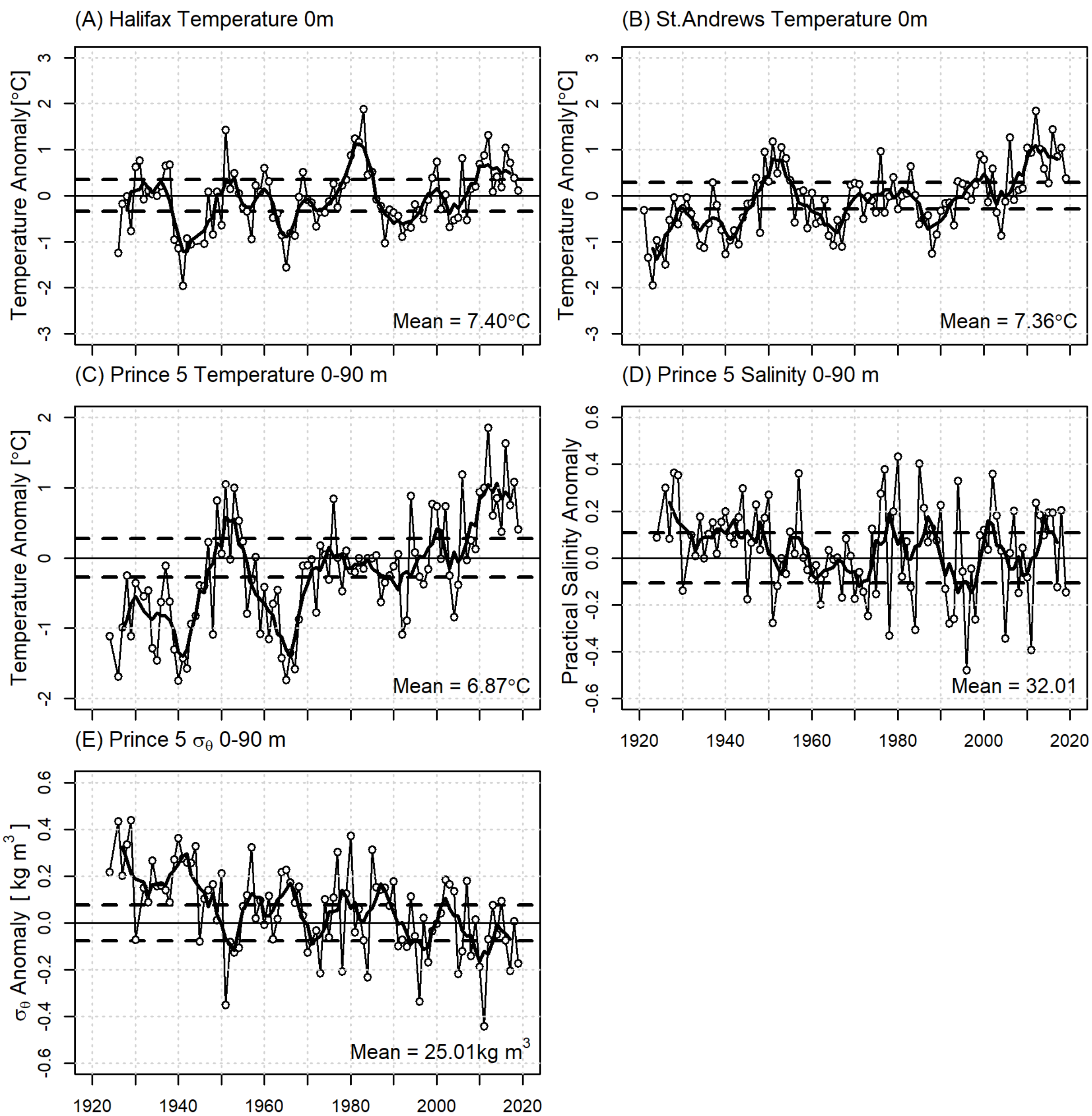

Figure 37. The annual surface temperature anomalies (dotted line with circles) and their 5-year running means (heavy black line) for (A) Halifax Harbour and (B) St. Andrews; annual depth-averaged (0-90 m) (C) Temperature, (D) salinity and (E) density anomalies for the Prince 5 monitoring station at the mouth of the Bay of Fundy. Horizontal dashed lines are the climatological average ±0.5 SD.

Temperatures from Long-term Stations

Drinkwater and Trites (1987) tabulated monthly mean temperatures and salinities from available bottle data for areas on the Scotian Shelf and in the eastern Gulf of Maine that generally correspond to topographic features such as banks and basins. Petrie et al. (1996) updated their report using these same areas and all available hydrographic data. An updated time series of annual mean and filtered (5 year running means) temperature anomalies at selected depths for six areas (see map Figure 38) is presented in Figure 39. The Cabot Strait temperatures represent a mix of Labrador Current Water and Warm Slope Water (e.g., Gilbert et al., 2005) entering the Gulf of St. Lawrence along Laurentian Channel; the Misaine Bank series characterizes the colder near bottom temperatures on the Eastern Scotian Shelf by either inshore Labrador Current water or cold-intermediate layer water from the Gulf of St. Lawrence (Dever et al., 2016); the deep Emerald Basin anomalies represent the Slope Water intrusions onto the Shelf that are subsequently trapped in the deep inner basins (note the large anomaly "events" in Figure 39C, for example, around 1980 and 2009 indicative of pulse of Labrador Slope Water); the Lurcher Shoals observations define the ocean climate on the southwest Scotian Shelf and the shallow waters entering the Gulf of Maine via the Nova Scotia Current; last, the Georges Basin series indicates the slope waters entering the Gulf of Maine through the Northeast Channel. Annual anomalies are based on the averages of monthly values; however, observations may not be available for each month in each area. For Cabot Strait, Misaine Bank, Emerald Basin, Georges Basin, eastern Georges Bank and Lurcher Shoals, 2019 annual anomalies are based on observations from five, two, five, eight, seven and two months, respectively.

In 2019, the annual anomaly was +1.6°C (+4.8 SD) for Cabot Strait at 200-300 m (the largest anomaly; four of the last five years were the warmest). For the shallow Misaine Bank on the eastern Scotian Shelf, the annual anomaly was -0.2°C (-0.3 SD) at 100 m. For the deep basins on the central Scotian Shelf and Gulf of Maine, the 2019 anomalies were +1.8°C (+2.2 SD) for Emerald Basin at 250 m (a record high, the last six years were the warmest in the record) and +1.7°C (+3.2 SD) for Georges Basin at 200 m (second warmest with 2018 the warmest, the last seven years were the warmest in the record). For the shallow banks in western Nova Scotia, the anomalies were -0.0°C (-0.1 SD) for eastern Georges Bank at 50 m and +0.3°C (+0.4 SD) for Lurcher Shoals at 50 m (2018 was the second highest with 2012 having the record). These values correspond to changes of +0.7°C, -0.7°C, +0.2°C, -0.2°C, -0.5°C, and -2.9°C, from the 2018 values.

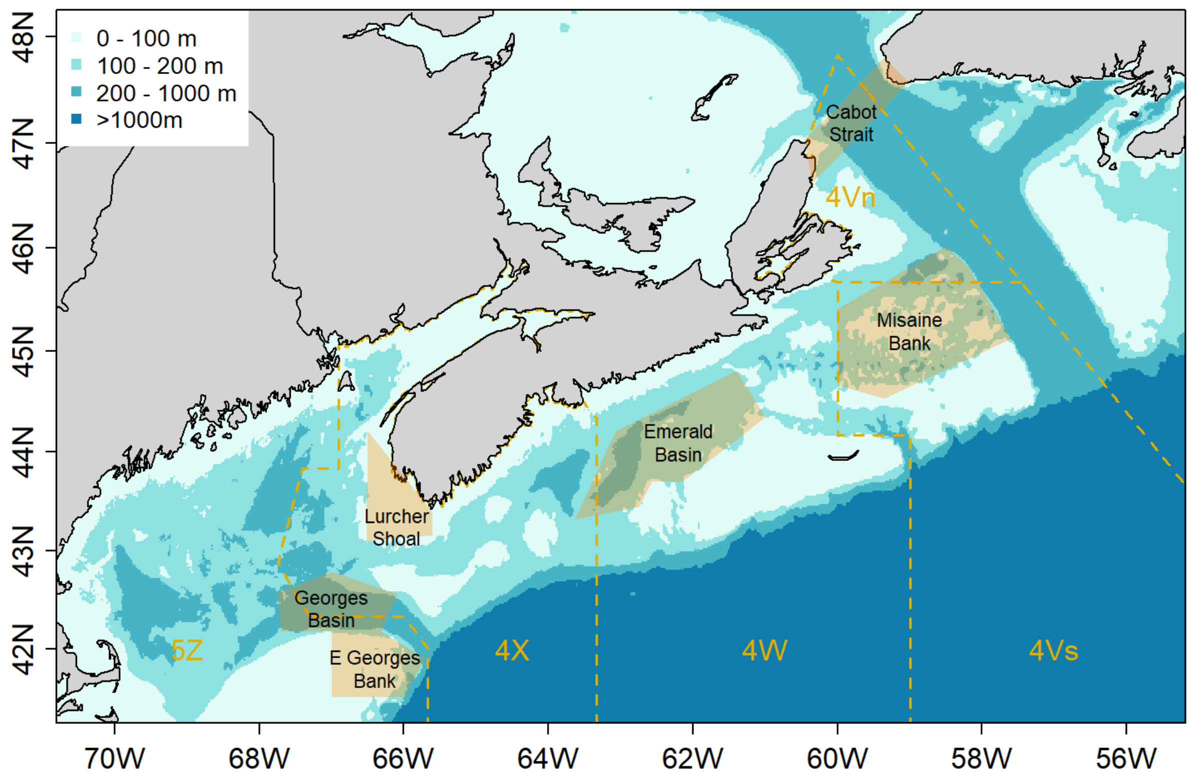

Figure 38. Areas on the Scotian Shelf and eastern Gulf of Maine used to characterize the different water masses.

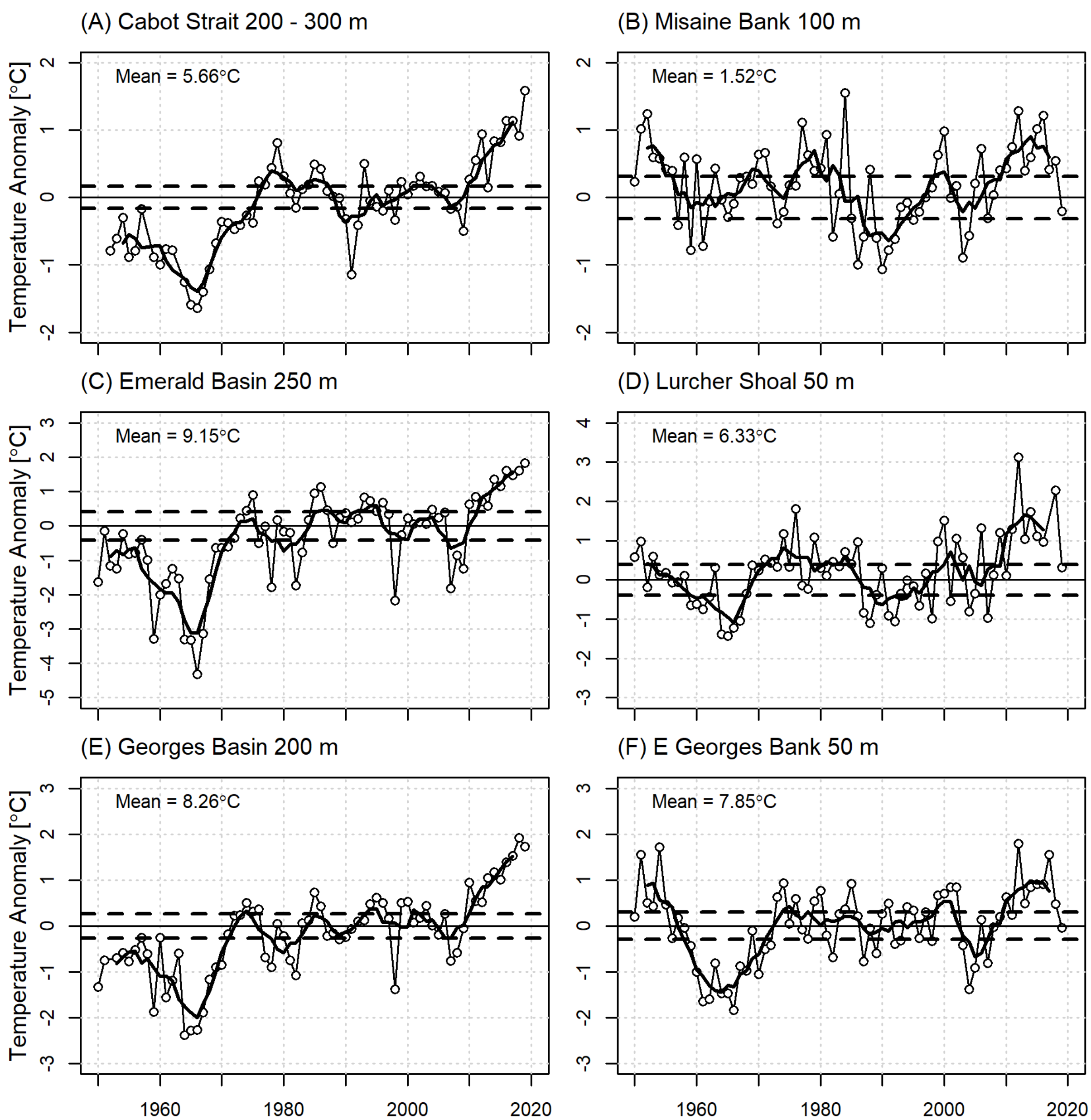

Figure 39. The annual mean temperature anomaly time series (dotted line with circles) and the 5 year running mean filtered anomalies (heavy solid line) on the Scotian Shelf and in the Gulf of Maine at (A) Cabot Strait (200-300 m); (B) Misaine Bank (100 m); (C) Emerald Basin (250 m); (D) Lurcher Shoals (50 m); and Georges Basin (200 m) (see Fig. 2). Horizontal dashed lines are the climatological average ±0.5 SD.

Temperatures during the Summer Groundfish Surveys

The broadest spatial temperature and salinity coverage of the Scotian Shelf is obtained during DFO's annual summer groundfish survey which covers the Scotian Shelf from Cabot Strait to the Bay of Fundy. The deep water boundary of the survey is marked roughly by the 200 m isobath along the shelf break at the Laurentian Channel, at the outer Scotian Shelf, and at the Northeast Channel into the Gulf of Maine towards the Bay of Fundy. A total of 236 CTD stations were sampled during the 2019 survey. The groundfish survey normally takes one month to complete with the area west of Halifax sampled first and the area east of Halifax sampled last.

The temperatures from the survey were combined and interpolated onto a 0.2° by 0.2° latitude-longitude grid using an objective analysis procedure known as optimal estimation. The interpolation method uses the 15 "nearest neighbours" with a horizontal length scale of 30 km and a vertical length scale of 15 m in the upper 40 m and 25 m at deeper depths. Data near the interpolation grid point are weighted proportionately more than those farther away. Temperatures were optimally estimated for at the standard depths (e.g. 0 m, 10 m, 20 m, etc.) and for near the bottom. Only the bottom temperatures are presented here (Figure 40).

Bottom temperatures anomalies for 2019 were positive for most of the region (Figure 41). The anomaly was positive for all of NAFO Divisions on the Scotian Shelf in 2019: +1.0°C (+2.4 SD) for 4Vn (the second warmest in the record; 2014 was the warmest); +0.8°C (+1.2 SD) for 4Vs; +0.9°C (+1.2 SD) for 4W and +1.2°C (+1.6 SD) for 4X (Figure 42 A-D). The volume of the Cold Intermediate Layer (CIL), defined as waters with temperatures <4°C, was estimated from the full depth CTD profiles for the region from Cabot Strait to Cape Sable (Figure 42E). For the period 1970 to 1989, the number of CTD profiles per year was limited; therefore, 5-year blocks of data (e.g. 1970-1974, centre date 1972) were used as input for the procedure to map the irregularly spaced data onto a regular grid. The data were then incremented by 1 year and a new set of estimates made (i.e., 1970-74, 1971-75, …). This procedure is similar to filtering (5-year running mean) the data for the 1970-89 period, effectively reducing the variance. Thus the long-term mean and particularly the SD (based on the 1981-2010 data in Figure 42E) could be affected. It is expected that the true SD is higher than the one derived here. There is considerable variation in the volume of the CIL from 1998 until 2009 (Figure 42E). The smallest volume was in 2012. In 2019, the CIL volume was slightly below normal.

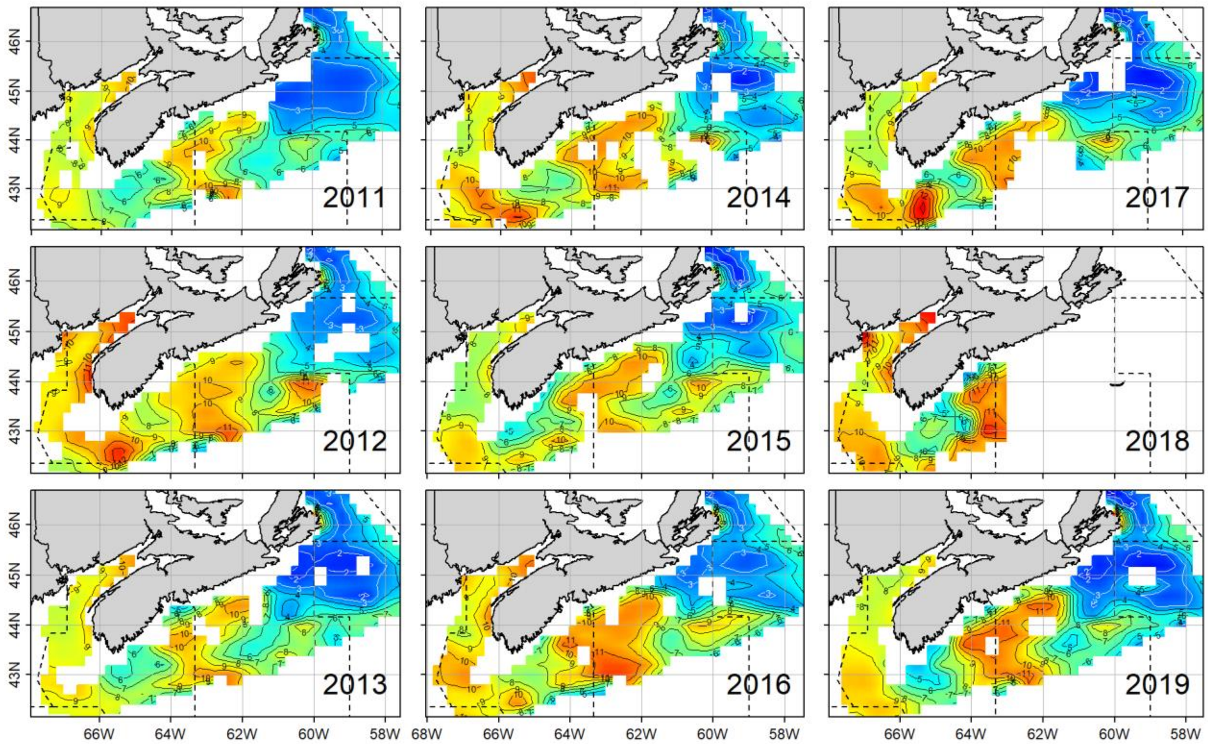

Figure 40. Bottom temperature determined from the July groundfish survey from 2011 to 2019. NAFO areas 4Vn, 4Vs, 4X and 4W are shown.

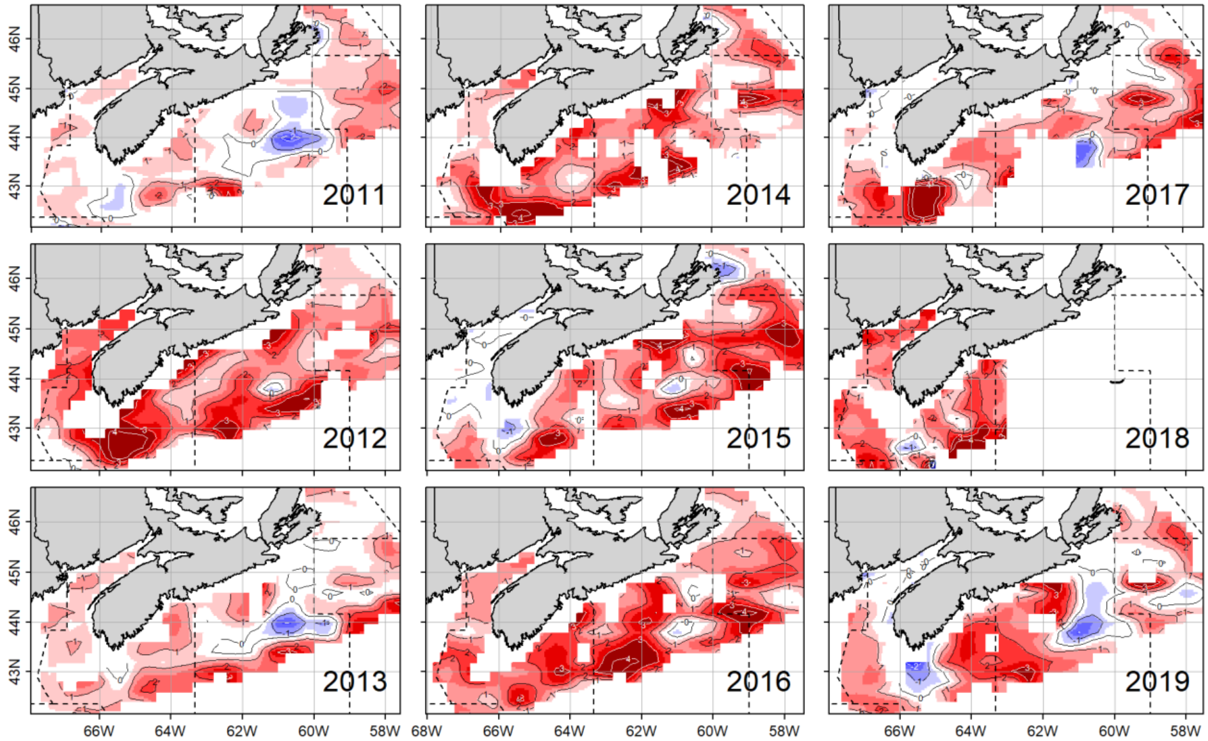

Figure 41. Bottom temperature anomalies determined from the July groundfish survey from 2011 to 2019. NAFO areas 4Vn, 4Vs, 4X and 4W are shown.

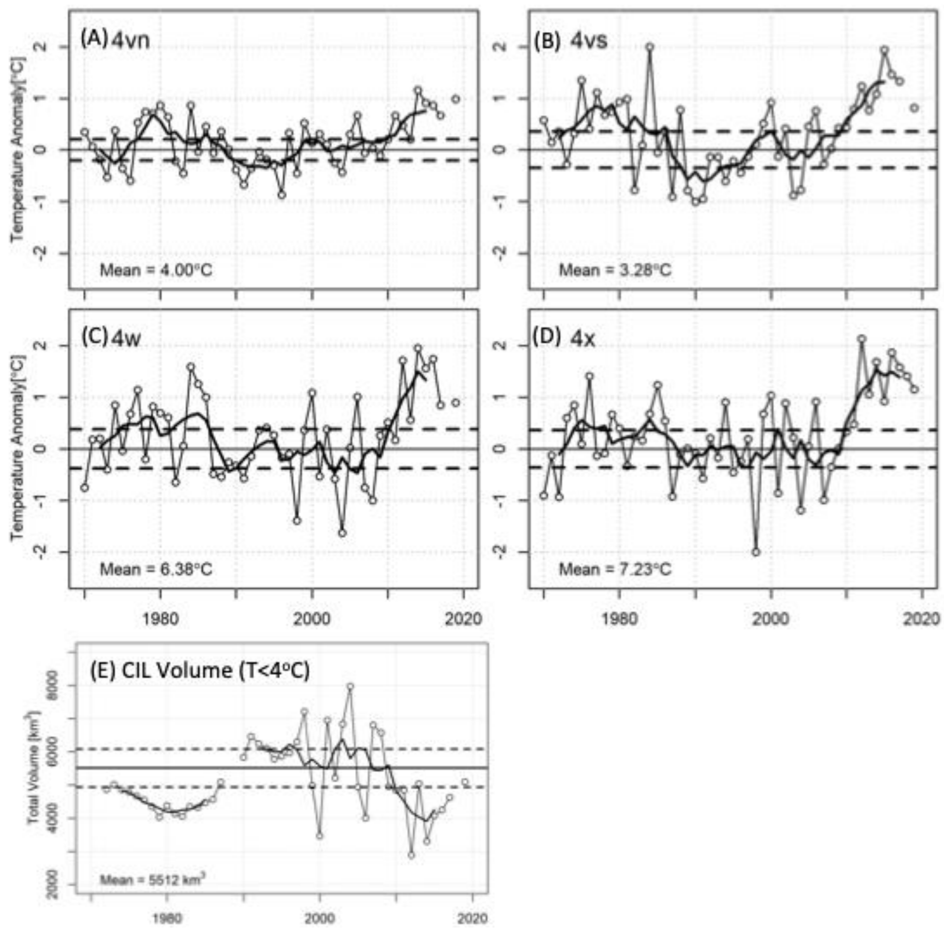

Figure 42. Time series of July bottom temperature anomalies (dashed lines with circles) and 5 year running mean filtered series (heavy line) for areas (A) 4Vn, (B) 4Vs, (C) 4W and (D) 4X. (E) Time series of the Cold Intermediate Layer (CIL, defined as waters with T<4˚C) volume on the Scotian Shelf based on the July ecosystem survey. The solid horizontal line is the 1981-2010 mean CIL volume and dashed lines represent ±0.5 SD.

Density Stratification

Stratification of the near surface layer influences physical and biological processes in the ocean such as vertical mixing, the ocean's response to wind forcing, the timing of the spring bloom, vertical nutrient fluxes and plankton distribution. Under increased stratification, there is a tendency for more primary production to be recycled within the upper mixed layer and hence less available for the deeper layers. The variability in stratification by calculating the density (σ_t) difference between 0 and 50 m was examined based on monthly mean density profiles on the Scotian Shelf. The long-term monthly mean density gradients for 1981-2010 were estimated; these were subtracted from the individual monthly values to obtain monthly anomalies. Annual anomalies were estimated by averaging all available monthly anomalies within a calendar year. This could be misleading if, in a particular year, most data were collected in months when stratification was weak, while in another year, sampling occurred when stratification was strong. However, initial results, using normalized monthly anomalies, were qualitatively similar to the plots presented here. The annual anomalies and their 5-year running means were for the Scotian Shelf. A value of 0.01 kg m^{-3}/m represents a difference of 0.5 kg m^{-3} over 50 m.

The dominant feature is the period from about 1950 to 1990 that featured generally below average stratification in contrast to the past 25 years that is characterized by above normal values (Figure 43). Since 1948, there has been an increase in stratification on the Scotian Shelf, resulting in a change in the 0-50 m density difference of 0.34 kg m^{-3} over 50 years. This change in mean stratification is due mainly to a decrease in the surface density, composed of equally of warming and freshening. Stratification in 2019 was significantly greater than in 2018 due to the surface freshening had a greater effect than the surface cooling.

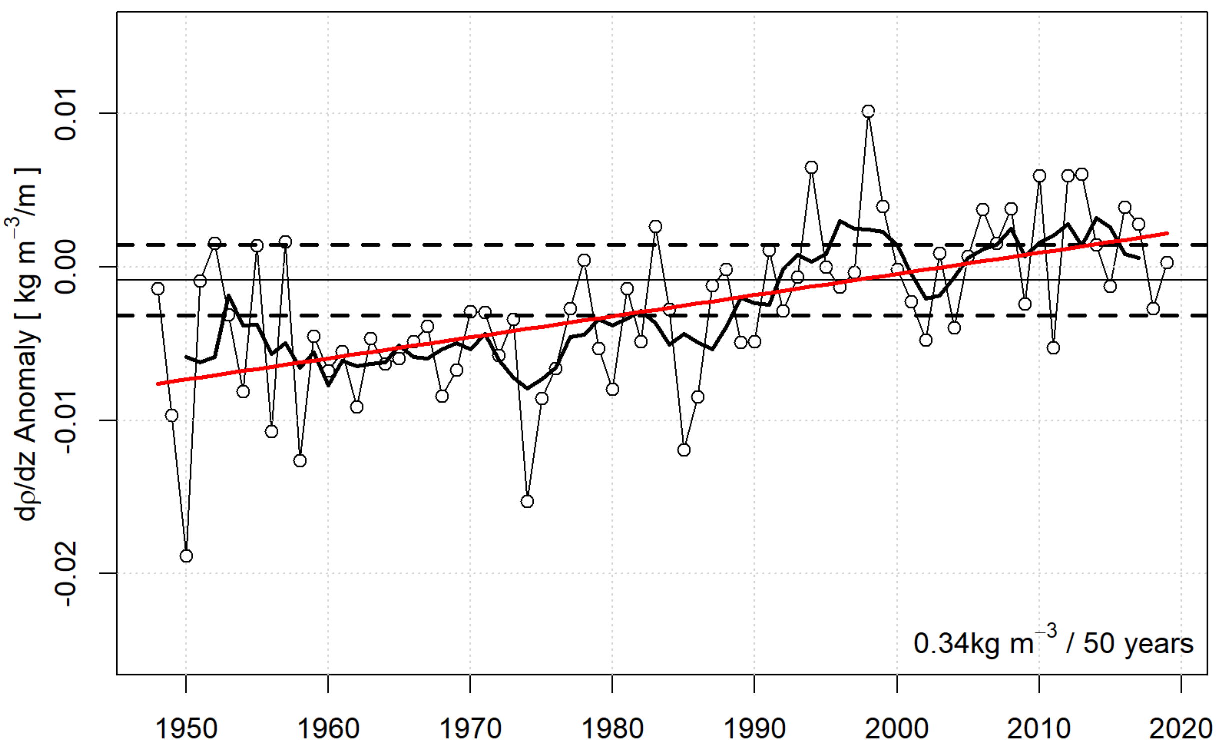

Figure 43. The mean annual anomaly (dashed line with circles) and 5-yr running mean (heavy solid line) of the stratification index (0-50 m density gradient) averaged over the Scotian Shelf. The solid

horizontal line is the 1981-2010 mean CIL volume and dashed lines represent ±0.5 SD. The linear trend (red line) shows a change in the 0-50 m density difference of 0.34 kg m^{-3} over 50 years.

Labrador Current Variability in NAFO Sub-area 2,3 and 4

The circulation in NL region is dominated by the south-eastward flowing Labrador Current, which floods the eastern shelf areas with cold and relatively fresh subpolar waters (Figure 44). This flow can significantly affect physical and biological environments off Atlantic Canada on seasonal and interannual time scales. The shelf current originates near the northern tip of Labrador where outflow through Hudson Strait combines with the eastern Baffin Island Current and flows southeastward along the Labrador coast where it is strongly influenced by the seabed topography, following the various cross shelf saddles and inshore troughs. A separate offshore branch flows southeastward along the western boundary of the Labrador Sea. This current is part of the large-scale Northwest Atlantic circulation consisting of the West Greenland Current that flows northward along the West Coast of Greenland, a branch of which turns westward and crosses the northern Labrador Sea forming the northern section of the Northwest Atlantic subpolar gyre.

Further south, near the northern Grand Bank, the inshore branch becomes broader and less defined. In this region, most of the inshore flow combines with the offshore branch and flows eastward, with a portion of the combined flow following the bathymetry southward around the southeast Grand Bank, and the remainder continuing east and southward around the Flemish Cap. A smaller inshore component flows through the Avalon Channel and around the Avalon Peninsula, and then westward along the Newfoundland south coast. Off the southern Grand Bank the offshore branch flows westward along the continental slope, some of which flows into the Laurentian Channel and eventually onto the Scotian Shelf. This extension of the Labrador Current on the Scotian Shelf (SS) slope is referred to as the Shelf Break Current. Additionally, there are strong interactions between the offshore branch of the Labrador Current and large-scale circulation. A significant portion of the offshore branch combines with the North Atlantic Current and forms the southern section of the subpolar gyre. Further east, the Flemish Cap is located in the confluence zone of subpolar and subtropical western boundary currents of the North Atlantic. Labrador Current water flows to the east along the northern slopes of the Cap and south around the eastern slopes of the Cap. In the eastern Flemish Pass, warmer high salinity North Atlantic Current water flows northward contributing to a topographically induced anticyclonic gyre over the central portion of the Cap.

Satellite altimetry data are used over a large spatial area to calculate the annual-mean anomalies of the Labrador Current transport (Han et al., 2014). A total of nine cross-slope satellite altimetry tracks are used to cover the Labrador Current on the NL slope from approximately 47°N to 58°N latitude (Figure 44). Similarly, five tracks from approximately 55°W to 65°W longitude are used for the Shelf Break Current on the SS slope. The nominal cross-slope depth ranges used for calculating the transport are from 200 to 3,000 m isobaths over the NL slope and from 200 to 2,000 m isobaths over the SS slope.

An empirical orthogonal function (EOF) analysis of the annual-mean transport anomalies was carried out. An index was developed from the time series of the first EOF mode and normalized by dividing the time series by its standard deviation. The mean transport values are provided based on ocean circulation model output over the NL slope (Han et al. 2008) and over the SS slope (Han et al.1997). The mean transport of the Labrador Current along the NL slope is 13 Sv with a standard deviation of 1.4 Sv, and the mean transport of the Shelf Break Current on the SS slope is 0.6 Sv with a standard deviation of 0.3 Sv. The mean transport values will be updated as new model output becomes available. The standard deviation values will be updated as knowledge on nominal depth improves.

The Labrador Current transport over the NL slope was out of phase with that of the Shelf Break Current over the SS slope for most of the years over 1993-2019 (Figure 45). The transport was strongest in the early 1990s and weakest in the mid-2000s over the NL slope, and weakest during those time periods over the SS slope.

The Labrador Current and Shelf Break Current transport were positively and negatively correlated with the winter North Atlantic Oscillation Index, respectively. After three years (2016-2018) of above normal transport for the Labrador Current and below normal for the Shelf Break Current, the transport was back to normal in 2019 for both region at +0.53 SD and -0.46 SD, respectively.

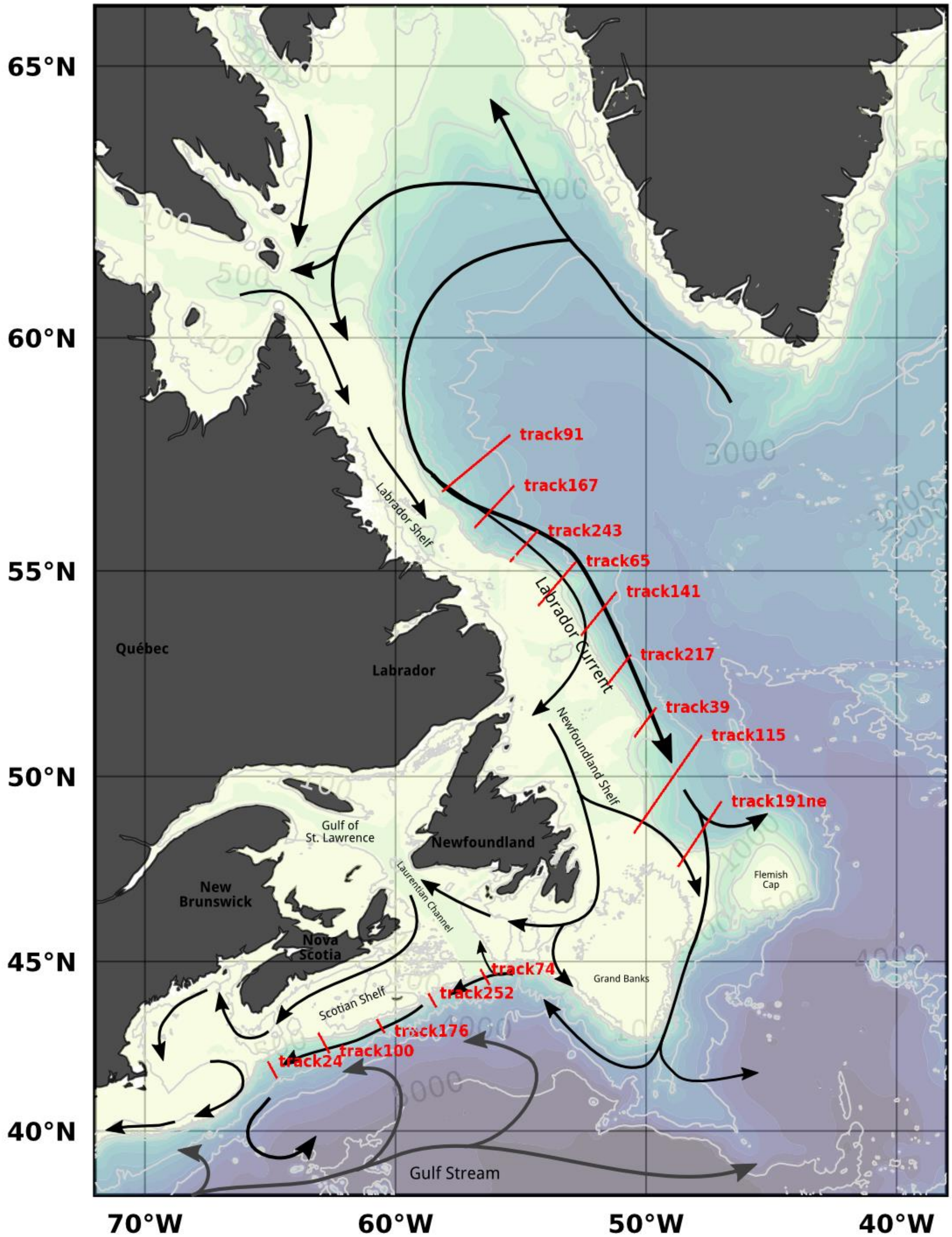

Figure 44. Map showing the Northwest Atlantic bottom topography (depth contour values in light gray) and schematic flow patterns (arrows). The transport is calculated across the cross-slope sections (red lines) identified by their satellite ground tracks numbers. The series of northern tracks are used

for the Labrador Current calculation on the Newfoundland and Labrador slope, while the series of tracks in the south are used for the Shelf Break Current transport on the Scotian Shelf slope.

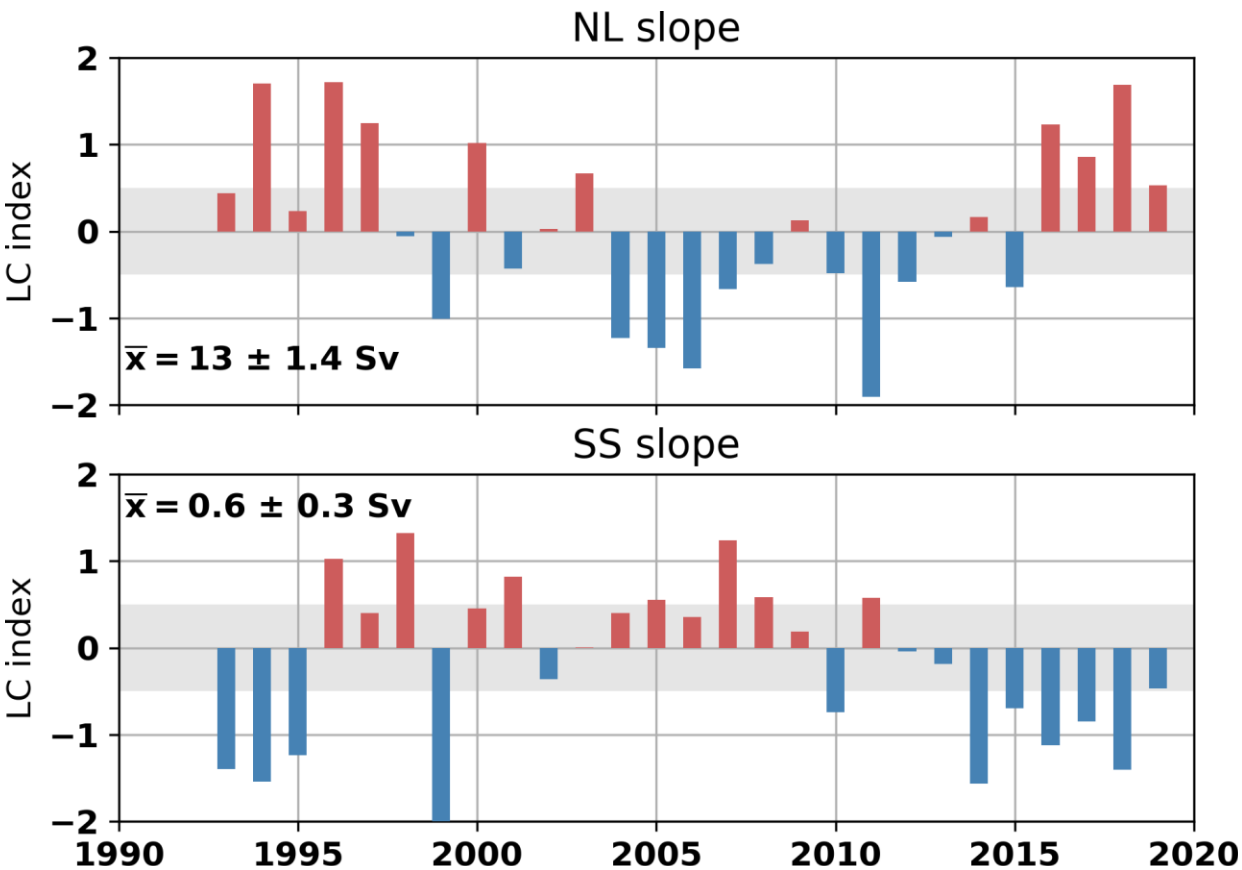

Figure 45. Normalized index of the annual-mean transport of the Labrador Current on the NL slope (top) and Shelf Break Current on the Scotian Shelf slope (bottom). Long-term averages over 1993-2019 (with standard deviation) are 13 ±1.4 Sv for the Labrador Current and 0.6 ±0.32 Sv for the Shelf Break Current. Shaded gray areas represent the ±0.5 SD range considered "normal".

Summary

An overview of physical environmental conditions for NAFO Divisions 2, 3 & 4 were presented. The highlights of 2019 can be summarized as follows:

- The annual air temperature was generally colder than average for sites in Newfoundland (St. John's and Bonavista), and much higher than average for the Arctic sites of Iqaluit (Baffin Island) and Nuuk (Greenland). On the Scotian Shelf and Gulf of Maine they were below normal or normal except for Boston which was nearly 2 SD above normal.

- Sea-surface temperature averaged over the ice-free months were normal to above normal on the Labrador Shelf and the northern Newfoundland Shelf, and varied from below normal to normal south and east of the Newfoundland shelf. In spite of regional disparities, the zonally averaged seasonal sea-surface temperature was below normal for the first time since 1992. However, this average would have been near-normal had it not been for tropical storm Dorian that hit the region in September.

- The sea-ice seasonal cycle exhibited a strong mid-season negative anomaly in ice volume in both Labrador and Newfoundland shelves. While the ice retreat timing was about normal on the Labrador shelf, it was early on the Newfoundland shelf.

- Summer cold intermediate layer metrics indicated normal to warmer-than-normal conditions across the zone.

- Bottom temperatures were mainly above normal across the zone except in NAFO Divisions 3LNO where they were near normal.

- Deep water temperature in Cabot Strait (200-300 m) and Emerald Basin (250 m) were at record high, while temperature in Georges Basin (200m) was the second warmest on record (last year was the warmest).

- High-frequency sites Station 27 and Halifax 2 exhibited below normal stratification.

- The Labrador Current weakened relative to 2018 on the NL slope, becoming close to normal.

Acknowledgments

We thank the many scientists and technicians at the Northwest Atlantic Fisheries Centre and at the Bedford Institute of Oceanography for collecting and providing much of the data contained in this analysis and to the Ocean Science Branch of Fisheries and Oceans in Ottawa for providing most of the historical data. Environment Canada provided the meteorological data. We also thank the captain and crew of the CCGS Teleost, Coriolis II and RRS James Cook for successful oceanographic survey during 2019. Finally, we thank the numerous technicians and scientists that contributed to the Atlantic Zone Monitoring Program for making this important work possible.

References

Colbourne, E. B., S. Narayanan and S. Prinsenberg. 1994. Climatic change and environmental conditions in the Northwest Atlantic during the period 1970-1993. ICES Mar. Sci. Symp., 198:311-322.

Colbourne, E. B., J. Holden, D. Senciall, W. Bailey, J. Craig and S. Snook. 2015. Physical Oceanographic Environment on the Newfoundland and Labrador Shelf in NAFO Subareas 2 and 3 during 2014. NAFO SCR. Doc. 2015/011. Serial No. N6431.

Cyr, F., Colbourne, E., Holden, J., Snook, S., Han, G., Chen, N., Bailey, W., Higdon, J., Lewis, S., Pye, B. and Senciall, D. 2019. Physical oceanographic conditions on the Newfoundland and Labrador Shelf during 2017. DFO Can. Sci. Advis. Sec. Res. Doc. 2019/051.

Cyr, F., Snook, S., Bishop, C., Galbraith, P.S., Pye, B., Chen, N., and, Han, G. 2020. Physical Oceanographic Conditions on the Newfoundland and Labrador Shelf during 2019, DFO Can. Sci. Advis. Sec. Res. Doc. [submitted] vi + 55 p.

Dever, M., Hebert, D., Greenan, B.J.W, Sheng, J. and Smith, P.C. (2016) Hydrography and Coastal Circulation along the Halifax Line and the Connections with the Gulf of St. Lawrence, Atmosphere-Ocean, 54:3, 199-217, DOI: 10.1080/07055900.2016.1189397

Dickson, R. R., J. Meincke, S. A. Malmberg and A. J. Lee. 1988. The "great salinity anomaly" in the northern North Atlantic 1968–1982. Progress in Oceanography, 20(2), 103-151.

Doubleday, W. G., Editor. 1981. Manual on groundfish surveys in the Northwest Atlantic. NAFC. Sco. Coun. Studies, 2: 56p.

Drinkwater, K.F. and R.W. Trites, 1987: Monthly means of temperature and salinity in the Scotian Shelf region, Can. Tech. Rep. Fish. Aquat. Sci., 1539, 101 p.

Drinkwater, K. F. 1996. Climate and oceanographic variability in the Northwest Atlantic during the 1980s and early-1990s. J. Northw. Atl. Fish. Sci., 18: 77-97.

Galbraith, P.S., Chassé, J., Shaw, J.-L., Caverhill, C., Dumas, J., Lefaivre, D. and Lafleur, C. 2020. Physical Oceanographic Conditions in the Gulf of St. Lawrence during 2019. DFO Can. Sci. Advis. Sec. Res. Doc. [submitted]. iv + 85 p.

Gilbert, D., B. Sundby, C. Gobriel, A. Mucci and G.-H. Tremblay, 2005: A seventy-two-year record of diminishing deep-water oxygen in the St. Lawrence estuary: The northwest Atlantic connection, Limnol. Oceanogr., 50, 1654-1666.

Han, G., Chen, N., and Z. Ma. 2014. Is there a north-south phase shift in the surface Labrador Current transport on the interannual-to-decadal scale? Geophys. Res. 119: 276-287.

Han, G., Lu, Z., Wang, Z., Helbig, J., Chen, N., and B. deYoung. 2008. Seasonal variability of the Labrador Current and shelf circulation off Newfoundland. Geophys. Res. 113.

Han, G., Hannah, C.G., Smith, P.C., and J.W. Loder. 1997. Seasonal variation of the three-dimensional circulation over the Scotian Shelf. Geophys. Res. 102:1011-1025.

ICNAF. 1978. List of ICNAF standard oceanographic sections and stations. ICNAF selected papers #3.

Petrie, B., S. Akenhead, J. Lazier and J. Loder. 1988. The cold intermediate layer on the Labrador and Northeast Newfoundland Shelves, 1978-1986. NAFO Sci. Coun. Studies 12: 57-69.

Petrie, B., K. Drinkwater, D. Gregory, R. Pettipas, and A. Sandström, 1996: Temperature and salinity atlas for the Scotian Shelf and the Gulf of Maine, Can. Data Rep Hydrog. Ocean Sci. 171, 398 p.

Petrie, B., 2007: Does the North Atlantic Oscillation affect hydrographic properties on the Canadian Atlantic Continental Shelf?, Atmos.-Ocean, 45, 141-151.

Petrie, B., R. G. Pettipas and W. M. Petrie. 2007. An overview of meteorological, sea ice and sea surface temperature conditions off eastern Canada during 2006. DFO Can. Sci. Advis. Sec. Res. Doc. 2007/022.

Therriault, J.-C., Petrie, B., Pepin, P., Gagnon, J., Gregory, D., Helbig, J., Herman, A., Lefaivre, D., Mitchell, M., Pelchat, B., Runge, J., and Sameoto, D. 1998. Proposal for a northwest Atlantic zonal monitoring program. Can. Tech. Rep. Hydrogr. Ocean Sci. 194: vii+57 pp.

Thyng, K. M., Greene, C. A., Hetland, R. D., Zimmerle, H. M., & DiMarco, S. F. (2016). True colors of oceanography. Oceanography, 29(3), 10.

Vincent, L. A., X. L. Wang, E. J. Milewska, H. Wan, F. Yang, and V. Swail. 2012. A second generation of homogenized Canadian monthly surface air temperature for climate trend analysis. J. Geophys. Res. 117, D18110, doi:10.1029/2012JD017859.